DISSERTATIONES GEOLOGICAE UNIVERSITATIS TARTUENSIS

19

DISSERTATIONES GEOLOGICAE UNIVERSITATIS TARTUENSIS
19

DEVELOPMENT OF IMPACT-INDUCED HYDROTHERMAL SYSTEM AT KÄRDLA IMPACT STRUCTURE

EVELIN VERŠ

TARTU UNIVERSITY
PRESS

Institute of Geology, Faculty of Biology and Geography, University of Tartu, Estonia.

This dissertation is accepted for the commencement of degree of Doctor of Philosophy (in Geology) at the University of Tartu on October, 19, 2006 by the Council of the Faculty of Biology and Geography of the University of Tartu.

Opponent: Prof. Dr. phil. Alexander Deutsch, Institut für Planetologie, Westfälische Wilhelms-Universität Münster, Germany

The thesis will be defended at the University of Tartu, Vanemuise 46, room 246, on December, 08, 2006 at 12.15.

Publication of this thesis is granted by the Faculty of Biology and Geography, University of Tartu.

ISSN 1406–2658
ISBN 9949–11–477–2 (trükis)
ISBN 9949–11–478–0 (PDF)

Tartu Ülikooli Kirjastus
www.tyk.ee
Tellimus nr. 597

CONTENTS

ORIGINAL PUBLICATIONS

Publication I

Versh E., Kirsimäe K., Jõeleht A. and Plado J. 2005. Cooling of the Kärdla impact crater: I. The mineral paragenetic sequence observation. Meteoritics & Planetary Science 40(1), 3–19.

Publication II

Jõeleht A., Kirsimäe K., Plado J., **Versh E.** and Ivanov B. 2005. Cooling of the Kärdla impact crater: II. Impact and geothermal modeling. Meteoritics & Planetary Science 40(1), 21–33.

Publication III

Versh E., Kirsimäe K. and Jõeleht A. in press. Development of potential ecological niches in impact-induced hydrothermal systems: the small-to-medium size impacts. Planetary and Space Science. doi:10.1016/j.pss.2005.12.022.

Author's contribution

Publication I: The author was primarily responsible for fieldwork, data analysis, interpretation and writing of the manuscript.

Publication II: The author contributed to the fieldwork, data collection, analysis and complemented to the writing of the manuscript.

Publication III: The author was responsible for the fieldwork, data analysis, interpretation and writing of the manuscript.

1. INTRODUCTION

Hydrothermal alteration, i.e. interaction of rock-forming minerals with solutions that have temperatures higher than expected from the regional geothermal gradient in the given area (Utada 1980), is a common natural phenomenon that occurs in a wide variety of geological settings and rock types. Formation of a hydrothermal (HT) system (i.e., heated fluid flow through rocks) needs water, fractures in the ground rock and primarily — the heat source. As a consequence, hydrothermal phenomena are usually found in close relation to endogenous processes, such as volcanic activity, ocean spreading and continental rifting.

The energy released by a meteorite impact, exogenous in nature, results in fracturing and heating (up to melting and vaporization) of the projectile and target rocks. Strong differential temperatures remaining in the fractured and/or displaced crater basement rocks due to the post-shock residual heat can also create a hydrothermal circulation system if water (including groundwater or permafrost resources) is present at the crater site (Abramov and Kring 2004; Jõeleht et al. 2005). Evidences of impact-induced hydrothermal (IHT) activity have been found at numerous terrestrial impact craters varying in size (from 1.8 to 250 km) and target composition (e.g., Koeberl et al. 1989; McCarville and Crossey 1996; Ames et al. 1998; Sturkell et al. 1998; Naumov 2002; Osinski et al. 2001; Kirsimäe et al. 2002; Hagerty and Newsom 2003; Hecht et al. 2004; Naumov 2005; Versh et al. 2005). The IHT activity has been suggested for impact craters on Mars as well (e.g., Allen et al. 1982). In contrast to hydrothermal processes caused by igneous and metamorphic events, impact-generated fluid circulation systems have become the subject of scientific interest only during the last two decades (Naumov 2005). However, the formation and development of the IHT systems is still under debate.

Development and formation of an IHT system largely depends on the dimensions of an impact and the presence of impact melting (e.g., Naumov 2005 and references therein; Versh et al. in press). In large-scale impacts, where initially impermeable melt-sheet can cover most of the crater depression, the IHT circulation is originally initiated in an annular trough between peak ring and final crater rim (e.g., Abramov and Kring 2004). However, in small-to-medium scale craters without significant melting, an IHT system is formed usually in and around the central high (e.g., Jõeleht et al. 2005). Likewise, the life-time and alteration intensity of the system varies significantly with crater size, depending on the amount of melting and governing mode of the heat transport. In small-scale structures with limited melting the IHT system is formed shortly after the impact and the cooling is governed mainly by convective heat transport leading to more rapid temperature decrease. Development of the IHT system, which is part of the post-impact cooling process, can be recognized by means of mineralogical studies that describe the thermal and compositional evolution of the post-impact fluids as well as the geochemical/mineralogical alteration of the primary impactites. However, fast temperature changes and evolving post-impact fluids in small-to-medium size structures make it difficult to assess their IHT system development.

Objectives

The aim of this thesis is to investigate thermal, geochemical and mineralogical changes in time and space in a 4-km diameter Kärdla structure on the Hiiumaa Island near the west coast of Estonia. It is one of the best-preserved and well-investigated impact structures of its size (e.g., Puura and Suuroja 1992; Plado et al. 1996; Suuroja et al. 2002; Puura et al. 2004) and can serve as a model structure for impact-induced hydrothermal activity in small-to-medium sized impact craters.

This thesis has three main objectives:

(1) to identify mineralogical and geochemical changes in impactites during the different evolutionary phases of the IHT system;

(2) to explore how the physical (e.g., fluid temperature) and chemical (e.g., pH, oxidizing-reducing) conditions are set and evolving through the life-time of the IHT activity;

(3) to examine how a hydrothermal system, initiated by a meteorite impact, produces new environments suitable for high-temperature microbial life; what are the characteristics of these ecological niches and how do they change in space and time.

The thesis consists of three papers focused on mineralogical (paper I), impact and geothermal modeling studies in the Kärdla crater (paper II) and evaluation of development of ecological niches in small-to-medium size craters (paper III).

Paper I

Versh E., Kirsimäe K., Jõeleht A. and Plado J. 2005. Cooling of the Kärdla impact crater: I. The mineral paragenetic sequence observation. Meteoritics & Planetary Science 40(1), 3–19.

This and the following paper are focused on the Kärdla structure situated in the Island of Hiiumaa, near the west coast of Estonia. The IHT mineral paragenetic sequence in Kärdla impactites is presented and described by mineralogical, chemical and initial stable isotope studies. The mineralization sequence is characterized in the most altered central area and in the rim wall of the structure, which describes development of this area shortly after the impact from an early vapor-dominated fluid stage right after the impact, up to the later liquid-dominated stages when temperatures were dropping close to the ambient conditions. The main results are:

The IHT mineralization sequence with falling temperatures started with plagioclase alteration to submicroscopic adularia at temperatures higher than 300°C. This stage was followed by hornblende chloritization during transition from vapor- to liquid-dominated system at temperatures of 300 to 150(100)°C. The second chlorite-feldspar-quartz stage of hydrothermal mineralization was completed by precipitation of microscopic idiomorphic (euhedral) K-feldspar in fractures and cavities in the impact breccia. The final stage was characterized by the sequence of calcite generation I, dolomite, quartz, calcite II, chalcopyrite/ pyrite, Fe-oxyhydrate, and calcite III precipitation at temperatures below 100°C.

The IHT system at the Kärdla structure can be considered as a model for medium-to-small size impact structures. Its architecture is characterized by pervasive alteration in the upper central area of the crater and by the fracture limited fluid-rock interaction at the rim and in the deeper central portion of the crater depression. It represents a single thermal event, which displays an irreversible cooling path that has resulted in a series of alteration products. The character and spatial position of the IHT mineralization suggest that geochemical transport was restricted to a "semi-closed" system of fluid-rock interactions.

Paper II

Jõeleht A., Kirsimäe K., Plado J., Versh E. and Ivanov B. 2005. Cooling of the Kärdla impact crater: II. Impact and geothermal modeling. Meteoritics & Planetary Science 40(1), 20–32.

The aim of this paper was to study the time scale and contribution of different thermal processes involved in the cooling of the Kärdla impact crater. The numerical heat and multi-phase fluid transfer modeling was used. To estimate heating caused by the impact as well as the post-impact temperature distribution in the crater structure, numerical impact modeling was also performed. For the estimation of post-impact temperatures, the source data needed as input for the geothermal modeling, the lateral and vertical variations in mineralogical-geochemical data by Versh et al. (2005) and Kirsimäe et al. (2002) were used. The main results are:

The maximum crater depth of 1.2 km (transient cavity) was reached in 6–7 seconds after which the central uplift started to rise. The excavation in the radial direction continued and the final crater diameter was achieved approximately 20 seconds after the impact. The rise of central uplift continued until 30–35 seconds and then collapsed to some extent. The highest simulated post-impact temperatures, which slightly exceeded 800°C, were present in the near-surface part at the centre of the uplift. At distances of 250, 450 and 700 meters from the crater centre the post-impact temperatures of <650°C,

<480°C and <300°C were distributed, respectively. At the rim the near-surface temperatures were around 100°C, in the shocked ejecta fragments and injected breccia dikes, however, the temperatures up to 200°C may have existed.

The post-impact cooling of the Kärdla crater was rapid. The highest post-shock temperatures in the central area of the structure decreased 50% from their initial values in 1200–1500 years and 80% in less than 4000 years. Transition from convective-dominated to conduction-dominated heat transfer system took place about 3000–4000 years after the impact, whereas it took about 9000–10,000 years for the IHT flow system to cease. However, the thermal equilibration of the impact-heated rocks took much longer time and the heat flow density anomaly became instrumentally undetectable only 40,000–50,000 years after the impact.

Paper III

Versh E., Kirsimäe K. and Jõeleht A. in press. Development of potential ecological niches in impact-induced hydrothermal systems: the small-to-medium size impacts. Planetary and Space Science. doi:10.1016/j.pss.2005.12.022.

In this paper, development of IHT zones potentially habitable for thermophilic and hyperthermophilic microorganisms was studied. The numerical modeling and mineralogical-geochemical data suggest that in small-to-medium size impact craters with insignificant melting, the suitable conditions for hydrothermal microbial communities are established during a geologically short time (from tens to few hundreds of years) after the impact in most parts of the crater. In the central uplift area the microbial colonization is inhibited for about a thousand years. However, this area retains the optimum temperatures (45–120°C) needed for hydrothermal microorganisms for the longest period. In the crater depression and rim area the initial temperatures, suggested by the impact modeling, were much lower — from 150°C to ambient temperatures, except locally somewhat higher in fracture zones and suevite pockets.

Geochemical and mineralogical data suggest, in general, neutral pH 7 (±1) fluids of the IHT systems, which is, compared to volcanic hydrotherms, richer in dissolved oxygen and low in reduced compounds. This may indicate the presence of sulfur reducing microorganisms in the possible IHT communities. Furthermore, these microbes cannot be highly specialized, because especially in small-scale craters impact-induced hydrotherms change rapidly in space and environmental quality. Therefore, the potential habitats created in IHT systems would be occupied by organisms capable of adapting to the changing conditions by applying alternative metabolic processes.

2. GEOLOGICAL SETTING

2.1. Location and geological background

This thesis focuses on the Kärdla impact structure located on the Hiiumaa Island (58º58´40´´N, 22º46´45´´E), 25 km off the northwestern coast of Estonia (Fig. 1). The structure is 4 km in (rim-to-rim) diameter and ~540 m deep with a central uplift exceeding 100 m in height. The crater formed in a shallow (<100 m deep) epicontinental Ordovician sea into two-layered rock target of Early Paleozoic siliciclastic and carbonate sediments covering Precambrian crystalline basement (Puura and Suuroja 1992). The estimated age of the structure is early Caradoc (~455 Ma) and corresponds to the transition between the *Angochitina curvata* and *Lagenochitina dalbyensis* chitinozoan Biozones (Grahn et al. 1996). The structure is buried under the Ordovician, Silurian and Quaternary sedimentary cover and is barely expressed in the present-day topography. The thickness of the post-impact sedimentary rocks in the crater depression reaches 300 m, outside of the crater structure 90 m and 15–20 m above the crater rim-wall.

The pre-impact bedrock section composed of sedimentary rocks overlying the crystalline basement of the Paleoproterozoic metamorphic rocks. The sedimentary succession of the target consisted mostly (>90% of the section thickness) of Ediacaran, Lower Cambrian and Lower Ordovician weakly cemented terrigenous rocks: sand- and siltstone, clays, and a thin (~15 m) layer of Ordovician carbonates. The present-day porosity of these sediments is ~20–30% (Jõeleht et al. 2002), which suggests that the section was, accounting only the mechanical compaction, about 30% thicker (up to ~200 m) at the time of the Kärdla impact.

The Paleoproterozoic crystalline basement, representing a 1.7–2.0 Ga old Svecofenninan crustal segment (Puura and Huhma 1993; Gorbatchev and Bogdanova 1993), is composed of regionally metamorphosed amphibolite facies migmatitic granites and quartz-feldspar gneisses with amphibolites, biotite gneisses and biotite-amphibole gneisses (Koppelmaa et al. 1996). The amphibolitic rocks form up to 22%, biotite-amphibole gneisses and biotite-plagioclase gneisses 6%, and granitic rocks (granitoids, granite gneisses and quartz-feldspar gneisses) up to 72% of the basement in the area. The eastern part of the structure at the Paluküla rim wall is mainly composed of amphibolites, whereas the main part of the crater depression and western rims are granites and quartz-feldspar gneisses (Koppelmaa et al. 1996).

Figure 1. Location of the Kärdla and other terrestrial impact structures in the Baltic Sea area, where post-impact hydrothermal alteration has been detected (after Naumov 2002, Figure 1 and references therein; Suuroja and Suuroja 2000), from which detailed IHT mineralogical-geochemical research has been previously conducted only in Siljan and Lockne structures (Komor et al. 1988; Hode et al. 2003; Sturkell et al. 1998).
Impact structures: 1 — Kärdla; 2 — Gardnos; 3 — Jänisjärvi; 4 — Lappajärvi; 5 — Lockne; 6 — Logoisk; 7 — Mien; 8 — Mishina Gora; 9 — Misarai; 10 — Neugrund; 11 — Sääksjärvi; 12 — Siljan; 13 — Söderfjärden; 14 — Suavjärvi.

2.2. Impactites

The well-preserved crater depression in Kärdla is filled with complete set of impactites (i.e., rocks affected by an impact resulting from collision of planetary bodies; Stöffler and Grieve 1994) characteristic to those produced by impacts in marine environment with no or limited melting (Suuroja et al. 2002 and references therein). The section of the crater filling impactites consists, from the bottom to the top, of autochthonous (monomict), allochthonous, slumped and fallback (polymict) breccias covered with resurge conglomerates, conglomeratic turbidites and sands eroded from the uplifted rim walls (Suuroja et al 2002; Puura et al 2004). Herein the term "monomict" refers to *in situ* brecciation of a particular lithology and uniform (low) degree of shock; and "polymict" to a mixture of one or more lithological types of clasts with different degree of shock, mixing and homogenization of one or more target lithologies (Stöffler and Grieve 1994).

The porosity of the shock-affected rocks in Kärdla increases from ≤5% in the fractured basement to ~18% in the impact breccias (Plado et al. 1996). The shock metamorphic features from shock stages 1–3 (e.g., kink-banding, planar deformation features (PDFs), isotropization and partial melting) in quartz, microcline and/or biotite are present only in the allochthonous breccia units (Suuroja 1999; Puura et al. 2004). However, the volume of rocks subjected to post-impact chemical/mineralogical alteration is considerably larger, extending also into the (par)autochthonous breccias and the fractured basement.

Autochthonous breccias (i.e., massive monomict breccias and shocked rocks of the crater basement; Stöffler and Reimold in press); are composed of cataclastic crystalline basement rocks, which are fractured to various scales. The intensity of fracturing decreases gradually with depth and, according to geophysical data and reconstruction of the transient cavity, extend probably about 1 km beneath the crater floor (Plado et al. 1996). In autochthonous breccias fine-grained breccia dikes are common; they decrease in number and size with depth (in K-1, to a depth of 800 m; Puura et al. 2004). Within the fractured crystalline rock dikes of matrix-rich impact breccia can be found at the northeast crater rim as well (core P-11; Puura et al. 2004).

Allochthonous breccias (i.e., impact breccia in which component materials have been displaced from their point of origin, including dike and clastic matrix breccias; Stöffler and Grieve 2003) consist of poorly mixed polymict crystalline (mainly granitic) and sedimentary rock derived breccia (inter)layers. The crystalline-derived breccia units (523–471 m and 380–356 m in K-1; 356–400 m in K-18; Puura et al. 2004) are similar in texture and composition — they contain small grains of sedimentary material within granitioid or amphibolite blocks, fragments (with diameter of 0.2–5 cm or 5–30 cm, often altered; Põldvere 2002) and fine-grained matrix. The fine-grained, mainly crystalline-derived matrix is more or less strongly welded. Clastic sand to pelitic particles in matrix of the upper layers is observable (Puura et al. 2004). The color of the cementing matrix varies between light greenish-gray or grayish-brown and pinkish-red (in places reddish-brown or -gray), containing mineral or rock clasts crushed to submicroscopic scale. The intervals 522.8–493.0 and 378.5–360.5 m can be described as suevitic and suevite-like breccias respectively, by the occurrence of dispersed (rarely exceeding 20%) and strongly altered melt particles (Põldvere 2002; Suuroja et al. 2002).

The sedimentary-derived allochthonous breccia units are composed mainly of sedimentary rocks with few clasts of crystalline rocks (in the second layer, 356–300 m; Puura et al. 2004). In the upper part (~315 m) the abundance of crystalline clasts increases. These units consist of large block and smaller fragments of sand-, clay- and limestone, they are cement-poor and mainly of slump origin. The inter-clast cement occurs as soft sedimentary rock powder with clasts of sedimentary origin.

The resurge breccias consist of clasts and blocks predominantly from the topmost part of the target rocks (e.g., 40% of limestone) with some clasts from suevite-like breccias (Suuroja et al. 2002). Outside of the crater the continuous 0.01–3.5 m thick ejecta (i.e., solid, liquid and vaporized rock ejected ballistically from an impact crater; Stöffler and Grieve 2003) layer is distributed within a distance of 50 km as a sandy (silt- to gravel-sized debris of target rocks) layer in the bedrock of Ordovician limestone (Suuroja and Suuroja 2006). The distal ejecta consists mostly of silt- to gravel-sized debris of the target rocks (mostly Cambrian siliciclastic and Paleoproterozoic metamorphic rocks) with coarser clasts in the lower part of the layer at closer areas to the impact centre. The ejected material contains up to 1 vol % of quartz grains with PDFs (Suuroja and Suuroja 2006).

3. PREVIOUS STUDIES AT THE KÄRDLA CRATER

An unexpected geological feature, afterwards identified as a rim wall of the Kärdla structure, was discovered in 1967. During a drilling of groundwater well the crystalline rocks were penetrated at depths of 22 m at the Paluküla village, where the normal depth for crystalline basement was expected to be at 250 m (Viiding et al. 1969). From 1968 until late 1990s several research and mapping teams have thoroughly investigated the Kärdla structure (Kala et al. 1971; Suuroja et al. 1974; Kala et al. 1974; Barankina and Gromov 1973; Kala et al. 1976; Gromov et al. 1980; Suuroja et al. 1981; Suuroja et al. 1991; Suuroja et al. 1994; Suuroja et al. 1997). From 1967 to 1990 altogether about 160 drill cores were drilled in and around the Kärdla crater area, including the deepest (815.2 m) drill core K-1 (Soovälja) in Estonia (Põldvere 2002).

The Kärdla structure was at first called an explosion crater in mid-1970s (Puura 1974) and its post-Cambrian age was suggested (Pirrus 1976). Later biostratigraphic studies established its Middle Ordovician (Caradoc) age (Bauert et al. 1987; Grahn et al. 1996). The impact features (PDFs etc.) were first discovered by Masaitis et al. (1980) and Feldman et al. (1981). It was followed by the first overviews on morphology and development of the structure (Kala et al. 1984; Puura and Suuroja 1984), which were specified by studies on its development (Bauert et al. 1987) and formation (Puura et al. 1989). Alternatively, Zhukov et al. (1987) proposed the cryptovulcanic origin of the Kärdla structure. Kleesment et al. (1987) presented more detailed lithological and mineralogical characterization of the impact-related terrigenous sediments.

Puura and Suuroja (1992) presented detailed description of the structure and its impactites, while Lindström et al. (1992) suggested a hypothesis of Kärdla, Tvären and Lockne impact structures as possible coeval structures formed by a single Ordovician asteroid swarm. However, later biostratigraphic studies established slight age differences of these craters (Grahn et al. 1996). In 1994 Kärdla was presented as a good example of epicontinental marine impact structure, having a complete impact-related stratigraphic section from autochthonous breccias formed during the impact event up to allochthonous, slumped and fallback breccias from the crater modification stage (Puura et al. 1994). The long-term influence of the uplifted rim to the carbonate sedimentation in the area after the impact event was studied by M. Semidor (1998) and Ainsaar et al. (2002). The lithological studies of the ejecta layer showed that the long-term effect of the impact was restricted to local changes in the sea bed relief and related to facies changes in the nearest surroundings of the crater (Suuroja and Suuroja 2006).

The geophysical signatures and petrophysical properties of the Kärdla impactites, gravity and magnetic anomalies caused by the crater morphology, impact breccias and post-impact sedimentary fillings were investigated by J. Plado (1995; 2000) and Plado et al. (1996). U. Preeden (2004) showed, by the comparison of impact breccia matrix fine-grained fraction from Kärdla, Neugrund (9 km), Åvike (10 km) and Lumparn (9 km) craters to glacial moraine, that the fragmentation of target rocks by the crater-forming shock wave has resulted in similar grain-size distribution as the fragmentation by glacier dynamics. Koppelmaa et al. (1996) presented petrographical, mineralogical and geochemical data of the crystalline basement rocks (Paleoproterozoic migmatized metamorphic rocks and late-kinematic granites) in the Kärdla crater area, that were used for reference in several subsequent studies.

As a result of extensive drilling and geological mapping in the Hiiumaa Island the formation of the crater during the impact process through the stages of contact/compression, excavation, modification, generated tsunami and post-impact development (filling, burial, erosion, tectonic, and glacial effects) of the area was summarized by K. Suuroja (1996) and later enhanced by morphological and general geological studies by Suuroja et al. (2002). Detailed analyses on the occurrence of shock metamorphic features in impact breccias (S. Suuroja 1994) and spatial distribution of planar deformation features (PDFs) in quartz (Preeden 2002; Puura et al. 2004) were studied and lithological classification of the Kärdla impactites was presented (S. Suuroja 1999). A comprehensive report on mineralogical, chemical and biostratigraphy analyses, physical properties and petrological-lithological description of the deepest drill core K-1 was published in the special issue of the journal Estonian Geological Sections (Põldvere 2002).

In recent years the mixing-rate calculations, results on (shock)petrography studies and geochemical analyses of the Kärdla impactites and target rocks have been presented (Puura et al. 2004; Suuroja et al. 2002); as well as more detailed study on the changes in the impactites' chemical composition (enrichment in potassium, decrease in sodium and calcium) and mineralogy (replacement of plagioclase by orthoclase adularia, chloritization of amphibolites; Puura et al. 2000; Kirsimäe et al. 2002) has been performed. The impact-induced and diagenetic changes (PDFs and PFs in quartz, lowered crystallinity in cracked grains, C-rich amorphous material and pyrite-bearing apatite coatings) in mineral grains of the sandy ejecta layer were studied by Kleesment et al. (2006).

Based on the alteration of the fractured basement rocks and impactites, and fluid inclusion evidences a possible impact generated hydrothermal system at Kärdla was first described by Kirsimäe et al. (2002).

4. MATERIAL AND METHODS

Three drill cores (K-1, K-18 and K-12) from the interior of the Kärdla structure and three from the rim areas (at Paluküla; F-241, P-11 and P-17) penetrating into the disturbed and/or brecciated crater material were used in the study. The deepest drill core (K-1) reveals material from parautochthonous, autochthonous, allochthonous and resurge breccias reaching the depth of 815 m near the central uplift. The borehole K-18 provided material down to the upper part of allochthonous breccias from the central uplift and K-12 to the upper part of allochthonous breccias in the annular depression. The crater margin area at the NE rim was accessed to various depths into the brecciated basement rocks: down to 248 m in drill core F-241 (26.0–247.7 m), to 80 m in P-17 (50.6–80.5 m) and to 64 m in P-11 (26.6–55 m).

To describe the distribution, scale and spatial extent of the post-impact hydrothermal alteration the drill cores were logged, photographed and sampled. A total of 103 hand specimens were collected and macroscopically studied for the alteration petrology and mineralogy under the binocular microscope. Representative samples were further examined by X-ray diffractometry (XRD) to define vein minerals, and studied for stable isotopes ($\delta^{18}O$ and $\delta^{13}C$) composition of secondary dolomite and calcite (for the details see Versh et al. 2005, Publication I).

Together 111 thin sections from samples taken from different positions in the crater structure, including its inner and marginal parts were studied by light microscopy. The alteration changes in impactites' texture, mineralogical and geochemical composition were studied under the petrographical microscope to determine the IHT mineral paragenetic sequence. Selected thin sections were studied by means of electron microprobe (EPMA) for quantitative chemical analyses, element mapping and imaging (for details see Versh et al. 2005, Publication I).

5. RESULTS AND DISCUSSION

5.1. Mineralogical changes in the impactites

Mineralogical evidences of the IHT activity has been found at a number of terrestrial impact craters; mainly in a form of alteration of impactites (melt, suevites and impact breccias), and vein or fracture fillings. In terrestrial impact craters the alteration is represented by intermediate type of Ca- or K-alteration series (e.g., McCarville and Crossey 1996; Osinski et al. 2001; Naumov 2002; Osinski 2005; Hecht et al. 2004; Zürcher and Kring 2004; Puura et al. 2000). The assemblages of clay minerals — zeolites — calcite — pyrite are predominant alteration products (Naumov 2005). The high-to-medium temperature alumosilicate IHT mineralization stages are generally characterized by different silica modifications (quartz, cristobalite and opal); hydrous phyllosilicates (chlorites, illite, mixed-layer minerals, smectites); and tectosilicates (zeolites and K-feldspar; Naumov 2002; 2005). The low-temperature stage (<100°C) is mainly characterized by carbonate, sulfide, and/or Fe-oxyhydrate minerals. However, the formation of a specific mineral assemblage(s) in a given crater depends on large number of variables as impact target composition; magnitude of the heating and nature of the heat source (e.g., melt sheet, central uplift or crater rim); intensity of the water/rock interaction (i.e., water availability at the impact site); and IHT fluid chemical and physical parameters (incl. fluid kinetics).

In Kärdla impactites the IHT alteration occurs in the form of replacement-type mineralization of silicate-clay alteration, vein and vug mineral fillings, and impregnated mineralization of the fine-grained breccia matrix. It is expressed in alumosilicate — carbonate — (sulfide) mineral associations (Versh et al. 2005, Publication I), whereas commonly occurring zeolites (Naumov 2002 and references therein) are not present.

5.1.1. Replacement-type alteration of primary impactites

The most significant IHT modification in Kärdla impactites is associated with the replacement-type alumosilicate alteration of plagioclase and hornblende, the two prevailing minerals in the pre-impact crystalline basement (Versh et al. 2005, Publication I). In the granitic impactite-sequences authigenic submicroscopical adularia type K-feldspar masses (together with microscopic xenomorphous iron-rich clay material occasionally accompanied by Fe-oxyhydrate impregnation) completely or partly replace altered and fractured plagioclase crystals. Petrographic analyses indicate that the outer boundaries of the submicroscopic K-feldspar masses in some places have later been either partly recrystallized into or overgrown by the euhedral K-feldspar form.

In amphibolitic sequences hornblende, some biotite and rarely occurring pyroxene are replaced by authigenic clay minerals, adularia, Fe-oxyhydrate and/or authigenic quartz phases. The clay mineral phases are represented by trioctahedral Fe-rich chlorite, mixed-layered corrensite, and corrensite-chlorite minerals (Kirsimäe et al. 2002). The EPMA analyses revealed three chemically different chlorites: (1) Mg-clays; (2) Mg-Fe clays; and (3) Fe-clays, which probably represent the compositional variation in the chlorite — chlorite-corrensite — corrensite series (Versh et al. 2005, Publication I). In the fine-grained matrix of the suevitic allochthonous breccia (in allogenic sequence, as well as in the injection dikes in parautochthonous rocks) chlorite and/or corrensite replace both, amphibolite and devitrified glass or melt clasts. In the groundmass of the allochthonous and/or autochthonous breccias xenomorphous quartz, calcite or dolomite aggregates as pore/vug fillings (i.e., cement between rock and mineral clasts) can be found.

5.1.2. Vein- and vug-filling mineral assemblages

In Kärdla the hydrothermal vein minerals (i.e., mineral deposits sealing a fracture and altered wall rock; Meunier 1995) line walls of fractures produced by the impact, fill dissolution or impact-generated vugs and cement the rock and/or mineral clasts (Versh et al. 2005, Publication I). The earlier alumosilicate phase (coinciding with the alumosilicate alteration) and a later phase with carbonate — quartz — sulfide — (hydro)oxide mineral assemblages can be distinguished.

Paragenetically, the earliest, chlorite(-corrensite) veins occur as aggregates of microscopic, radially oriented euhedral flakes or irregularly stacked microscopic layers lining the fracture walls and cavities that are later filled with either adularia, carbonates or quartz. Next in the paragenetic sequence was euhedral adularia which crystals line the fracture systems or fill cavities later sealed by quartz, calcite and/or dolomite. Quartz and adularia also fill small vugs and pores between or within the rock clasts in the breccia matrix. In some cases their intergrowths are also visible. The spatial relationships and morphology of late-stage carbonate minerals reveal at least three different calcite generations and dolomite. The white to transparent or pinkish calcite aggregates, mainly in the form of the first (scalenohedral) and second (rhombohedral crystals) generations are usually found in the amphibolitic rocks where fractures are in most cases sealed by the calcite. In the granitic parts calcite fillings are less abundant and many fractures in the autochthonous breccia have remained open. Rarely the veins are filled with pink dolomite rhombohedral to saddle-shaped crystal aggregates. According to XRD and EPMA analysis the majority of calcite in Kärdla is a pure to low-magnesian calcite with 0–4 mole% of $MgCO_3$, whereas rarely high-magnesian calcites with 6 mole% of $MgCO_3$ occur (the third generation; Versh et al. 2005, Publication I). This is rather common to most of the IHT systems where calcite appears to be low-magnesian calcite with <5 wt% of $MgCO_3$; e.g., in Lappajärvi (Goldsmidt et al. 1955), Ries (Stöffler et al 1977), St. Martin (Simonds and McGee 1979), Zapadnaya (Tatarintsev et al. 1981), Sudbury (Ames 1999), Kara (Naumov 2002) and Chicxulub Structures (Zurcher and Kring 2004).

The Fe-oxyhydrates (hematite and goethite) and rare sulfides (mainly chalcopyrite) are mainly associated with carbonate filled fractures (i.e., veins) and cavities (i.e., vugs). Hematite occurs as abundant spherulitic aggregates intertwined with calcite. In some places <1 mm thick hematite veins inside fractured and altered amphibolitic basement rocks were also observed. On the surfaces of calcite and dolomite crystal aggregates small reddish-brown spherules or spherulitic aggregates of goethite, sparse <0.5 mm size tetrahedral single crystals or small aggregates of chalcopyrite, and bipyramidal hexagonal prisms of authigenic quartz (colorless, transparent and with no visible inclusions) crystals were observed. The xenomorphous quartz, calcite or dolomite aggregates as pore/vug fillings (i.e., cement between rock and mineral clasts) in the groundmass of the allochthonous and/or autochthonous breccias is also evident.

5.1.3. K-enrichment

The impactites in Kärdla are characterized by major mineralogical and chemical changes with respect to the crystalline basement rocks outside of the crater (Puura and Suuroja 1992; Puura et al. 2000; Koppelmaa et al. 1996). This phenomenon (enrichment in potassium and respective decrease in calcium and/or sodium) has been documented in several impact craters with similar crystalline and/or sedimentary target lithologies: e.g., in Ames (Koeberl et al. 2001), Beaverhead (Fiske et al. 1994), Boltysh (Masaitis et al. 1980; Gurov et al. 1986), Brent (Grive 1978), Chicxulub (Hecht et al. 2004; Zürcher and Kring 2004), Gardnos (French et al. 1997), Gosses Bluff (Milton and Sutter 1987), Ilynets (Gurov et al. 1998), Jänisjärvi (Masaitis et al. 1980), Kaluga (Masaitis et al. 1980), Neugrund (Suuroja and Suuroja 2000; 2004), Newport (Koeberl and Reimold 1995) and Rochechouart (Oskierski and Bischoff 1983; Reimold et al. 1984).

The K-enrichment in impactites can be explained as K-metasomatosis, which is a process by which the chemical composition of a rock, in respect to potassium, is changed by interaction with fluids. In the Kärdla impactites it is mineralogically expressed primarily by two generations of authigenic adularia (K-feldspar): (1) submicroscopic masses intertwined with clay material; and (2) microscopic- to macroscopic crystal euhedral aggregates (see chapters 5.1.1 and 5.1.2; Puura et al. 2000). According to geochemical and XRD analyses, the two generations have no significant chemical or structural differences (Versh et al. 2005, Publication I). New K-feldspar is structurally a single monoclinic adularia type orthoclase with strained lattice parameters which are intermediate between typical orthoclase and low microcline, but that are rather stable through the sequence. The pre-impact K-feldspar from crystalline basement is a maximum triclinic microcline that can also be found as relicts in the altered samples.

The origin and high abundance of adularia in the Kärdla impactites is somewhat unclear. Paragenetic relationships indicate that it (the first generation) was one of the first mineral phases forming in the IHT-system and it is evidently related to the hydrothermal alteration (chapter 5.1.1). However, the adularia precipitation and/or recrystallization continued at later stages of the impact cooling (second generation) and it cannot be excluded that feldspathization of impactites occurred also during the post-impact geological development of the structure. It is not possible to determine the lower stability limit for the authigenic K-feldspar as it can form during devitrification of rock (volcanic and possibly impact) glasses at moderate to low diagenetic temperatures (Kastner and Siever 1979). Moreover, authigenic monoclinic adularia type orthoclase K-feldspar in the Kärdla impactites is a typical representative of secondary low temperature feldspars which are exclusively the extreme pure end-members of the alkali feldspar series showing various degrees of structural Al/Si ordering from low-triclinic to disordered monoclinic (Kastner and Siever 1979; Worden and Rushton 1992).

Kärdla impactites are notably devoid of zeolite minerals, which are frequently reported in the IHT-systems (Naumov 2002 and references therein). However, the zeolites are thermodynamically metastable phases, which tend to recrystallize into stable feldspar minerals. This would explain the controversy that zeolites are not common in the IHT mineralization in old (>150–200 Ma) structures (e.g., Naumov 2005).

5.2. The IHT alteration development in space and time

5.2.1. Intensity and the extent of the alteration

Water availability in the target area is a primary control on the intensity of the water-rock interaction during the impact cooling. Consequently, the most extensive IHT alteration takes place in the impact craters formed into ocean, shelf or intra-continental shallow marine/lake basin. The studied Kärdla crater represents a shallow shelf sea impact (~100 m of water-depth) and the IHT system was mainly fed by seawater intruding through the disturbed and fractured basement. The resulting mineralogical-geochemical changes are characteristic of high-to-medium water-rock alteration (Naumov 2005); its intensity (i.e., abundance of the authigenic phases) depends on the distance from the heat source.

As in some other impact structures (e.g., Puchezh-Katunki and Manson; Naumov 2002; McCarville and Crossey 1996) vertical and lateral zones of different IHT alteration types in the Kärdla structure can be distinguished. However, the absence of coherent melt sheet (in the annular depression) and zeolites in IHT mineral assemblages (in the central uplift) resulted in somewhat dissimilar IHT assemblages of the main zones' mineral types. Also, the distribution of major oxides and alkali in Kärdla differs from those outlined by Naumov (2005; see chapters 5.2.2 and 5.2.3). In the central (uplift) area of the Puchezh-Katunki, Ries, Boltysh and Siljan structures (Naumov 2002; 2005; and references therein) upper smectite-zeolite and lower chlorite-anhydrite zones have been described wherein several subzones (by Ca/Na and Al/Si ratio in zeolites and high-alumina Mg-Fe varieties of smectites) are distinguished. Equally, based on XRD and microprobe studies on altered amphibolite rock samples in Kärdla (Kirsimäe et al. 2002) one can distinguish an upper chlorite-adularia zone (with maximum generation temperatures of 200–300ºC and higher) and lower corrensite-calcite zone (max. <200 ºC). At the location of 450 m from the crater centre (drill core K-1) the transition between the two zones is quite sharp and lies between fractured and strongly fractured basement rocks at the depth of 590 m; whereas more close to the centre, at the distance of 250 m (drill core K-18) the transition is more gradual and located near the border of the allochthonous and autochthonous breccias (approximately at the depth of 400 m). The authigenic quartz is more or less equally distributed in both zones; however, the general decrease of fracturing and hydrothermal alteration with depth limits its occurrence in the lower zone.

Likewise, the IHT alteration types in the periphery of the central uplift (the annular depression; drill core K-12) are somewhat distinct from those at the central uplift. The distribution of a widespread goethite-hematite impregnation marks distinctive zones with the transition at the depth around 442 m within the upper allochthonous breccias: (1) an upper hematized zone represented mainly in the resurge and slumped breccia with purple matrix; and (2) lower adularia-chlorite zone in the allochthonous breccia with green to gray matrix. At the crater rim the low-temperature IHT minerals dominate. Also, in the IHT chlorite to corrensite series a spatial (both vertical and lateral) decrease of iron (and increase of Mg) from upper central area in depth and towards the rim wall was detected: (1) Fe-clays in the upper central uplift area (in a suevitic breccia lens in the slumped breccia); (2) Fe-Mg clays in the lower central area and the rim wall (near the border of the allochthonous and autochthonous breccia and the fractured basement, the allochthonous breccia lens in post-impact sediments; respectively); and (3) Mg clays in the rim wall (allochthonous breccia lens in the post-impact sediments).

Generally, the hydrothermal alteration in the Kärdla crater is rare or absent in the resurge and sedimentary slump breccias, respectively, but abundant in the allochthonous and autochthonous breccias, whereas the intensity of the alteration decreases with the depth. The alteration is most widespread and complete in the upper portion of the allochthonous breccias within and around the central uplift where the silicate-clay alteration is dominant. In this area almost all hornblende and plagioclase along with the impact glass is replaced mainly by clay (chlorite/corrensite) and K-feldspar minerals. The alteration zones reach progressively outwards from the fractures into the host rock, and up to one-third of the plagioclase and hornblende volume is replaced with the authigenic minerals. The variation in alteration intensity is reflected by the style of the alteration, which changes from open-space fracture fillings to more replacement-type mineralization from the rim walls and deeper parts of the crater towards the upper-central areas.

The fracture-limited fluid-rock interaction occurs at the rim and in the deeper central areas of the crater depression. At the rim wall, hydrothermal alteration is localized along the fractures and impact-injected breccia lenses, where the carbonate and sulfide/Fe-oxyhydrate assemblages dominate over the authigenic feldspar–chlorite–quartz minerals. The occurrence of plagioclase K-alteration and hornblende chloritization is restricted to fracture planes and grain boundaries within the breccia lenses. At the rim some goethite spherules are partly inter-grown with calcite crystals outer boundaries indicating their simultaneous precipitation.

5.2.2. The evolutionary stages and lifetime of the IHT system

The mineral paragenetic associations with fluid inclusion, geothermobarometric (Kirsimäe et al. 2002) and stable isotope (Versh et al. 2005, Publication I) studies indicate the existence of three evolutionary stages of the IHT system that describe the post-impact cooling of the Kärdla impact structure from the early feldspar — chlorite — quartz to late carbonate and Fe-oxyhydrate stage. Based on mineral associations and the dominant fluid environment regimes, we can distinguish: (1) early stage of vapour-dominated silicate alteration, (2) the middle stage of vapour- to liquid-dominated silicate mineralization, and (3) the late stage of liquid-dominated carbonate — sulfide/Fe –oxyhydrate — quartz mineralization.

The homogenization temperatures of quartz fluid inclusions indicate that during the first evolutionary stage directly after the crater formation the maximum temperatures were as high as 400–500°C; whereas the majority of inclusions were trapped at fluid temperatures of 150 to 300 ºC (Kirsimäe et al. 2002). The latter temperature interval is also indicated by corrensite-chlorite geothermometry of the widespread Fe-chloritization in amphibolitic impact-sequences with maximum equilibrium temperatures in the upper portion of impactite sequence of 200–300°C, whereas chloritization intensity was found to decrease with decreasing fracturing downward into the crater floor where chlorite occurs only in immediate proximity of the fracture planes and corrensite prevails within macroscopically unaltered amphibolite blocks, indicating maximum temperatures below 200°C (Kirsimäe et al. 2002). As microcrystalline adularia was the first mineral to form, it must have precipitated from fluids with temperature higher than those of clay minerals, i.e. above 300 ºC during a vapor-dominated early stage of the IHT silicate (potassium) alteration.

The mineralogical data are in good accordance with the transient fluid flow and heat transfer simulations (Jõeleht et al. 2005, Publication II), which show that immediately after the impact the initial temperatures in the central area of the structure were well above the boiling point (>350°C; Fig. 2.a). The vapor-dominated fluid during the first stage of the impact cooling is supported by submicroscopical structure of the adularia, which suggests kinetically controlled and a rapid crystal growth at a large number of simultaneously formed nucleation sites.

Due to efficient heat loss at groundwater vaporization front the vapor-dominated area disappeared quickly (in few tens to hundreds of years; Fig. 2.b, c) and progressive cooling of the system resulted in a transition to mixed two-phase vapor-liquid dominated fluid at temperatures 300–150(100)ºC. This second stage is associated with the most intensive chloritization, followed by precipitation of euhedral microcrystalline adularia (Ksp II) and quartz in remaining fractures and cavities.

The third stage of mineralization took place in liquid fluid environment with temperatures below 100 ºC by precipitation of mainly carbonate minerals (with minor Fe-oxyhydrates, sulfides and low-temperature silicates) into open vugs and fractures. The third generation of calcite was the last mineral precipitated in this system, probably at temperatures close to ambient conditions (Versh et al. 2005, Publication I). The minimum temperature of the IHT solution may be somewhat arbitrary and is limited by kinetic effects of water-rock interaction. As the temperature is lower, close to the areas thermal gradient, any reaction between rock and solution proceeds more slowly and therefore the production of secondary minerals is hard to recognize in the rocks during short periods of interaction (Inoue 1995).

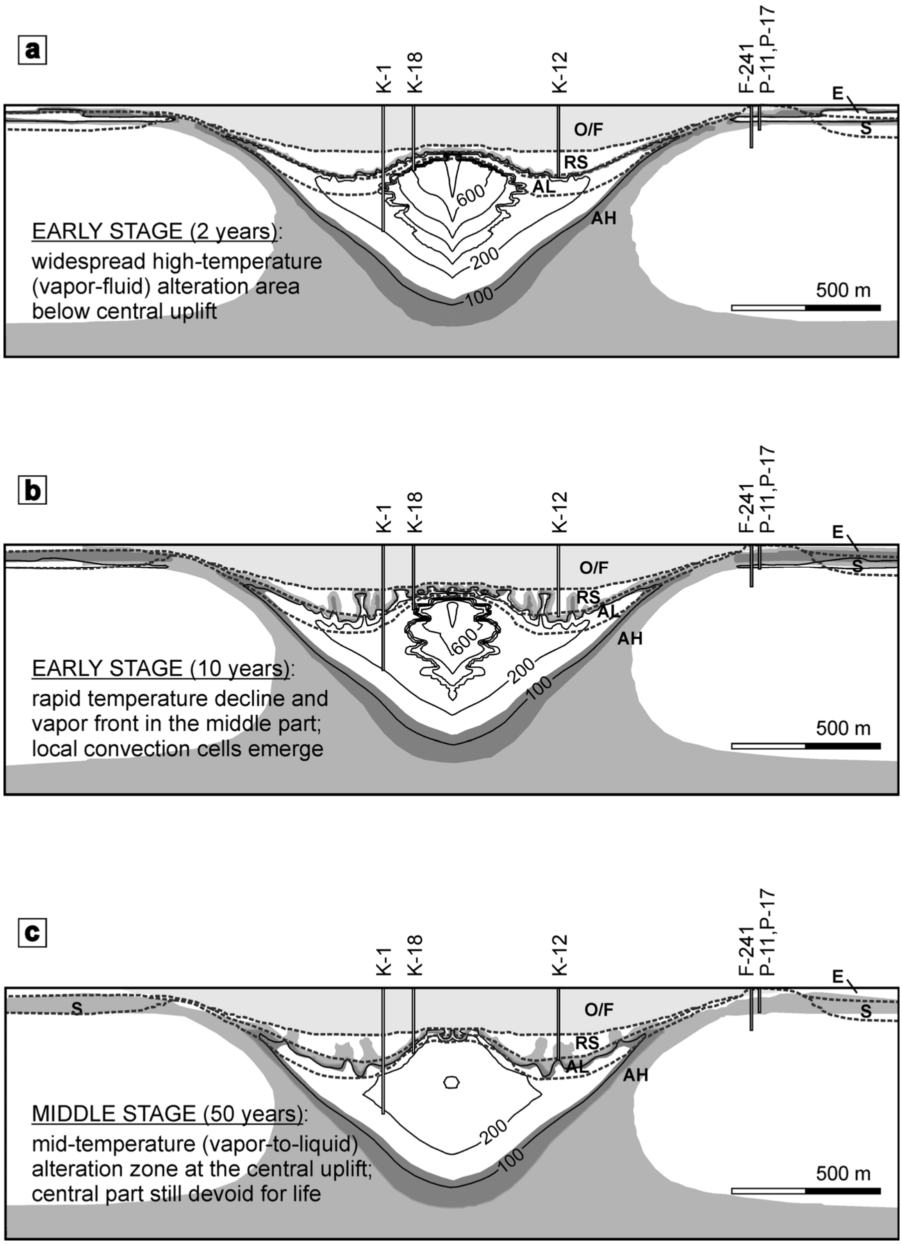

Figure 2. The evolution of the IHT system in the Kärdla impact structure. The numerical modeling isotherms after every 100ºC (d and e after ever 50ºC) and location of studied drill cores are given. The dark gray area represents temperature interval 120–80ºC (habitable zone for hyperthermophiles) and lighter gray 80–45 ºC (habitable zone for thermophiles). AH — (par)autochthonous breccia and fractured basement; AL – allochthonous breccia; RS — resurge and slumped breccia; S — pre-impact sediments; O/F — Ordovician sea/crater-filling sediments; E — ejected material.

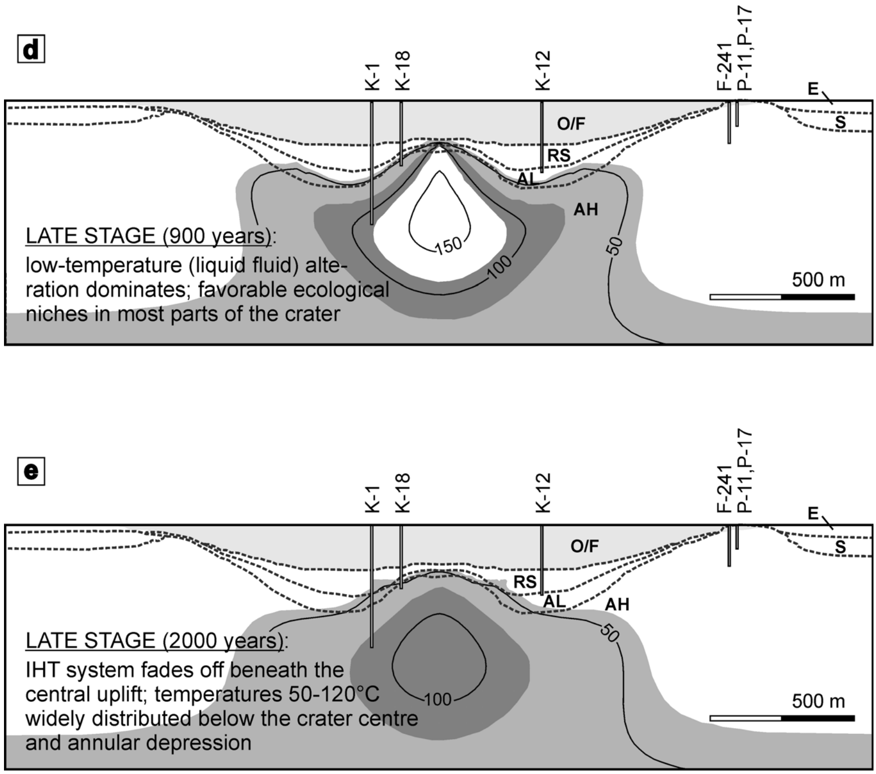

Figure 2. Continued

5.2.3. Composition and development of IHT fluids

The chemical composition of an IHT fluid depends upon the composition of crystalline or sedimentary rocks present at the impact site as well as on the fluid source. Utada (1980) divided the hydrothermal alteration in young orogenic belts into three types by the temperature and activity ratio of aqueous cation species in the hydrothermal solution: (1) acid type alteration with low cation/hydrogen ratios in the solution; (2) intermediate alteration subdivided into Ca-Mg-series and K-series with medium cation/hydrogen ratios; and (3) alkaline type subdivided into Na- and Ca-series with high cation/hydrogen ratios. Each alteration type includes mineral zones corresponding to different fluid temperature conditions.

In this sense a typical IHT mineralization corresponds most closely to the alkaline (e.g., Naumov 2002) and/or intermediate (e.g., Hecht et al. 2004; Zürcher and Kring 2004) type of the HT alteration, whereas the presence of Na-Ca, Ca-Mg or K-series depends most possibly on the specifics of an impact: target rock composition (granitic or maffic), size, i.e., magnitude of heating (removal of volatiles), as well as on the nature of the IHT fluids (saline brines, seawater, undersaturated fresh-water resources etc). The mineralogical characteristics of the IHT alteration in Kärdla correspond to the K-series during the first two stages, which then evolves into Ca-Mg-series during the last stage of the impact cooling. The rather low salinity of the secondary fluid inclusions in quartz from Kärdla crater (in average ≤5 wt% $NaCl_{eq}$; Kirsimäe et al. 2002) suggests that the hydrothermal system was recharged by infiltration of relatively undersaturated water, which was highly reactive towards the main rock-forming silicate minerals. As the K-feldspar nucleation and stability is primarily controlled by the variation in pH and dissolved silica activity (Garrels and Christ 1965; Velde 1985), the rapid precipitation of K-feldspar during the first stage of the impact cooling suggests rather high pH (≥8) of the circulating fluid. This is possibly related to the effective removal of evolved gas and strong reactivity of high-temperature solutions with the surrounding rocks, which efficiently consumed the available H^+ ions through anion hydrolysis of primary silicates. At later stages the pH of initial fluid was lowered, but remained high enough (>7) to promote the II type of K-feldspar and carbonate mineral precipitation.

Owing to the interactions of alumosilicate minerals and water the IHT fluid at Kärdla became gradually enriched respect to Ca and Mg at last stages of cooling. Ca and Mg were most probably released by hydrothermal chloritization of amphibole minerals during the second stage of alteration and in addition by the transformation of plagioclase into K-feldspar. The subsequent precipitation of calcite/dolomite was controlled by the availability of Ca and Mg ions in the convecting fluids, as the formation of either calcite or dolomite depends on Ca/Mg ratio in the solutions (Reeder 1983). The sequence of carbonate mineral precipitation suggests that calcite I (first generation) formed in a solution supersaturated with respect to calcite, which resulted in an efficient removal of Ca from the solution, thus, allowing the precipitation of dolomite as the next carbonate phase. Conditions favorable for calcite II precipitation were achieved after Mg removal by dolomite formation. The calcite II generation has abnormally shifted lattice parameters, which suggest involvement of Mn or Fe. The formation of calcite II was followed by precipitation of sulfides and Fe-oxyhydrates, probably at the expense of Fe released by hornblende chloritization. In places, goethite spherule intergrowth with calcite I scalenohedral crystals suggests that occasionally the goethite precipitation started shortly before the calcite I ended. Calcite III was the last mineral precipitated in this system, probably at the temperatures close to ambient conditions (Versh et al. 2005, Publication I).

The IHT mineralization at Kärdla suggest that unlike in the volcanic HT environments that are generally low in oxygen and rich in reductants, the impact-induced systems seem to be more rich in dissolved oxygen, but not necessarily oxidative, and low in reduced compounds. Sulfides, although present in the altered Kärdla impactites, are not dominant mineral phases (Versh et al. in press, Publication III).

5.3. Biological implications of impact-induced hydrothermal systems

The role of meteorite impacts in the biological evolution is controversial — large-scale impacts can cause extinctions of different scale and global and local disturbances in the development of some ecosystems, but by this also create opportunities for other organisms or new dissimilar ecosystems. Impact heating and the super-high pressures wipe out all living matter at the immediate vicinity of the impact site, and in large-scale impacts, the biological devastation may obtain a global scale. On the other hand, the cooling impact structures may have deserved as suitable ecological niches for life (e.g., Cockell and Lee 2002; Cockell et al. 2002). The impact-induced hydrothermal systems may host the thermophilic and/or hyperthermophilic microorganisms that are interesting to study in respect to exobiological perspectives. Also, the study of IHT systems may contribute to the understanding of early life on the Archean Earth (Mojzsis and Harrison 2000).

The results of transient fluid flow and heat transfer simulations both in small and large scales structures (Jõeleht et al. 2005, Publication II; Abramov and Kring 2004) suggest that the central areas of the crater, in and around the central uplift, are not habitable immediately after the impact. In small-to-medium sized craters with insignificant melting, the temperatures in the central area are well above the boiling point (250–290°C, depending on hydrostatic pressure) and a vapor-dominated area forms (Jõeleht et al. 2005, Publication II). In large impact structures the central peak-ring and peak-ring depression are filled with impact melt and/or melt-rich breccias and target rocks and impactites suffer from effective heat sterilization in large rock-volumes. However, in small-scale structures, due to efficient heat removal at the liquid/vapor front, the superheated area diminishes rapidly in order of few hundred years, whereas in the crater depression and the rim area the initial temperatures predicted by impact modeling are much lower — from 150°C to the ambient temperatures at the outer rim. Under these circumstances the conditions favorable for thermophilic microorganisms (temperatures below 100°C) are reached in less than 500–1000 years in most areas of the crater (Figure 2). Moreover, in these impact structures the organisms, that survived the impact and heat sterilization, are readily present in the environment and capable to colonize the system in a short time after the impact. Simulated impact experiments suggest that the bacteria spores (*Bacillus subtilis*) survive the pressures of 32 GPa and temperatures peaked at 250°C (Horneck et al. 2001). In the small-scale impacts like the Kärdla these conditions are met only in the very central areas.

The suitable zones for hyperthermophilic (80–120°C) and thermophilic (45–80°C) organisms change significantly in space and volume with the time. As a general consequence, independently of size, structure and lifetime of IHTs, the volume of space that is habitable for hydrothermal microbial communities (temperature range 45–120°C) grows rapidly during the first period of the cooling, but then fades off with the gradual decrease and deepening of the habitable zone(-s) towards the crater centre. In small-scale structures the cooling of the rim is quite fast as is demonstrated in Versh et al. in press, Publication III, figure 3, but in large structures with coherent and extensive melt sheet in the rim area the IHTs are initiated and stay there until the melt sheet has cooled down to 350–400°C and the hydrothermal circulation in the crater centre can start. Although in the central uplift region the possible microbial colonization is inhibited for about a thousand years, this is the rock body, which retains the optimum temperatures (45–80°C) needed for thermophiles and/or hyperthermophiles (80–107°C) for the longest period. The thermal equilibration of the whole impact takes much longer time. Even though the maximum temperature disturbance after 10,000 years is only about 190°C, the heat flow density is two times higher than in the surrounding areas.

The structure of the possible microbial community at a particular IHT system is primarily defined by the environmental conditions depending on the temperature and geochemical characteristics of the fluid (fluid-rock interaction) within the system, but also the circumstances of photosynthesis. In terrestrial hydrotherms (hot springs) thermophilic photoautotrophs predominate over other groups, whereas at deep-sea hydrothermal vents, the chemosynthetic (chemolithoautotrophic) groups are using the energy from the interaction of reduced compounds in the hydrothermal fluid (sulphur, iron etc.) and surrounding oxidized seawater (Van Dover 2000). The IHT systems differ from most of the known volcanic (both terrestrial and deep-sea) hydrotherms in many aspects — by the temperature history, fluid flow characteristics and chemistry, size etc. As an example, at the large craters the IHT systems that are volumetrically an order of magnitude larger, compared to volcanic hydrotherms, can be generated (Abramov and Kring 2004).

As discussed above (see chapters 5.1. and 5.2.), the mineral assemblages and geochemical characteristics of the hydrothermal minerals in the IHT systems suggest alkaline and near neutral environments (pH 6–8) as the result of anion-hydrolysis of the mainly alumosilicate composition rocks and impact derived impact-melts/glasses. Also, the solution maintains Eh values above -0.5 V (at least for a neutral environment) in the course of the hydrothermal process indicated by the presence of sulfide and rare Fe-oxide minerals.

These constrained environmental variables suggest some limitation/specification among possible thermophilic and/or hyperthermophilic microorganisms that could potentially colonize the system. If most of the Archaea and Bacteria are neutrophiles and can easily grow in the very slightly acidic-alkaline pH range (6–8) of the impact-induced environment, then unlike the volcanic environments that are generally low in oxygen and rich in reductants (Barns and Nierzwicki-Bauer 1997), the impact-induced systems seem to be richer in dissolved oxygen, but not necessarily oxidative, and low in reduced compounds. This would suggest the preference of sulphur-reducing microorganisms in the

IHT communities, whereas many sulphate reducers are also able to use the molecular H_2, on which rely most of the chemolithotropic reactions used by microorganisms in hydrothermal vents (McCollom and Schock 1997).

At the same time, the microorganisms in impact-induced hydrotherms cannot be/have been very highly specialized as far as these hydrotherms, especially in small-scale craters, change rapidly in the space and environmental quality. The space habitable for the most primitive hydrothermal microbial communities (temperature range 45–120°C) grows rapidly during the first period of the impact cooling reaching the maximum in some thousand years and then fades off in few tens of thousands years with the gradual decrease and deepening of the habitable zone(-s) towards the crater centre (Figure 2). This implies that the potential habitats in IHT systems would be occupied by organisms capable adapting to the changing conditions by applying alternative metabolic processes.

Post-impact environmental recovery of the craters' intra- and outer space offers possibilities for microbiota and metazoa to invade and (re-)colonize new, dissimilar ecological niches — crater lakes or disturbed surface and subsurface areas (Cockell et al. 2002; Kring 2000a; 200b; Versh et al. in press, Publication III). However, so far no approved evidence for life at IHT systems has been found which can be a result of the complicated recognition of ancient microorganism activity and lack of detailed microbiological studies.

CONCLUSIONS

In the Kärdla structure the development of impact-induced hydrothermal (IHT) chemical and mineralogical alteration of impactites and physical-chemical conditions of convective fluids were studied. The mineralogical, geochemical and stable isotope studies suggest three different stages of the evolving IHT system, characterized by different fluid-state conditions, temperature, alteration type and mineral phases. The system represents a single thermal event with irreversible cooling path. The alteration of impactites was pervasive in the upper central area, i.e., in the vicinity of the central uplift. At the rim and in the deeper central portion of the crater depression it was confined to fracture limited fluid-rock interaction. The IHT system studied at the Kärdla structure can therefore be considered as a model for medium-to-small size impact structures. Regardless of the absence of a thick melt sheet in Kärdla a spatial IHT zoning pattern is still visible.

Mineralogically the earliest phases of the IHT development are characterized by alumosilicate alteration of pre-impact minerals plagioclase and hornblende. The authigenic euhedral to submicroscopic adularia, chlorite and quartz formed during the early vapor- and middle vapor-to-liquid stages. According to geothermal modeling immediately after the crater modification stage had ended, temperatures in the central part of the crater reached well above the boiling point (>350°C). As the chloritization of hornblende took place at temperatures 300 to 150(100)°C (Kirsimäe et al. 2002) the earlier plagioclase/adularia alteration occurred at more elevated temperatures. At the crater rim the alteration was localized along fractures and impact-injected breccia lenses. Here, the late (<100°C, low-temperature) stage carbonate and sulfide/Fe-oxyhydrate assemblages dominate over authigenic feldspar — chlorite — quartz minerals.

The alteration from the first two stages in Kärdla corresponds to the K-series, which then evolved into Ca-Mg-series during the last stage of the impact cooling. According to geochemical and mineralogical data the environmental conditions in terrestrial IHT systems vary within a narrow interval of pH 6–8 as a result of anion hydrolysis of mainly alumosilicate target rocks and impact-derived impact melts/glasses. Compared to volcanic hydrotherms they are apparently richer in dissolved oxygen, but not necessarily oxidative, and low in reduced compounds.

Like hydrothermal systems generated by endogenic processes, the IHT systems can create potential ecological niches for high-temperature microbial organisms. The latter may represent interest in the context of early life and astrobiological studies.

In most parts of the Kärdla crater the suitable conditions for hydrothermal microbial communities were established shortly (tens to few hundreds of years as maximum) after the impact. In the most heated and at first inhabitable central uplift area the conditions favorable for thermophilic microorganisms (temperatures below 120 ºC) were reached in 500–1000 years after the impact. The overall cooling to ambient temperatures in the deeper parts of the central uplift lasted for thousands of years.

Environmental characteristics of IHT fluids suggest a preference for sulfur reducing microorganisms in the possible IHT communities. However, the potential habitats created in IHT systems could be occupied by organisms capable of adapting to the changing conditions by applying alternative metabolic processes.

REFERENCES

Abramov O. and Kring D. A. 2004. Numerical modeling of an impact-induced hydrothermal system at the Sudbury crater. *Journal of Geophysical Research* 109: E10007.

Ainsaar L., Suuroja K. and Semidor M. 2002. Long-term effects of the Kärdla crater (Hiiumaa, Estonia) on Late Ordovician carbonate sedimentation. *Deep-Sea Research II* 49(6): 1145–1155.

Allen C. G., Gooding J. L. and Keil K. 1982. Hydrothermally altered impact melt rock and breccia: Contributions to the soil of Mars. *Journal of Geophysical Research* 87: 10083–10101.

Ames D. E. 1999. *Geology and regional hydrothermal alteration of the crater-fill Onaping Formation: Association with Zn-Pb-Cu mineralization, Sudbury Structure, Canada.* Ph. D. Thesis. Carleton University, Ottawa, Canada, 460 pp.

Ames D. E., Watkinson D. H. and Parrish R. R. 1998. Dating of a hydrothermal system induced by the 1850 Ma Sudbury impact event. *Geology* 26: 447–450.

Barankina I. F and Gromov O. B. 1973. *Preliminary results of granite building stone exploration in the Paluküla structure area (Hiiumaa Island, Estonia) in 1972*. Geological Survey of Estonia, Tallinn, Report No. 3261. (in Russian)

Barns S. M., Nierzwicki-Bauer S. A. 1997. Microbial diversity in ocean, surface and subsurface environments. In: J. F. Banfield, K. H. Nealson (Eds.). *Geomicrobiology: Interactions Between Microbes and Minerals.* Reviews in Mineralogy, Vol. 35. Mineralogical Society of America, Washington DC, pp. 35–79.

Bauert H. A, Männil R. M. and Suuroja K. A. 1987. On the age of the Kärdla crater. *Abstracts of the 48th All-Soviet Meteoritic Conference*. Estonian Academy of Sciences. (in Russian)

Cockell C. S. and Lee, P. 2002. The biology of impact craters — a review. *Biological Reviews* 77: 279–310.

Cockell C. S., Lee P., Osinski G., Horneck G. and Broady P. 2002. Impactinduced microbial endolithic habitats. *Meteoritics & Planetary Science* 37: 1287–1298.

Feldman V. I, Granovski L. B. and Dabisha F.I. (eds.) 1981. *Impactites*. University of Moscow, Moscow, 240. (in Russian)

Fiske P. S., Hargraves R. B., Onstott T. C., Koeberl C. and Hougen S. B. 1994. Pseudotachylites of the Beaverhead impact structure: Geochemical, geochronological, petrographic, and field investigations. In: B. Dressler, R. A. F. Grieve, V. L. Sharpton (Eds.). *Large Meteorite Impacts and Planetary Evolution.* Geological Society of America Special Paper 293: 163–176.

French B. M., Koeberl C., Gilmour J., Shirey S. B., Dons J. A., Naterstad J. 1997. The Gardnos impact structure: petrology and geochemistry of target rocks and impactites. *Geochimica et Cosmohimica Acta* 61: 873–904.

Garrels R. M. and J. C. Christ. 1965. *Solutions, minerals, and equilibria*. San Francisco, Freeman, Cooper.

Goldsmidt J. R., Graf D. L. and Joensuu O. I. 1955. The occurrence of magnesian calcites in nature. *Geochimica et Cosmochimica Acta* 7: 212–230.

Gorbatchev R. and Bogdanova S. 1993. Frontiers in the Baltic Shield. *Precambrian Research* 64: 3–21.

Grahn Y., Nõlvak J. and Paris F. 1996. Precise chitinozoan dating of Ordovician impact events in Baltoscandia. *Journal of Micropalaentology* 15: 21–35.

Grive R. A. F. 1978. The petrochemistry of the melt rocks at Brent crater and their implication for the condition of impact. *Meteoritics* 13: 484–487.

Gromov O. B., Gromova G. A. and Fokin A. M. 1980. *Report on results of preliminary geophysical mapping for area of subsurface mapping on Island of Hiiumaa*. Geological Survey of Estonia, Tallinn, Report No. 3720, 95 p. (in Russian)

Gurov E. P., Kolesov G. M. and Gurova E. P. 1986. Composition of impactites of the Boltysh astrobleme. *Meteoritika* 45: 150–155. (in Russian)

Gurov E. P., Koeberl C., and Reimold W. U. 1998. Petrography and geochemistry of target rocks and impactites from the Ilynets Crater, Ukraine. *Meteoritics & Planetary Science* 33: 1317–1333.

Hagerty J. J. and Newsom H. E. 2003. Hydrothermal alteration at the Lonar Lake impact structure, India: Implications for impact cratering on Mars. *Meteoritics & Planetary Science* 38: 365–381.

Hecht L., Wittmann A., Schmitt R. T. & Stöffler D. 2004. Chemical composition of impact melts and the effects of post impact alteration in suevitic rocks at the YAX-1 drill core, Chicxulub crater, Mexico. *Meteoritics and Planetary Science* 39: 1169–1187.

Horneck G., Stöffler D., Eschweiler U., Hornemann U. 2001. Bacterial spores survive simulated meteorite impact. *Icarus* 149: 285–290.

Inoue A. 1995. Formation of clay minerals in hydrothermal environments. In: B. Velde (Ed.). *Origin and mineralogy of clays. Clays and the environment.* Springer Verlag, Berlin, Heidleberg, pp. 269–329.

Jõeleht A., Kirsimäe K., Shogenova A., Shliaupa S., Kukkonen I. T., Rasteiniene V. and Zabele A. 2002. Thermal conductivity of Cambrian siliciclastic rocks from the Baltic basin. *Proceedings of the Estonian Academy of Sciences. Geology* 51: 5–15.

Jõeleht A., Kirsimäe K., Plado J., Versh E. and Ivanov B. 2005. Cooling of the Kärdla impact crater: II. Impact and geothermal modeling. *Meteoritics & Planetary Science* 40: 20–32.

Kala E., Kajak K., Kajak H. and Elterman G. 1971. *Geological-hydrological complex mapping in scale 1:200 000 in Hiiumaa Island (sheet 0-34-XI)*. Geological Survey of Estonia, Tallinn, Report No. 3146, 624 p. (in Russian)

Kala E., Suuroja K. and Petersell V. 1974. *Geological description and technological-economical expertise of granitoids at Paluküla*. Geological Survey of Estonia, Tallinn, Report No. 3295, 50 p. (in Russian)

Kala E., Suuroja K. and Tassa V. 1976. *Preliminary exploration report of Paluküla granitoids*. Geological Survey of Estonia, Tallinn, Report No. 3379, 94 p. (in Russian)

Kala E., Puura V. and Suuroja K. 1984. The main signatures of the buried Kärdla crater. Proceedings of the Estonian Academy of Sciences. *Geology* 1: 1–7. (in Russian)

Kastner M. and Siever R. 1979. Low temperature feldspars in sedimentary rocks. *American Journal of Science* 279: 435–479.

Kirsimäe K., Suuroja S., Kirs J., Kärki A., Polikarpus M., Puura V. and Suuroja K. 2002. Hornblende alteration and fluid inclusions in Kärdla impact crater, Estonia: Evidence for impact-induced hydrothermal activity. *Meteoritics & Planetary Science* 37: 449–457.

Kleesment A., Pirrus E., Suuroja K and Tiirmaa R. 1987. The outer rim-wall geology of the buried Kärdla crater. *Proceedings of the Estonian Academy of Sciences. Geology* 36: 131–139. (in Russian)

Kleesment A., Konsa M., Puura V., Karhu J., Preeden U. and Kallaste T. 2006. Impact-induced and diagenetic changes in minerals in the sandy ejecta of the Kärdla crater, NW Estonia. *Proceedings of the Estonian Academy of Sciences, Geology* 55 (3): 189–212.

Koeberl C. and Reimold W. U. 1995. The Newport impact structure, North Dakota, USA. *Geochimica et Cosmochimica Acta* 59: 4745–4767.

Koeberl C., Fredriksson K., Götzinger M. and Reimold W. U. 1989. Anomalous quartz from the Roter Kamm impact crater, Namibia: Evidence for post-impact activity? *Geochimica et Cosmochimica Acta* 53: 2113–2118.

Koeberl C., Reimold W. U. and Kelley S. P. 2001. Petrography, geochemistry, and 40Ar/39Ar ages of impact melt rocks and breccias from the Ames impact structure, Oklahoma: The Nicor Chestnut 18-4 drill core. *Meteoritics and Planetary Science* 36: 651–669.

Koppelmaa H., Niin M. and Kivisilla J. 1996. About petrography and mineralogy of the crystalline basement rocks in the Kärdla crater area, Hiiumaa Island, Estonia. *Bulletin of the Geological Survey of Estonia* 6(1): 4–24.

Kring D. A. 2000a. Impact events and their effect on the origin, evolution, and distribution of life. *GSA Today* 10(8): 1–7.

Kring D. A. 2000b. Impact-induced hydrothermal activity and potential habitats for thermophilic and hyperthermophilic life. In: *Catastrophic Events & Mass Extinctions: Impacts and Beyond.* LPI meeting in July 9–12, 2000, Vienna, Austria Abstract Book, LPI Contribution No. 1053, Lunar and Planetary Institute, Houston, 106–107.

Lindström M., Floden T., Puura V. and Suuroja K. 1992. The Kärdla, Tvären and Lockne craters — possible evidences of an Ordovician asteroid swarm. *Proceedings of the Estonian Academy of Sciences, Geology* 41: 45–53.

Masaitis V. L., Danilin A. N., Mashchak M. S., Raikhlin A. I., Selivanovskaja T. V. and Shadenov Y. M. 1980. *Geology of astroblems*. Nedra, Leningrad, 231 p. (in Russian).

McCarville P. and Crossey L. J. 1996. Post-impact hydrothermal alteration of the Manson impact structure. In: C. Koeberl and R.R. Anderson (Eds.). *The Manson Impact Structure, Iowa: Anatomy of an Impact Crater*. GSA Special Paper 302, Geological Society of America, Boulder, Colorado, 347–376.

McCollom T. M. and Schock E. L. 1997. Geochemical constraints on chemolitho-autotrophic metabolism by microorganisms in seafloor hydrothermal system. *Geochimica et Cosmochimica Acta* 61: 4375–4391.

Meunier A. 1995. Hydrothermal alteration by veins. In: B. Velde (Ed.). *Origin and mineralogy of clays. Clays and the environment.* Springer Verlag, Berlin, Heidleberg, pp. 247–267.

Milton D. J. and Sutter J. F. 1987. Revised age for the Gosses Bluff impact structure, Northern Territory, Australia, based on 40Ar/39Ar dating. *Meteoritics* 22: 281–289.

Mojzsis S. J. and Harrison T. M. 2000. Vestiges of a beginning: clues to the emergent biosphere recorded in the oldest known sedimentary rocks. *GSA Today* 10(4): 1–6.

Naumov M. V. 2002. Impact-generated hydrothermal systems: Data from Popigai, Kara, and Puchezh-Katunki impact structures. In: J. Plado and L. J. Pesonen (Eds.). *Impacts in Precambrian Shields.* Impact Studies. Springer Verlag, Berlin, Heidelberg, 117–171.

Naumov M. V. 2005. I Principal features of impact-generated hydrothermal circulation systems: mineralogical and geochemical evidence. *Geofluids* 4: 1–20.

Osinski G. R. 2005. Hydrothermal activity associated with the Ries impact event, Germany. 5(3): 202 — 220.

Osinski G. R., Spray J. G. and Lee P. 2001. Impact-induced hydrothermal activity within the Haughton impact structure, arctic Canada: Generation of a transient, warm, wet oasis. *Meteoritics & Planetary Science* 36: 731–745.

Oskierski W. and Bischoff L. 1983. Petrographic, geochemical and structural studies on impact breccia dikes of the Rochechouart impact struture, SW France (abstract). *Lunar and Planetary Science XIV*: 584–585.

Pirrus E. 1976. About the age of Paluküla structure. *Geoloogiline kogumik* 3, Tallinn, 83–87. (in Estonian)

Plado J. 1995. *Geophysical signatures of the Kärdla impact crater, Hiiumaa Island, Estonia*. M. Sc. Thesis, Institute of Geology, University of Tartu, Tartu, 86 p.

Plado J. 2000. Gravity and magnetic signatures of meteorite impact structures. *Dissertationes Geologicae Tartuensis 10*. Institute of Geology, University of Tartu, Tartu, 86 p.

Plado J., Pesonen L. J., Elo S., Puura V. and Suuroja K. 1996. Geophysical research on the Kärdla impact structure, Hiiumaa Island, Estonia. *Meteoritics & Planetary Science* 31: 289–298.

Preeden U. 2002. *Shock metamorphic features in quartz and its position in the Kärdla crater, Estonia.* B. Sc. Thesis. Institute of Geology, University of Tartu, Tartu, 52 p. (in Estonian)

Preeden U. 2004. Impaktbretšade peenfraktsiooni lõimis Kärdla, Neugrundi, Åvike ja Lumparni kraatrites. M.Sc. Thesis, University of Tartu, Tartu, 75 p.

Puura V. 1974. The structure of the southern slope of the Baltic Shield. Ph.D. Thesis, Institute of Geology, Estonian Academy of Sciences, Tallinn, 28 p. (in Russian)

Puura V. and Huhma H. 1993. Palaeoproterozoic age of the East Baltic granulitic crust. *Precambrian Research* 64: 289–294.

Puura V. and Suuroja K. 1984. The Kärdla crater, a unique structure hidden in surface. *Eesti Loodus* 9: 559–565. (in Estonian)

Puura V. and Suuroja K. 1992. Ordovician impact crater at Kärdla, Hiiumaa Island, Estonia. In: L. J. Pesonen and H. Henkel (Eds.). Terrestrial Impact Craters and Crater form Structures with a Special Focus on Fennoscandia. *Tectonophysics* 216: 143–156.

Puura V. A., Kala E. A. and Suuroja K. A. 1989. The structure of the Kärdla astroblem. *Meteoritika* 48: 150–161. (in Russian)

Puura V., Lindström M., Floden T., Pipping F., Motusa G., Lehtinen M., Suuroja K. and Murnieks K. 1994. A Structure and stratigraphy of meteorite craters in Fennoscandia and the Baltic region: A first outlook. *Proceedings of the Estonian Academy of Sciences, Geology* 43: 93–108.

Puura V., Kärki A., Kirs J., Kirsimäe K., Kleesment A., Konsa M., Niin M., Plado J., Suuroja K. and Suuroja S. 2000. Impact-induced replacement of plagioclase by K-feldspar in granitoids and amphibolites at the Kärdla Crater, Estonia. In: I. Gilmour and C. Koeberl (Eds.). *Impacts and the Early Earth*. Lecture Notes in Earth Sciences 91, Springer, Berlin, Germany, 417–445.

Puura V., Huber H., Kirs J., Kärki A., Suuroja K., Kirsimäe K., Kivisilla J., Kleesment A., Konsa M., Preeden U., Suuroja S. and Koeberl C. 2004. Geology, petrography, shock petrography, and geochemistry of impactites and target rocks from the Kärdla crater, Estonia. *Meteoritics & Planetary Science* 39: 425–451.

Põldvere A. 2002. *Soovälja (K-1) drill core*. Estonian Geological sections, Bulletin 4. Geological Survey of Estonia, 61 p.

Reeder J. R. (ed.) 1983. *Carbonates: mineralogy and chemistry*. Reviews in mineralogy 11, Mineralogical Society of America, Washington, 394 p.

Reimold W. U., Oskierski W. and Schafer H.. 1984. The Rochechouart impact melt: Geochemical implications and Rb-Sr chronology (abstract). *Lunar and Planetary Science XV*: 685–686.

Semidor M. 1998. *Middle Ordovician sedimentary conditions in the area influenced by the Kärdla impact crater*. M. Sc. Thesis. Institute of Geology, University of Tartu, Tartu, 52 p. (in Estonian)

Simonds C. H. and McGee P. E. 1979. Petrology of impactites, Lake St.Martin, Manitoba, impact structure (abstract). *Lunar and Planetary Science Conference X.* 1125–1127.

Sturkell E. F. F., Broman C., Forsberg P. and Torssander P. 1998. Impact-related hydrothermal activity in the Lockne impact structure, Jamtland, Sweden. *European Journal of Mineralogy* 10: 589–606.

Stöffler D. and Grieve R. A. F. 1994. Classification and nomenclature of impact metamorphic rocks: A proposal to the IUGS subcommission on the systematics of metamorphic rocks. *Lunar and Planetary Sciences 25:* 1347–1348.

Stöffler D. and Grieve R. A. F. 2003. *Towards a unified nomenclature of metamorphic petrology, Chapter 11: Impactites.* A proposal on behalf of the IUGS Subcommission on he Systematics of Metamorphic RocksWeb version of 30.04.2003.

Stöffler D. and Reimold W. U. in press. Geological setting, properties, and classification of terrestrial impact formations.

Stöffler D., Ewald U., Ostertag R. and Reimold W. U. 1977. Research drilling Nördlingen 1973 (Ries) — composition and texture of polymict impact breccias. *Geologica Bavarica* 75: 163–189.

Suuroja K. 1996. *Formation and evolution of the Kärdla impact crater in Estonia.* M. Sc. Thesis, Institute of Geology, University of Tartu, Tartu, 57 p. (in Estonian)

Suuroja K. and Suuroja S. 2000. Neugrund Structure — the newly discovered submarine Early Cambrian impact crater. In: I. Gilmour and C. Koeberl (Eds.). I*mpacts and the Early Earth.* Lecture Notes in Earth Sciences 91. Berlin: Springer. pp. 389–416.

Suuroja K., Gromov O., Kala E., Gromova G., Petersell V. and Puura V. 1974. *Report on the exploration of crystalline basement uplifts in northeast Hiiumaa and evaluation of their usage for granite building stone*. Geological Survey of Estonia, Tallinn, Report No. 3288, 212 p. (in Russian)

Suuroja K., Mardla A. and Puura V. 1981. *Descriptions of geological and structural maps in scale 1:200 000 for pre-Quaternary mineral resources in west Estonia*. Geological Survey of Estonia, Tallinn, Report No. 3877, 120 p. (in Russian)

Suuroja K., Koppelmaa H. and Niin M. 1991. *Subsurface mapping in Hiiumaa in scale 1:200 000, in 1986-1991*. Geological Survey of Estonia, Tallinn, Report No. 4518, 210 p. (in Russian)

Suuroja K., Kadastik E. and Mardim T. 1994. *Report of the complex geological mapping in scale 1:50 000 in Hiiumaa Island*. Geological Survey of Estonia, Tallinn, Report No. 4696. (in Estonian)

Suuroja K., Kadastik E., Mardim T. and Suuroja S. 1997. *The detailed geological mapping of the Kärdla crater area in scale 1:50 000*. Geological Survey of Estonia, Tallinn, Report No. 5820. (in Estonian)

Suuroja K., Suuroja S., All T. and Floden T. 2002. Kärdla (Hiiumaa Island, Estonia) — the buried and well-preserved Ordovician marine impact structure. *Deep-Sea Research II* 49/6: 1121–1144.

Suuroja S. 1994. *Shock-metamorphic features in the crystalline rocks of Kärdla crater, Estonia.* B. Sc. Thesis. Institute of Geology, University of Tartu, Tartu, 49 p. (in Estonian)

Suuroja S. 1999. *Lithology of the Kärdla crater breccias*. M. Sc Thesis. Institute of Geology, University of Tartu, Tartu, 78 p. (in Estonian)

Suuroja S. and Suuroja K. 2004. The Neugrund Marine Impact Structure (Gulf of Finland, Estonia). In: H. Dypvik, M. Burchell and P. Claeys (Eds.). *Cratering in Marine Environments and on Ice.* Impact Studies. Berlin: Springer. pp. 75–95.

Suuroja S. and Suuroja K. 2006. Kärdla Impact (Hiiumaa Island, Estonia) — Ejecta Blanket and Environmental Disturbances. In: C. Cockell, C. Koeberl, I. Gilmour (Eds.). *Biological Processes Associated with Impact Events.* Impact studies. Springer Verlag, Berlin, 121–146.

Tatarintsev V. I., Krochuck V. M., Bondarenko I. N. and Legkova G. V. 1981. Sphalerite from an explosion structure on the Ukrainian Shield. In: *Mineralogy and Petrology of Ore Areas of the Ukrainian Shield.* Naukova Dumka, Kiev, Ukraine, pp 41-50. (in Russian)

Utada M. 1980. Hydrothermal alteration related to igneous acidity in Cretaceous and neogene formations of Japan. In: S. Ishihara and S. Takenouchi (Eds.). *Granitic magmatism and related mineralization. Mining Geology Special Issue* 8: 67–83.

Van Dover C. L. 2000. *The Ecology of Deep-Sea Hydrothermal Vents*. Princeton University Press, Princeton, NY.

Velde B. 1985. *Clay Minerals: A physico-chemical explanation of their occurrence.* Development in Sedimentology 40, Elsevier, Amsterdam.

Versh E., Kirsimäe K., Jõeleht A. and Plado J. 2005. Cooling of the Kärdla impact crater: I. The mineral parasequence observations. *Meteoritics & Planetary Science* 40: 3–19.

Versh E., Kirsimäe K. and Jõeleht A. in press. Development of potential ecological niches in impact-induced hydrothermal systems: the small-to-medium size impacts. *Planetary and Space Science.* doi:10.1016/j.pss.2005.12.022.

Viiding H., Kala E. and Pobul E. 1969. The mystery of the Paluküla is resolving. *Eesti Loodus* 8: 464–474. (in Estonian)

Worden R. H. and Rushton J. C. 1992. Digenetic K-feldspar textures: A TEM study and model for diagenetic feldspar growth. *Journal of Sedimentary Petrology* 62: 779–789.

Zhukov F., Petersell V. and Fomin J. 1987. Palaeozoic volcanism occurrences in Estonia. *Proceedings of the Estonian Academy of Sciences. Geology* 36, 6–13. (in Russian)

Zürcher L. and Kring D. A. 2004. Hydrothermal alteration in the core of the Yaxcopoil-1 borehole, Chicxulub impact structure, Mexico. *Meteoritics and Planetary Science* 39: 1199–1221.

SUMMARY IN ESTONIAN

Plahvatusjärgse hüdrotermaalse süsteemi areng Kärdla meteoriidikraatris

Meteoriidiplahvatusel hetkeliselt vabanev energia põhjustab tekkiva kraatri kivimite kuumutuse. Juhul, kui kivimites leidub küllaldaselt (põhja)vett või kui on tegemist merre kukkunud meteoriidi plahvatusega, võivad meteoriidikraatrites moodustuda lokaalsed hüdrotermaalsed süsteemid. Selliste plahvatusjärgsete ehk impakt-indutseeritud hüdrotermaalsete (IHT) protsesside uurimine on viimasel kümnendil olnud üks kiiremini arenevaid impaktgeoloogia teemasid. Selle teema peamised uurimisvaldkonnad on: (1) IHT kui loodusliku nähtuse olemuse selgitamine; (2) meteoriidikraatrite jahtumise uurimine; ja (3) IHT süsteemide võimaliku osatähtsuse selgitamine maavälise elu ja varajast elu Maal toetava mehhanismina. IHT süsteemid on erinevalt endogeensetest hüdrotermidest (nt vulkaaniliste piirkondade ja ookeani keskahelike hüdrotermaalsed süsteemid) väga kitsa levikuga, suhteliselt lühiajalised ning pöördumatult jahtuva temperatuuritrendiga.

Käesoleva doktoritöö eesmärk on selgitada mineraloogilisi, geokeemilisi ja arvutimodelleerimise meetodeid kasutades, milline oli IHT süsteemi areng 4-km läbimõõduga Kärdla meteoriidikraatris, sh:

(1) selgitada, millised mineraloogilised ja geokeemilised muudatused toimusid kraatri kivimites IHT süsteemi erinevate arenguetappide jooksul;
(2) uurida millised olid algsed füüsikalised ja keemilised tingimused, kuidas need tekkisid ja edasise IHT tegevuse ajal muutusid;
(3) selgitada, kuidas meteoriidiplahvatuse järgselt tekkinud hüdrotermaalses süsteemis võivad kujuneda uued elukeskkonnad, mis on sobilikud kuumalembestele (termofiilsetele) mikroorganismidele;
(4) millised on selliste ökoloogiliste niššide iseloomulikud tunnused ning kuidas need muutusid ruumis ja ajas.

Kärdla kraater on üks maailma paremini säilinud ja enim uuritud meteoriidikraatreid ning sobilik väikese- kuni keskmisemõõduliste meteoriidikraatrite mudelstruktuuriks. Tehtud mineraloogiliste ja geokeemiliste uuringute tulemused näitavad, et Kärdla IHT süsteemi iseloomustab kolmeetapiline areng, mis väljendab fluidi olekumuutusi algsest aurulisest keskkonnast kuni valdavalt veelise fluidi tsirkulatsiooni kujunemiseni. Hüdrotermaalsete mineraalide tekkimise järjekord ehk parageneetiline rida väljendab tasakaaluliste mineraalsete faaside moodustumist plahvatusjärgsete fluidi-temperatuuride langusel, mille kolm etappi on: (1) varajane aurulise fluidi staadium (>300°C), mida iseloomustab krüptokristallilise adulaari tüüpi K-päevakivi tekkimine; (2) peamine staadium kahe-faasilise (aur-vesi) tsooni arenguga temperatuuridel 300 kuni 150(100)°C, mida iseloomustab kloriidi/korrensiidi, submikroskoopilise idiomorfse plokilise K-päevakivi ja kvartsi moodustumine; ning (3) hiline, valdavalt veelise fluidi staadium (<100°C) kaltsiit I, dolomiidi, kvartsi, kaltsiit II, kalkopüriidi/püriidi, Fe-oksihüdraatide ja kaltsiit III tekkimisega. Ülalmainitud tulemused on kooskõlas kraatri jahtumise geotermaalse arvutimodelleerimise tulemustega, millest saab järeldada, et kahe esimese staadiumi alumosilikaatne mineraalne kooslus (K-päevakivi — kloriit/korrensiit– kvarts) tekkis suhteliselt lühikese aja jooksul (vähem kui 4000–5000 aastat peale kraatri tekkimist), samas kui karbonaadi — kvartsi — sulfiidi — Fe-oksihüdraatide moodustumine võis toimuda kuni umbes 10 000 aasta vältel peale kraatri tekkimist.

Meteoriidiplahvatused on kõige enam tuntud nende võimalike katastroofiliste tagajärgede poolest bioloogilisele evolutsioonile. Samas ei ole plahvatuse mõju bioloogilisele arengule üksnes hävitav vaid selle tulemusena võib tekkida uus, märkimisväärselt teistsugune ökosüsteem, andes eksistentsi ja/või arenguvõimalusi teistele organismidele. Plahvatuse poolt purustatud kivimid ja meteoriidikraatritega seotud IHT süsteemid võisid olla üheks võimalikuks alternatiivseks prebiootiliste reaktsioonide toimumispaigaks planeetide varajasel arenguetapil ning iseäranis varasel Maal, kuna nad pakuvad eluks (vähemalt meile tuntud vormis) vajaliku vett ning energiat, sh lahustunud toitaineid. Seetõttu on IHT süsteemid teaduslikult huvitavad objektid kõige vanemate ja primitiivsemate organismide — (hüper)-termofiilsete mikroobsete organismide — võimaliku elutegevuse uurimiseks. Kuna igas vett ja/või vee-jääd sisaldavas planetaarses kehas võib selline IHT süsteem kujuneda, siis on põhjendatud võimaliku primitiivse elu jälgede otsingud taolistest kohtadest teistel planeetidel, iseäranis Marsil.

Modelleerimise tulemused näitavad, et väikese- kuni keskmisemõõduliste kraatrite jahtumisel kujunevad termofiilisetele (45–80ºC) ja hüpertermofiilsetele (80–120ºC) organismidele sobilike temperatuurivahemikega asustamiskõlblikud tsoonid juba 500–1000 aastat pärast kraatri teket. Jahtumise algfaasis, kui kraatri keskosas domineerivad auru-fluidid (temperatuuridel üle 250–290°C), on kraatri keskosa asustuskõlbmatu, samas säilib seal termofiilide ja hüpertermofiilide seisukohalt optimaalsed kõrgendatud temperatuurid kõige kauem.

Suurtes meteoriidikraatrites, kus kuumutuse käigus moodustuv impaktsula võib täita kogu topograafilise kraatrisüvendi, on kivimite ja võimalike plahvatusjärgsete hüdrotermaalsete fluidide temperatuur eluks sobilikust piirist mitu korda kõrgem pikema perioodi vältel ning seetõttu on süsteemide asustamine võimalik alles kümneid kuni sadu tuhandeid aastaid hiljem. Lisaks pikaajalistele kõrgetele temperatuuridele peab suurte struktuuride korral arvestama impaktplahvatuse (ülihelikiirusliku lööklaine ning impaktkuumutuse) steriliseeriva mõjuga. Steriliseeriv mõju on väiksemates kraatrites aga minimaalne.

Seni, vähesed avaldatud IHT süsteemide ehitust ja kujunemist käsitlevad artiklid on keskendunud vaid suurtele (>50 km läbimõõduga) kraatritele ning väikese- kuni keskmisemõõduliste kraatrite uuringud praktiliselt puudusid. Seega on antud töö tulemused originaalsed kogu maailma kontekstis ja omavad suurt tähtsust sarnaste protsesside mõistmiseks väikse kuni keskmise suurusega meteoriidikraatrites, andes seni puudunud kompleksse lähenemise IHT süsteemi tekkest ja arengust ning bioloogilistest aspektidest ühe kraatri näitel.

ACKNOWLEDGEMENTS

The author is grateful to supervisor Prof. Kalle Kirsimäe (Institute of Geology, Univesity of Tartu) who provided valuable assistans and support during the doctoral studies and preparation of this thesis.

The author is grateful to Väino Puura (Institute of Geology, University of Tartu) and Kalle-Mart Suuroja (Estonian Geological Survey) for providing samples and help in related research. Jaan Aruväli (Institute of Geology, University of Tartu) and Tõnu Martma (Institute of Geology at Tallinn University of Technology) are thanked for their help and assistance in carrying out the XRD and stable isotope analyses. The author is very grateful to Argo Jõeleht, Väino Puura and Leho Ainsaar (Institute of Geology, University of Tartu) for instructive and helpful discussions during the preparation of this thesis and in related research fields.

Roald Tagle, Tobias Salge, Lutz Hecht, Dieter Stöffler and Thomas Kenkmann are thanked for many-sided technical support in carrying out the EPMA and SEM studies, fruitful and instructive discussions, helpful remarks, and warm hospitality at the Institute of Mineralogy, Museum of Natural History, Humboldt University in Berlin. Bjørn Buchardt is thanked for good instructions and helpful discussions, technical support and warm hospitality at the Geological Institute, University of Copenhagen.

The Lunar and Planetary Institute, European Science Foundation ESF-IMPACT program, The Barringer Crater Company and NordForsk are thanked for student travel grant awards or financial support to attend and present results at conferences.

The compilation of this thesis and comprised work was financially supported by the Estonian Science Foundation grants No. 4541, 5372, 5851; a DAAD (Deutscher Akademischer Austausch Dienst) research scholarship, a Danish Government Scholarship and a research scholarship by University of Münster.

PUBLICATIONS

Meteoritics & Planetary Science 40, Nr 1, 3–19 (2005)
Abstract available online at http://meteoritics.org

Cooling of the Kärdla impact crater: I. The mineral paragenetic sequence observation

Evelin VERSH,* Kalle KIRSIMÄE, Argo JÕELEHT, and Jüri PLADO

University of Tartu, Institute of Geology, Vanemuise 46, Tartu 51014, Estonia
*Corresponding author. E-mail: evelin.versh@ut.ee

(Received 1 June 2004; revision accepted 29 November 2004)

Abstract–The impact-induced hydrothermal system in the well-preserved, 4 km-diameter Kärdla impact crater on Hiiumaa Island, western Estonia, was investigated by means of mineralogical, chemical, and stable C and O isotope studies. The mineralization paragenetic sequence, with gradually decreasing temperature, reveals at least three evolutionary stages in the development of the post-impact hydrothermal system: 1) an early vapor-dominated stage (>300 °C) with precipitation of submicroscopic adularia type K-feldspar; 2) the main stage (300 to 150/100 °C) with the development of a two-phase (vapor to liquid) zone leading to precipitation of chlorite/corrensite, (idiomorphic) euhedral K-feldspar, and quartz; and 3) a late liquid-dominated stage (<100 °C) with calcite I, dolomite, quartz, calcite II, chalcopyrite/pyrite, Fe-oxyhydrate, and calcite III precipitation.

INTRODUCTION

Energy released by a meteorite impact results in the heating, melting, and vaporization of the projectile and target rocks. The remaining target rocks then start to cool to the ambient conditions. In dry environments (e.g., on the Moon), the heat loss occurs mainly by conduction and radiation transfer. However, if water is present at the crater site, cooling of the impact-heated rocks can also occur by convective heat transfer by hydrothermal circulation systems. Evidence of impact-induced hydrothermal activity have been found at numerous terrestrial craters varying in size (from 250 to 1.8 km) and in target composition (e.g., Ames et al. 1998; Naumov 2002; Osinski et al. 2001; Hagerty and Newsom 2003), and it is suggested for impact craters on Mars as well (e.g., Allen et al. 1982; Newsom 1980; Newsom et al. 1996).

Impact-induced hydrothermal systems are important to study for many reasons. First, their development and cooling is still a topic of debate. In most cases described so far, evidence of hydrothermal alteration is mainly found both in and around the crater central uplift, for example in the Kärdla, Manson, Puchezh-Katunki, and Siljan structures (Kirsimäe et al. 2002; McCarville and Crossey 1996; Naumov 2002; Hode et al. 2003; respectively), whereas at times it has been recognized around the central uplift and at the crater rim (e.g., at the Haughton crater; Osinski et al. 2001). Second, mineral deposits formed and/or modified by hydrothermal fluids are of significant economic interest, for example at Sudbury (Ames et al. 2002). Third, in recent years, studies of the thermal history of impact structures have been made with emphasis on creating new habitable environments for high-temperature anaerobic microbial life forms (e.g., Cockell and Lee 2002).

The development and cooling of impact-induced hydrothermal systems can be recognized by: 1) mineralogical and geochemical studies that describe the thermal and chemical evolution of the post-impact fluids over time; and 2) numerical modeling which approximates the space and time for given (temperature) conditions. This paper is the first part of a detailed geological investigation of post-impact cooling of the medium- to small-size Kärdla impact structure. Here, we present the results of mineralogical, geochemical, and isotopic studies of the impact-induced hydrothermal mineralization paragenetic sequence developed at this structure. The results of impact and geothermal modeling studies are presented in the second part of this study (Jõeleht et al. 2005).

GEOLOGICAL SETTING

The Kärdla meteorite impact structure has a 4 km rim-to-rim diameter (Suuroja et al. 2002) and is located on the Island of Hiiumaa (centered at 58°58′40″N, 22°46′45″E) 25 km off the northwestern coast of Estonia (Fig. 1). The true depth of the structure is ~500 m and it hosts a 130-meter-high central uplift. The Kärdla structure is surrounded by an elliptical

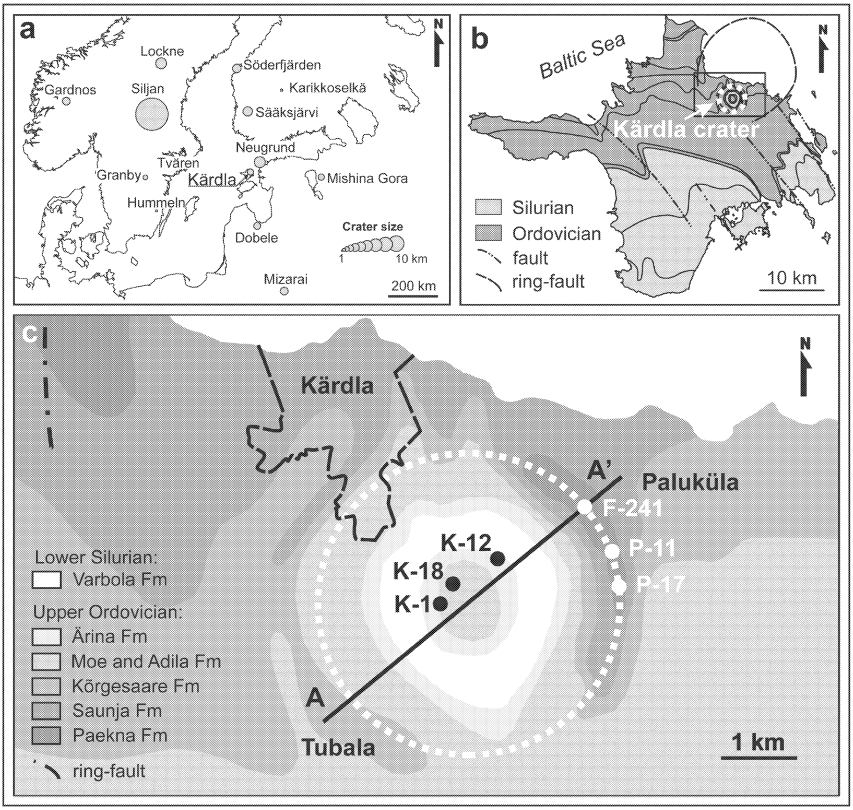

Fig. 1. a) Location of Kärdla and other Paleozoic or Ediacaran impact craters in the Baltic Sea region, northeastern Europe; b) geological map of Hiiumaa Island with the location of the crater and the surrounding ring fault; c) geological map of the Kärdla crater area with studied drill cores. The white dashed line shows the location of the crater rim, black line the cross section (A-A') presented in Fig. 2, and black dashed line a border of town Kärdla in the northwestern part of the crater.

ring-fault of 12–15 km in diameter, which corresponds to the outer boundary of dislocations in the target rocks caused by the impact (Suuroja et al. 2002; Puura and Suuroja 1992). The impact occurred in a shallow (<100 m deep; Puura and Suuroja 1992) Ordovician shelf sea about 455 Ma ago (Grahn et al. 1996). The structure is well preserved and buried under post-impact sediments of Ordovician, Silurian, and Quaternary age (Fig. 2).

Pre-Impact Target Rocks

The pre-impact bedrock section is composed of ~200 m of sedimentary rocks overlying a crystalline basement of Paleoproterozoic metamorphic rocks. The crystalline rocks belong to the 1.7–2.0 Ga Svecofenninan crustal segment (Puura and Huhma 1993) and consist of regionally metamorphosed amphibolite facies migmatite granites, quartz-feldspar gneisses with amphibolites, biotite gneisses, and biotite-amphibole gneisses (Koppelmaa et al. 1996). The amphibolitic rocks form up to 22%, biotite-amphibole gneisses and biotite-plagioclase gneisses ~6%, and granitic rocks (granitoids, granite gneisses, and quartz-feldspar gneisses) up to 72% of the basement in the area. The eastern part of the crater basement is mostly composed of amphibolites, whereas the crystalline rocks in the crater depression, including the western rim, are predominantly granites and quartz-feldspar gneisses.

Puura et al. (1983) detected that Precambrian weathering

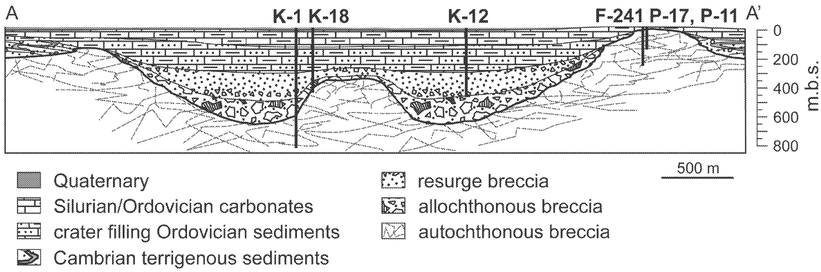

Fig. 2. Cross section of the crater structure in the southwest-northeast direction (shown in Fig. 1) with locations of studied drill cores. The vertical scales indicate meters below surface.

of crystalline bedrock below the contact with sedimentary rocks in the northeastern part of Hiiumaa Island reaches tens of meters below the Proterozoic peneplane. Remnants of the weathered surfaces are occasionally found in dislocated crystalline rock blocks at various depths in the crater rim at Paluküla (Puura and Suuroja 1992). Inside the crater structure, the majority of the weathered crystalline crust was ejected during the impact event. Its hydrothermally altered fragments are, therefore, rare and found only within the resurge and allochthonous breccia, whereas they are totally absent in the sub-crater basement rocks (V. Puura, personal communication).

At the time of impact, the sediments overlying the crystalline basement were composed mostly (>90% of the section) of Ediacaran, Lower Cambrian, and Lower Ordovician weakly cemented terrigenous rocks (sand-, silts-, and claystones); and a thin (~15 m) layer of Lower to Middle Ordovician carbonates (Suuroja et al. 2002).

Impactites

The crater depression is filled with a practically uneroded complex of autochthonous and allochthonous impact breccias that are covered by resurge breccia (Fig. 2). The latter consists of resurge conglomerates, conglomeratic turbidites, and sands which were eroded from uplifted walls before complete burial under the post-impact sediments (Puura and Suuroja 1992). The autochthonous breccias are composed of cataclastic crystalline basement rocks fractured and brecciated in various scales—from meter-size blocks and breccia dikes down to millimeter to submillimeter-size clasts in the breccia matrix, and micro-fracturing of mineral grains (Puura et al. 2000). The allochthonous fragmental breccias consist of a polymict mixture of crystalline and sedimentary rock fragments. No evidence of an impact melt sheet in the crater interior has been found; however, the suevitic breccia units do contain small, devitrified melt clasts (Suuroja et al. 2002).

The impactites at Kärdla are characterized by major mineralogical and chemical changes with respect to the crystalline basement rocks outside the crater. These include, for example, chloritization of amphibole in autochthonous and allochthonous breccias (Kirsimäe et al. 2002), and replacement of plagioclase with orthoclase-type K-feldspar in impact affected granites and amphibolites (Puura et al. 2000; 2004). The latter is chemically expressed by Na and Ca depletion, and K-enrichment (Puura and Suuroja 1992).

Possible hydrothermal alteration of the impactites in the Kärdla structure was first discussed by Kirsimäe et al. (2002) who suggested that impact-induced hydrothermal processes occurred at temperatures of about 100–300 °C, based on low salinity fluid inclusions in quartz and pervasive hornblende chloritization in autochthonous and allochthonous breccias.

Post-Impact Rocks

The normal, slow-rate sedimentation of cold to temperate water marine carbonate sediments at the crater site resumed shortly after the impact, and the crater was buried under Upper Ordovician and Lower Silurian marine limestone (Ainsaar et al. 2002). In the crater depression, the thickness of the post-impact sedimentary rocks reaches 275 m, whereas in the surrounding area it is on average ~90 m thick and only 15–20 m above the highest rim wall at Paluküla (Fig. 2). The bedrock at the crater area is covered with a 24 m thick layer of Quaternary glacial, marine, and lacustrine deposits, reaching only 0.2–2 m at the elevated crater rim walls (Suuroja et al. 2002).

Sulfide (galena, sphalerite, and pyrite) mineralization of a not well-known origin has been discovered on the outer slopes of the buried rim wall at Paluküla within strongly dolomitized Ordovician reef limestones which overlie brecciated Cambrian siliciclastic target rocks (Suuroja 2002) and within the limy sandstone layer covering the ejected impact breccias near the Tubala rim wall (Suuroja et al. 1994). Neither the spatial extent nor the exact age of this mineralization is known. Suuroja et al. (1994) and K. Suuroja (2002) have suggested that it is not genetically related to the impact or to the impact-induced hydrothermal activity and is believed to be post-Ordovician in age.

MATERIAL AND ANALYTICAL METHODS

Using various mineralogical and geochemical methods, four distinctive impactite types at Kärdla were investigated: resurge deposits, allochthonous impact breccias, autochthonous impact breccias (drill cores K-18, K-1, and K-12), and fractured crystalline basement rocks with breccia vein pockets (P-11, P-17, and F-241). They represent the impact-related rocks from the central uplift, annular depression, and rim wall, (Figs. 1 and 2).

Drill core K-18 accesses a section of the resurge and allochthonous breccias in the central part of the crater, and penetrates to the brecciated crystalline rocks on the edge of the central uplift (at depths from 399 to 432 m; Fig. 3). Drill core K-1 penetrates the whole section of the resurge, allochthonous and autochthonous breccias inside the crater depression down to 815 m below the surface (Fig. 4). Drill core K-12 penetrates the resurge breccias and the uppermost part of the allochthonous breccias down to 485.6 m (Fig. 5) in the annular depression in the northeast. Drill cores F-241, P-11, and P-17 cut into brecciated and fractured basement rocks on the northeast-eastern part of the rim wall, and the analyzed samples represent three different depth intervals below the surface: 15–45, 70–80, down to 200–250 m (Fig. 5), respectively.

Macroscopic (inspection of all drill cores and 35 selected hand specimens in detail), microscopic (over 100 thin sections), and X-ray diffractometry (XRD) (75 samples) studies were made to define vein minerals and breccia matrix composition. XRD patterns of mineral fractions and whole rock samples were measured in powdered unoriented preparations with Dron-3M diffractometer using Ni-filtered Cu-$K\alpha$ radiation from 2 to 50° 2θ with 0.02° 2θ step size and 5 sec counting time. XRD measurements were carried out at the Institute of Geology, University of Tartu. The patterns were analyzed using AXES 1.9A (Mändar et al. 1996) and Siroquant 2.5™ (Taylor 1991) codes. Calcite and dolomite lattice parameters were found by applying the Powder Cell 2.3 refinement code (Kraus and Nolze 1996).

Quantitative chemical analyses, element mapping, and imaging were carried out on selected thin sections using a JEOL JXA 8800L microprobe operating at 15 kV and 15 nA, at the Institute of Mineralogy, Museum of Natural History, University of Humboldt in Berlin. Chemical analyses were done based on a calibration with international mineral standards. Counting times of 10 or 20 sec on peak and 5 or 10 sec on background were used. A beam size of 1 μm for silicates and 5 or 10 μm for carbonates and clay minerals was used. Element mapping was performed with a beam size of <1 μm.

Stable O and C isotopes were studied in 15 samples from vein-filling calcite and dolomite. The isotopic composition of oxygen and carbon for monomineral calcite and dolomite was determined from CO_2 gas obtained by reacting powdered samples with 100% phosphoric acid with a reaction time of 15 min at temperatures of 50 °C (calcite) and 100 °C (dolomite). Stable isotope composition fractions were measured with Finnigan-MAT "Delta-E" mass spectrometer at the Institute of Geology, Tallinn Technical University. Possible fluid temperatures at the time of the carbonate precipitation were calculated using the isotope fractionation-temperature equation:

$$10^3 \ln \alpha_{\text{mineral-water}} = a\,(10^6/T^2) + b\,(10^3/T) + c \quad (1)$$

where α is the fractionation factor between mineral and water (the fluid); T is the fluids' temperature in Kelvin; a, b, and c are equation constants. The following values were used for the constants: $a = 2.78$, $b = 0$, $c = -2.89$ for the calcite-water system (after O'Neill et al. 1969); and $a = 2.78$, $b = 0$, $c = 0.91$ for the dolomite-water system (after Land 1985). In the calculations, the HCO_3^- state of carbon in the fluid was assumed.

RESULTS

Hydrothermal Mineralization in Impact Breccia Matrices, Cavities, and Fractures

Macroscopic and microscopic petrological/ mineralogical studies reveal eight major post-impact hydrothermal mineral phases in the Kärdla rocks: 1) two morphologically different generations of authigenic K-feldspar; 2) Fe-chlorite/corrensite; 3) quartz; 4) three morphologically, chemically, and structurally distinctive generations of calcite; 5) dolomite; 6) hematite; 7) goethite; and 8) chalcopyrite/pyrite.

K-Feldspar

The morphology and size of the crystals, as well as their associations with other minerals, indicates the existence of two different generations of K-feldspar which, according to geochemical and XRD analyses, have no significant chemical or structural differences (Table 1). The paragenetic relations refer to the presence of earlier submicroscopical K-feldspar (Ksp I) and later idiomorphic rhombohedral-like euhedral microscopic K-feldspar (Ksp II) in impactite types studied from the Kärdla structure. The submicroscopical Ksp I masses completely or partly replace altered and fractured plagioclase crystals and occur together with xenomorphic iron-rich, probably clay material (Fig. 6). The euhedral Ksp II crystals line fracture systems (Fig. 7c) and cavities, as well as small vugs and pores between rock clasts in the fine-grained breccia matrix. Xenomorphous quartz and/or carbonate minerals fill the central part of these K-feldspar lined fracture systems and cavities (Figs. 7b–7d). Morphological studies indicate that the outer boundaries of the submicroscopic K-feldspar masses in some places have later been either partly recrystallized into or overgrown by the euhedral form (Ksp II). Some intergrowth with authigenic quartz is also visible (Fig. 7a).

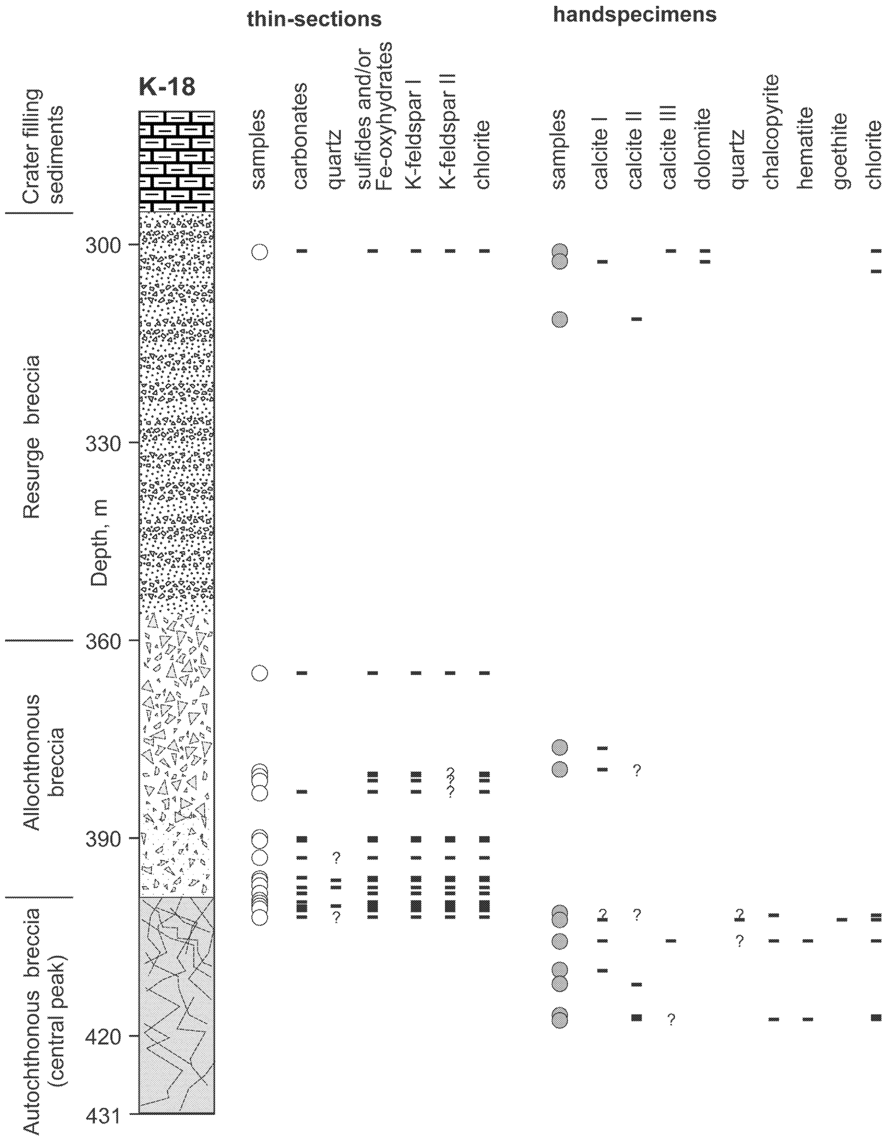

Fig. 3. Position of studied thin sections and hand specimens with distribution of hydrothermal minerals described in the text. Drill core K-18 from the northwestern edge of the central uplift.

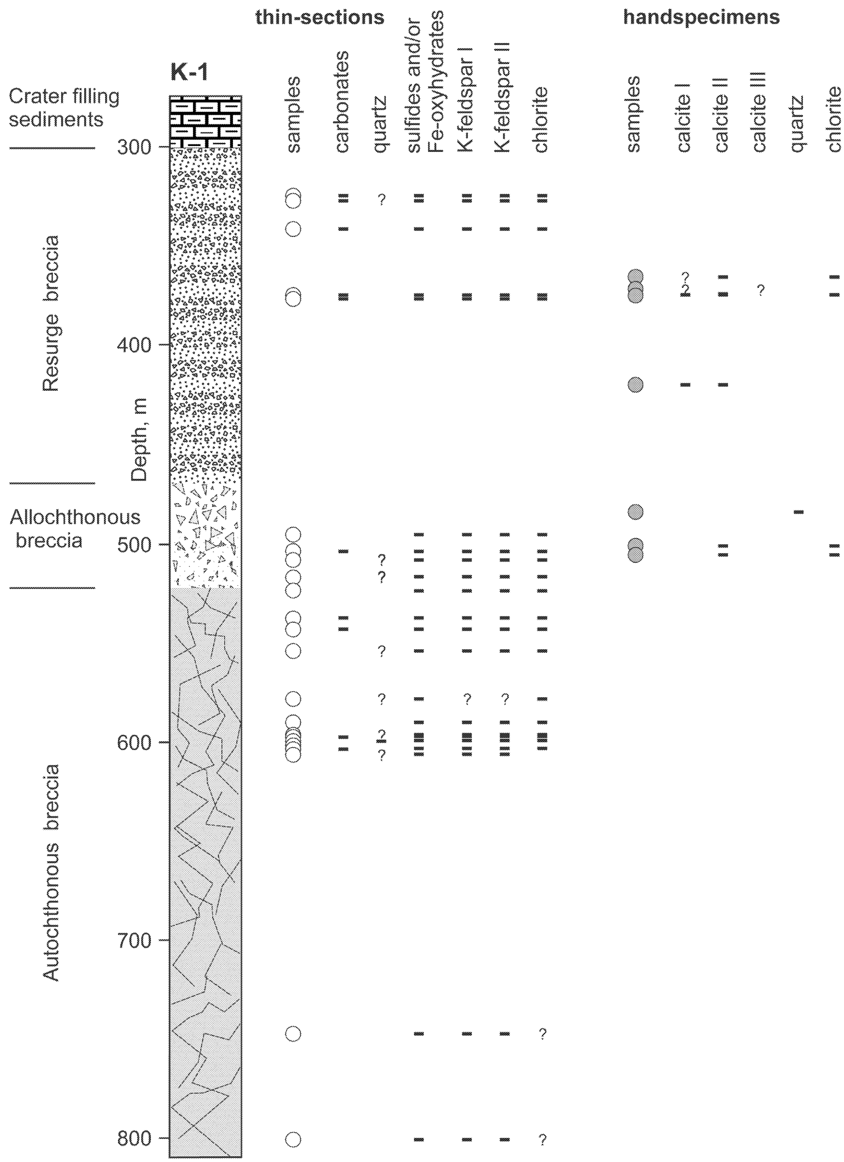

Fig. 4. Position of studied thin sections and hand specimens with distribution of hydrothermal minerals described in the text. Drill core K-1 from the west side of the crater depression, close to proposed location of central uplift.

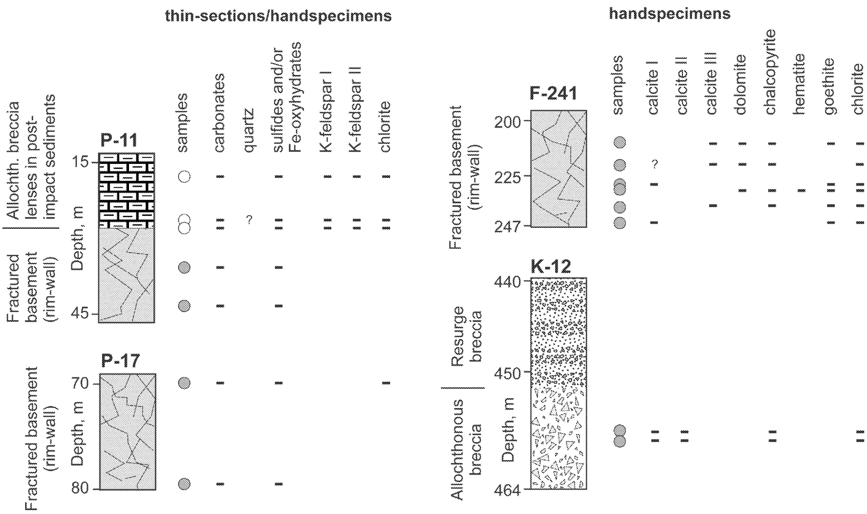

Fig. 5. Position of studied thin sections and hand specimens with distribution of hydrothermal minerals described in the text. Drill cores P-11, P-17, F-241 from the crater rim in the north-northeast and K-12 from the northeastern side of the crater depression.

Table 3. Electron microprobe analyses of authigenic clay minerals and pre-impact hornblende in the Kärdla impactites.

	Clay minerals (chlorite/corrensite)						Hornblende			
	Mg clays[a]		Mg-Fe clays[b]		Fe clays[c]		K-1	K-1	Average[d]	SD[d]
wt%	Average[d]	SD[d]	Average[d]	SD[d]	Average[d]	SD[d]	597.0	603.0	–	–
SiO_2	34.47	2.05	33.79	1.64	29.42	2.49	43.50	44.52	43.99	0.78
TiO_2	0.01	0.01	0.10	0.4	0.31	0.88	1.89	1.30	1.60	0.34
Al_2O_3	16.40	0.73	13.62	1.27	19.56	0.95	10.54	11.06	10.79	0.44
FeO	7.55	2.26	16.38	1.44	19.14	3.64	18.43	16.84	17.65	0.88
MnO	0.26	0.09	0.08	0.12	0.36	0.07	0.32	0.29	0.31	0.04
MgO	25.46	2.42	21.51	1.42	13.77	1.94	9.53	10.82	10.16	0.70
CaO	0.41	0.12	0.65	0.19	0.26	0.17	11.63	11.48	11.56	0.18
Na_2O	0.10	0.04	0.09	0.03	0.12	0.07	1.48	1.50	1.49	0.11
K_2O	0.47	0.43	0.15	0.13	1.08	1.05	1.34	1.26	1.30	0.09
Cr_2O_3	0.05	0.03	0.07	0.05	0.05	0.04	0.06	0.10	0.08	0.04
Total	85.18	–	86.44	–	84.07	–	98.72	99.17	98.93	–
n[e]	39	–	209	–	63	–	20	20	40	–

[a]Measured in thin sections from: P-11 017.8 m, P-11 026.4 m.
[b]Measured in thin sections from: K-1 597.0 m, K-1 599.0 m, K-1 603.0 m, K-18 398.4 m, P-11 017.8 m.
[c]Measured in a thin section from: K-1 373.5 m.
[d]Average and standard deviation in the Kärdla impactites. Sample names are given by the drill core number and depth (m). Results are given as an average of spot analyses in thin sections.
[e]Number of measurements (analyze spots).

Authigenic K-feldspar is a structurally single, monoclinic, adularia-type orthoclase with strained lattice parameters that are intermediate between typical orthoclase and low microcline. This adularia-type K-feldspar is characterized by rather stable lattice constants (a = 8.584 ± 0.0032 Å, b = 13.013 ± 0.0045 Å, c = 7.195 ± 0.0032 Å, γ = 115.83 ± 0.054°) throughout the studied section (35 samples from drill cores K-1 and K-18 representing the fine-grained breccia matrix in all four impactite rock types). The primary K-feldspar in the crystalline basement rocks, which is also found in the altered samples, is by XRD structure refinement, a maximum triclinic microcline as suggested by relevant typical lattice constants (a = 8.566 Å, b = 12.938 Å, c = 7.210 Å, α = 90.49°, β = 116.11°, γ = 88.15°). Composition of

Table 1. Electron microprobe analyses of authigenic adularia-type K-feldspar (Ksp I and II in the Kärdla impactites.

	Adular																
	Ksp I				Ksp II				Ksp I/KSP II (not separated)								
	K-1	K-18	Avg.[a]	SD[a]	K-18	K-1	Avg.[a]	SD[a]	K-1	K-1	K-18	K-18	K-18	K-18	P-11	Avg.[a]	SD[a]
wt%	599.0	301.0	–	–	301.0	599.0	–	–	373.5	516.2	365.0	390.4	401.0	402.0	026.4	–	–
SiO_2	64.74	64.90	64.79	0.46	64.12	64.85	64.24	0.92	62.21	60.21	63.47	62.04	61.48	61.55	63.63	62.09	1.16
Al_2O_3	17.31	17.98	17.55	0.39	17.11	17.84	17.23	0.61	18.93	19.75	18.28	18.32	17.94	18.42	18.34	18.35	0.49
FeO	0.08	0.04	0.07	0.06	0.28	0.41	0.30	0.26	0.32	0.78	0.08	0.19	0.41	0.16	0.15	0.22	0.23
MnO	0.01	0.01	0.01	0.01	n.d.	0.01	0.01	0.01	0.01	0.01	0.02	0.02	0.02	0.01	0.01	0.01	0.02
MgO	0.01	0.01	0.01	0.02	0.13	0.02	0.11	0.18	0.02	0.16	0.01	0.06	0.14	0.01	0.04	0.05	0.10
CaO	0.01	0.02	0.02	0.02	0.12	0.02	0.10	0.16	0.05	0.03	0.10	0.05	0.08	0.05	0.09	0.06	0.09
Na_2O	0.06	0.03	0.05	0.04	0.26	0.04	0.22	0.26	0.14	0.18	0.61	0.42	0.17	0.44	0.08	0.33	0.33
K_2O	16.74	16.67	16.72	0.56	15.90	16.76	16.05	0.83	16.70	16.99	16.16	16.47	16.48	16.32	16.74	16.47	0.59
Total	98.96	99.66	99.22	–	97.92	99.95	98.26	–	98.38	98.11	98.73	97.57	96.72	96.96	99.08	97.58	–
n[b]	22	12	34	–	15	3	18	–	11	1	7	34	19	33	14	119	–

[a]Average and standard deviation of the authigenic K-feldspar (adular) in the Kärdla impactites. Sample names are given by the drill core number and depth (m). The results are given as an average of spot analyses in thin sections.
[b]Number of measurements (analyze spots).

Table 2. Electron microprobe analyses of pre-impact plagioclase (oligoclase and albite) and K-feldspar (microcline) in the Kärdla impactites.

	Pre-impact plagioclase				Pre-impact K-feldspar						
	Oligoclase		Albite		Microcline						
	K-1	SD	P-11	SD	K-18	K-18	K-18	K-18	P-11	Average[a]	SD[a]
wt%	599.0	–	026.4	–	365.0	390.4	401.0	402.0	026.4	–	–
SiO_2	61.73	0.52	67.32	0.54	62.08	62.93	62.75	63.24	64.72	63.18	0.84
Al_2O_3	22.79	0.46	19.43	0.14	18.50	18.52	18.32	18.60	18.08	18.46	0.27
FeO	0.14	0.08	0.09	0.11	n.d.	0.04	0.10	0.08	0.24	0.08	0.08
MnO	0.01	0.02	0.01	0.02	n.d.	0.03	n.d.	0.01	0.02	0.02	0.03
MgO	n.d.	n.d.	0.01	0.01	n.d.	0.01	0.01	0.01	0.02	0.01	0.01
CaO	5.58	0.23	0.18	0.05	0.06	0.07	0.18	0.10	0.04	0.08	0.05
Na_2O	7.74	0.19	9.88	0.43	1.14	1.24	1.30	1.20	1.14	1.21	0.15
K_2O	0.38	0.18	1.22	0.69	15.06	15.16	14.50	15.17	15.59	15.17	0.38
Total	98.37	–	98.14	–	96.84	98.00	97.16	98.41	99.85	98.21	–
n[b]	10	–	5	–	1	7	1	3	2	14	–

[a]Average and standard deviation of pre-impact K-feldspar (microcline) in the Kärdla impactites. Sample names are given by the drill core number and depth (m). Results are given as an average of spot analyses in thin sections.
[b]Number of measurements (analyze spots).

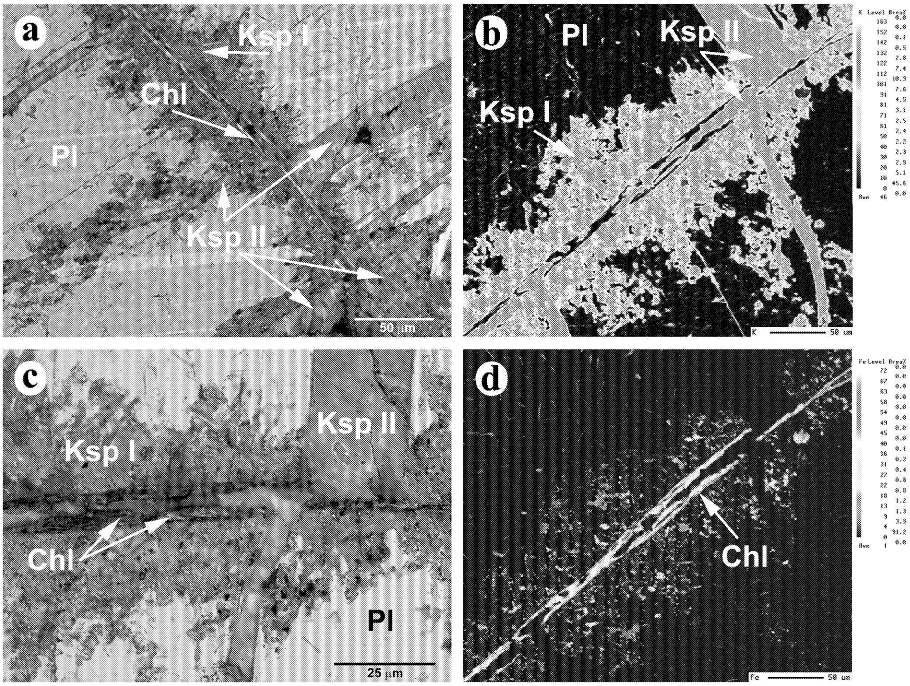

Fig. 6. Early stage hydrothermal alteration minerals in a fractured plagioclase crystal from autochthonous breccia in the central uplift (K-1 599.0 m): submicroscopic masses of K-feldspar (Ksp I) with iron-rich (probably) clay material replace the parent plagioclase (Pl) crystal near the fracture. Fracture walls are covered with authigenic chlorite (Chl) lamellas; fracture itself is filled with euhedral K-feldspar (Ksp II), the latter post-dating both Ksp I and chlorite. (a) and (c) are photomicrographs of a thin section with crossed polarized light; (b) and (d) are K and Fe element distribution maps, respectively.

the authigenic adularia is a pure end-member K-feldspar with Na_2O content of less than 0.1%, whereas the primary microclinic K-feldspar contains up to 1.3% of Na_2O (Table 2).

Chlorite/Corrensite

In all four impactite types at Kärdla, the authigenic chlorite phases, together with Fe-oxyhydrates and/or authigenic quartz, replace hornblende and some pyroxene or biotite crystals in amphibolitic rocks. The XRD results show that the chlorite phases are represented by trioctahedral Fe-rich chlorite, mixed-layered corrensite, and corrensite-chlorite minerals (Kirsimäe et al. 2002). The EPMA analyses revealed three chemically different chlorites: 1) Mg clays; 2) Mg-Fe clays; and 3) Fe clays (Table 3), which probably represent the compositional variation in chlorite, chlorite-corrensite, and corrensite series.

The chlorite veins observed in our study occur as aggregates of microscopic, radially oriented, masses of euhedral flakes lining the walls of fractures and cavities. These fractures and cavities are typically filled with carbonates (Figs. 8a and 8b) and/or quartz. However, in some fracture systems, chlorite was found to be formed after the precipitation of the Ksp I, but before the formation of the Ksp II. In these cases, Ksp II fills the inner part of the vein (Fig. 6c). According to the XRD and EPMA/SEM results, the authigenic chlorite also occurs sparsely throughout the studied sections in all types of the breccia matrix. In the matrix, chlorite and/or corrensite replace both amphibolite and/or devitrified glass clasts (Figs. 8a–8d).

Quartz

The paragenetic relationships suggest the possibility of two generations of authigenic quartz in the studied allochthonus and autochthonous breccia samples: 1) the aggregates (Figs. 7b and 7d) and microscopic intergrowths of quartz (Fig. 7a) associated with the formation of K-feldspar and the chloritization of hornblende/biotite, and 2) quartz

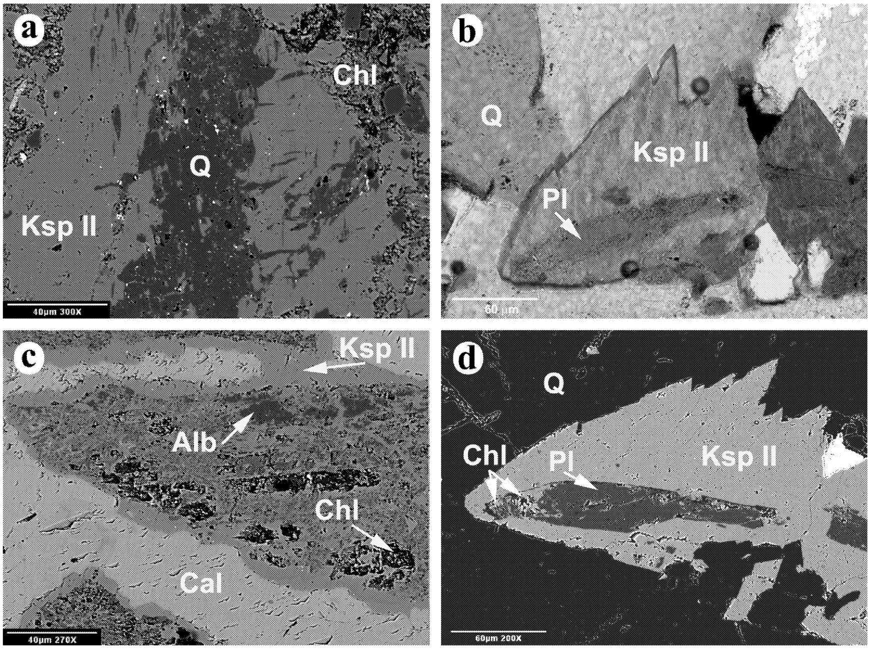

Fig. 7. Euhedral K-feldspar (Ksp II) paragenetic associations: a) Ksp II intergrowth with authigenic quartz (Q) (K-18 398.4 m); b) and d) Ksp II crystals replace plagioclase and grow into authigenic quartz (K-1 599.0 m); c) Ksp II aggregates line the walls of a fracture filled with calcite (Cal), and replace albite (Alb) in the groundmass together with clay minerals (Chl) (P-11 026.4 m). (a), (c), and (d) are secondary electron images; (b) is a photomicrograph with crossed polarized light.

associated with the precipitation of calcite. Bipyramidal hexagonal prisms of authigenic quartz were (macroscopically) observed on the surface of calcite I veins. Macroscopically, these quartz crystals are colorless, transparent, and have no visible inclusions. In thin section, the authigenic quartz occurs in several settings: as xenomorphous crystals and/or aggregates in the groundmass of the autochthonous breccias, or within chlorite masses in altered hornblende and melt clasts (Figs. 7b and 7d; 8c and 8d; respectively). In the latter, authigenic K-feldspar may also be found.

Carbonates

The spatial relationships and morphology of carbonate minerals reveal the presence of dolomite and at least three different calcite morphological generations that fill fractures and cavities in all four impactite types, although the third generation was not noted in any of the allochthonous breccia samples. Calcite occurs as: 1) transparent idiomorphic scalenohedral crystals filling and/or growing at the surface of open cavities between rock clasts or fractures inside the clasts (calcite I) (Fig. 9d); 2) light pink to white semitransparent rhombohedral crystals forming 1 to 2 mm thick veins (calcite II); and 3) transparent idiomorphic ditrigonal prisms or white monocrystals -(calcite III) on the top of 3 to 4 mm thick veins of rhombohedral and/or saddle-shaped dolomite (Fig. 9c). In the breccia matrix, calcite and dolomite also occur as xenomorphous pore/vug fillings (Figs. 9a and 9b). Usually, the cavities are lined with euhedral K-feldspar (Ksp II) and, toward the interior, filled with calcite and dolomite (Figs. 7c, 9a, and 9b). EPMA element mapping also revealed very small (<40–30 µm) K-feldspar particles inside a calcite III vein in one sample (core K-18 at 301.0 m).

Calcite structural lattice parameters indicate that the first and second generations are pure to low-magnesian calcites with 0–4 mol% of $MgCO_3$ and lattice parameters of a, b = 4.988–4.969 Å and c = 17.058–17.004 Å, while the third generation represents a high-magnesian state with 6 mol% of $MgCO_3$ and average lattice parameters of a, b = 4.963 Å and c = 16.965 Å. Iron and/or Mn contents in the second calcite generation are somewhat higher compared to the first and third generations. High Mn and Fe contents are also

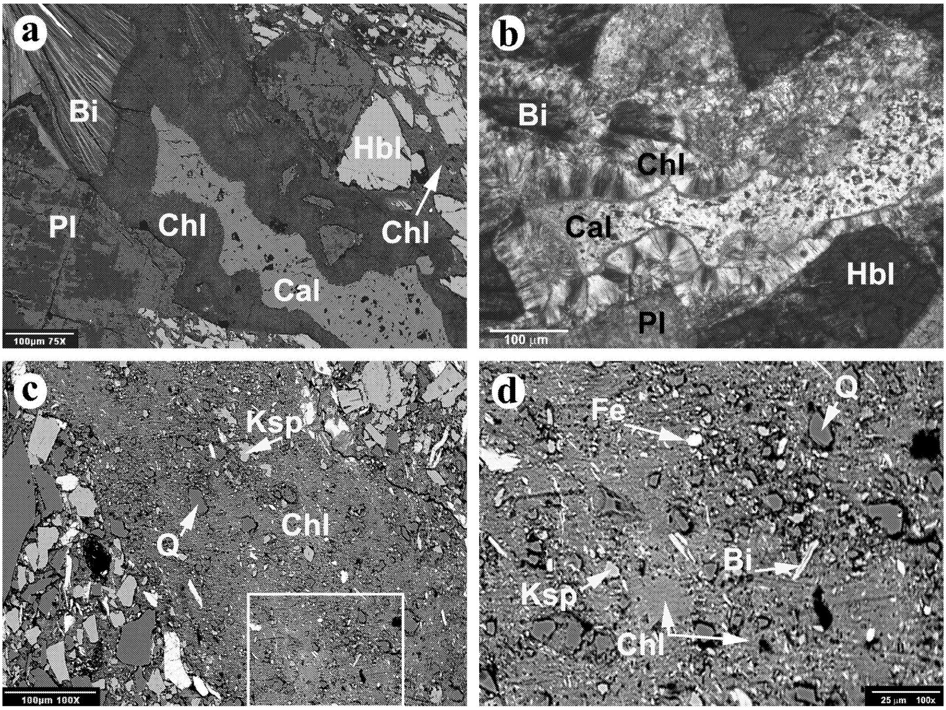

Fig. 8. Additional forms of authigenic clay minerals from autochthonous breccias in the central uplift: a) and b) chloritizied hornblende (Hbl) with chlorite vein of submicroscopic to radially oriented crystallites growing into a vug/void later filled with calcite (Cal) (K-1 603.0 m). Fragments of biotite (Bi) and plagioclase (Pl) crystals can be seen embedded into the chlorite vein. The dark alteration reaction front at the biotite-chlorite contact zone can be observed in the upper left in (a); c) and d) elongated altered melt clast with biotite, authigenic quartz (Q), K-feldspar (Ksp), and Fe-oxyhydrate or sulfide (Fe) crystals in submicroscopic chlorite and/or smectite groundmass (K-1 599.0 m). The flowing texture can be recognized by the chlorite/corrensite submicroscopic groundmass; d) detail of (c) showing a small sphere-shaped altered glassy melt spherule at the lower-middle left, consisting purely of authigenic clay minerals. (a), (c), and (d) are secondary electron images; (b) is a photomicrograph with crossed polarized light.

noticeable in the dolomite structure, having higher Mn and Fe values than typical sedimentary and/or diagenetic dolomites (Reeder 1983; Goldsmith et al. 1961; Table 4).

Fe-Oxyhydrates and Sulfides

Fe-oxyhydrates, hematite, and goethite in autochthonous and allochthonous breccias are mainly associated with carbonate-filled fractures (i.e., veins) and cavities (i.e., vugs). Hematite occurs as abundant spherulitic aggregates inside the calcite I, calcite II, and/or dolomite veins. Hematite is also abundant according to XRD analyses in the reddish colored matrix of the breccias. The latter is mainly present in the interval of 406.4–440.2 m of the resurge breccia in drill core K-12. The reddish interlayering with grayish, and rarely yellowish colored matrix can be also found in the allochthonous breccia and in the breccia pockets in the upper part of autochthonous breccia in drill core K-1. In a few cases, <1 mm thick hematite veins inside fractured and altered amphibolitic basement rocks were observed. Small reddish-brown spherules or spherulitic aggregates of goethite were found on the surface of calcite I, dolomite, and calcite III aggregates. In some samples, goethite spherules are partly intergrown with calcite I scalenohedral crystals (Fig. 9d).

Pyrite and chalcopyrite are the only sulfide minerals present in the Kärdla impactites. Pyrite occurs in a form of rare, small (~0.3–1.0 mm diameter) individual crystals and in some cases also as dendritic aggregates only in the matrix of a greenish-gray variety of fine-grained allochthonous breccia that dominates in drill cores K-1 and K-18. The chalcopyrite is more frequently found throughout K-18, K-12, and F-241 drill cores

Table 4. Electron microprobe analyses of authigenic pore/vug and fracture filling calcite and dolomite in the Kärdla impactites.

	Calcite											
	K-1	K-1	K-18	K-18	K-18	K-18	K-18	K-18	P-11	P-11	Avg.[a]	SD[a]
wt%	597.0	603.0	301.0	365.0	390.4	398.4	401.0	402.0	17.8	24.6	–	–
FeO	0.38	0.16	0.28	0.15	0.16	0.35	0.31	0.17	0.30	0.62	0.38	0.29
MnO	0.94	0.87	1.06	0.62	0.89	1.23	0.88	0.96	0.33	0.52	0.70	0.48
MgO	0.01	n.d.	n.d.	n.d.	n.d.	0.16	0.01	n.d.	0.08	0.05	0.06	0.11
CaO	54.97	54.69	54.49	56.05	53.99	54.71	54.23	55.37	55.45	54.48	54.89	1.05
CO_2	44.09	43.55	43.59	44.62	43.99	44.08	43.69	44.28	44.46	43.88	44.08	0.65
Total	100.39	99.27	99.42	101.44	99.03	100.53	99.12	100.78	100.62	99.55	100.11	–
n[b]	16	8	10	1	1	24	7	3	47	37	154	–

	Dolomite			
	K-18	K-18	Avg.[a]	SD[a]
wt%	301.0	402.0	–	–
FeO	5.76	5.26	5.71	0.46
MnO	1.25	0.82	1.20	0.26
MgO	17.03	15.96	16.92	0.68
CaO	29.48	30.52	29.59	0.95
CO_2	46.04	45.46	45.98	0.67
Total	99.56	98.02	99.40	–
n[b]	26	3	29	–

[a]Average and standard deviation of the authigenic calcite and dolomite in the Kärdla impactites. Sample names are given by the drill core number and depth (m). The results are given as an average of spot analyses in thin sections.
[b]Number of measurements (analyze spots).

in the form of sparse <0.5 mm size tetrahedral crystals or small aggregates on the surface of calcite I or dolomite crystals (Fig. 9c). Associations with carbonate minerals suggest possibly two intervals of chalcopyrite formation. The paragenetic relationship of the rare pyrite with other impact-induced hydrothermal minerals is not clear, neither is its relationship with later galena, sphalerite, and pyrite mineralization within the Ordovician limestones and sandstones overlying the buried crater rims described by Suuroja (2002).

Stable Isotopic Composition of Calcite and Dolomite

According to $\delta^{13}C$ and $\delta^{18}O$ analyses, authigenic calcite and dolomite in the Kärdla breccias are significantly depleted in heavier isotopes (Fig. 10) compared to normal marine carbonates of the same age and from the same area (Ainsaar et al. 1999). This suggests the involvement of light organic carbon and higher formation temperatures during the precipitation (Rye and Ohmoto 1974; Taylor 1974). Similar negative values of heavy carbon isotopes in post-impact hydrothermal calcite were found in the Lockne impact crater, Sweden (Sturkell et al. 1998), which indicates mixing of marine and organic source carbon.

Calcite and dolomite generation temperature calculations indicate that during the precipitation of calcite I, the fluid temperatures were about 75–45 °C, 75–35 °C at dolomite precipitation, around 55–40 °C during the formation of calcite II, and 50–30 °C during the precipitation of calcite III (Fig. 11). In these calculations, the initial fluid $\delta^{18}O$ composition was assumed to be close to the mean Ordovician seawater (–2‰ SMOW; Tobin and Walker 1997). The mean Ordovician seawater was chosen as most probable fluid source for the hydrothermal system at Kärdla due to the results of earlier fluid inclusion studies (Kirsimäe et al. 2002), which show rather low salinity (<13 wt% of $NaCl_{eq}$, mostly ≤5 wt% $NaCl_{eq}$) of the trapped fluids. This suggests that the hydrothermal system was driven by the recharge infiltration of seawater (3.0–3.5 wt% $NaCl_{eq}$) through the disturbed sedimentary cover and fractured crystalline basement.

DISCUSSION

Shock-Metamorphic Effects and Post-Shock Temperatures

Post-shock temperatures in the crater rocks control the formation and development of impact-induced hydrothermal systems and are proportionally related to impact-generated shock wave pressures. The peak shock pressures produced in a meteorite impact range from <2 GPa near the final crater rim to >100 GPa near the impact point (French 1998). The most frequent PDF orientations along the $\{10\bar{1}3\}$ and $\{10\bar{1}2\}$ planes in shocked quartz of the Kärdla impact breccias (Puura et al. 2004) indicate peak shock pressures of 20 to 35 GPa (according to Grieve et al. 1996) and correspond to maximum post-shock temperatures of at least 170–300 °C.

Post-shock temperatures gained from PDFs agree with fluid inclusion homogenization temperature T_h measurements

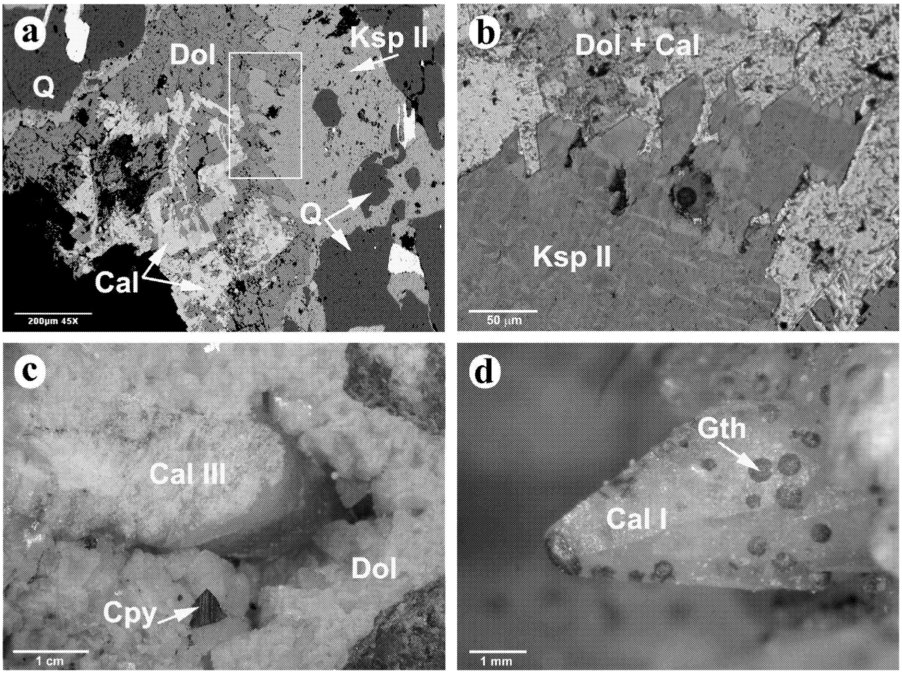

Fig. 9. Voids and fractures filled with authigenic carbonate, quartz, K-feldspar, sulfide, and Fe-oxyhydrate minerals: a) and b) euhedral K-feldspar (Ksp II) on the walls of a fracture filled with dolomite (Dol) and calcite (Cal) (K-18 301.0 m); b) a detail of (a) showing the euhedral structure of K-feldspar II; c) tetrahedral chalcopyrite (Cpy) and white calcite III crystal growing into an empty space of a void lined with earlier 3 to 4 mm thick vein of saddle-shaped dolomite crystals (F-241 219.9 m); d) goethite (Gth) spherulitic aggregates partly grown inside calcite I scalenohedron crystals (F-241 246.4 m). (a) is a secondary electron image and (b) a photomicrograph with crossed polarized light of a thin section; (c) and (d) are photomicrographs of broken surfaces.

and corrensite-chlorite geothermometry (Kirsimäe et al. 2002). The T_h of quartz fluid inclusions formed by impact-generated hydrotherms encompasses a wide range of post-shock temperatures with mean values between 150 and 300 °C. In addition, widespread Fe-chlorite formation in the area of the central uplift signifies maximum equilibrium temperatures of 200–300 °C during the hydrothermal alteration. Chloritization intensity decreases with decreasing fracturing downward into the crater floor, where chlorite occurs in the immediate proximity to the fracture planes only and corrensite prevails within macroscopically unaltered amphibolite blocks, indicating that maximum temperatures in that part were below 200 °C.

The fluid inclusion data indicate that the maximum temperatures reached 400–500 °C directly after the crater formation. No evidence for the presence of high-temperature hydrothermal mineral assemblages (e.g., epidote, garnet, etc.), have yet been found. This suggests that the initial high-temperature stage (>300 °C) was too short for the alteration to achieve equilibrium phases. However, based on the textural relationships and the geothermal modeling by Jõeleht et al. (2005), we suggest that this high-temperature phase can be evidenced by the submicroscopic masses of adularia type K-feldspar which formed at the expense of shock-destructured plagioclase during a high-temperature vapor-dominated alteration stage at temperatures of >300 °C. The following stage of chloritization and formation of microscopic euhedral K-feldspar was followed by carbonate/sulfide/Fe-oxyhydrate precipitation at much lower rate and characterize the latest cooling phase of the system development.

Temperature Evolution and Paragenetic Sequence of Hydrothermal Mineralization

The range of fluid inclusion T_h from 440 to 110 °C (Kirsimäe et al. 2002), chlorite associations equilibrium

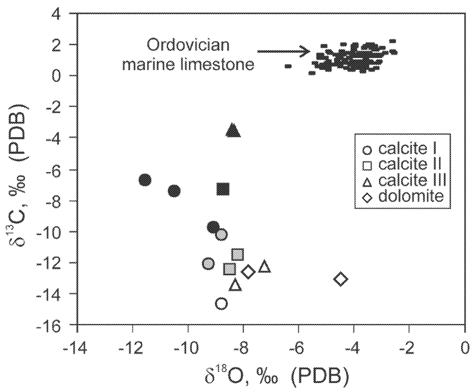

Fig. 10. $\delta^{18}O$ and $\delta^{13}C$ composition of authigenic calcite and dolomite in drill cores K-18 (filled with black), K-12 (filled with gray), and F-241 (filled with white) in comparison with Late Ordovician marine limestone from the crater area (data from Ainsaar et al. 1999). C and O isotope values are given in respect to standard Pee Dee Belemnite (PDB).

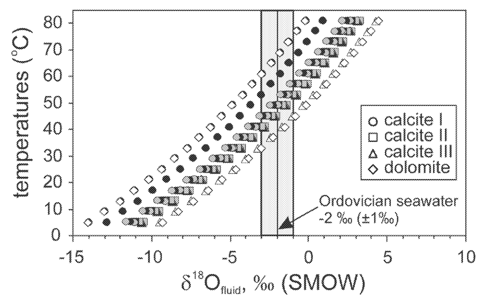

Fig. 11. Temperature versus $\delta^{18}O$ composition of water (Ordovician seawater −2‰) that precipitated the authigenic calcite and dolomite in the Kärdla impactites. The plotted ±1‰ variation range considers a mixing realm with meteoric water. $\delta^{18}O$ values are given in respect to standard mean ocean water (SMOW). For symbolized fillings, see caption of Fig. 10.

formation temperatures from 300 to 150(100) °C (Kirsimäe et al. 2002), and supposed fluid temperatures of <100 °C from calcite and dolomite oxygen isotope equilibrium fractionation temperatures outline the thermal evolution of the hydrothermal system at Kärdla. Based on the above and also on the spatial relationships between the various authigenic phases, we propose a model for the mineral paragenetic sequence of the post-impact hydrothermal system (Fig. 12). Based on mineral associations and the dominant environment regimes, the development of the hydrothermal system can be divided into three stages: 1) early stage vapor-dominated silicate mineralization; 2) middle stage vapor to liquid dominated silicate alteration; and 3) late stage liquid-dominated carbonate-sulfide/Fe-oxyhydrate-quartz mineralization.

The first two stages are characterized by two major silicate mineralization episodes. The submicroscopical K-feldspar was the first mineral that formed at the highest fluid inclusion trapping temperatures of 500–300 °C in the vapor-dominated system. The submicroscopical structure of Ksp I suggests kinetically controlled and rapid crystal growth at a large number of nucleation sites that were simultaneously formed in a vapor dominated fluid, whereas a monoclinic adularia type Al/Si ordering of the feldspar structure indicates moderate to low supersaturation of the fluid with respect to K-feldspar (Worden and Rushton 1992). The high lateral and vertical migration power of the vapor phase resulted in pervasive alteration of shock-destructured plagioclase in various settings within allochthonous and autochthonous breccias. However, the relative abundance of adularia in the Kärdla impactites (Puura et al. 2000, 2004) suggests that the alteration was most intensive in the upper portion of the allochthonous breccias in and around the central peak.

Progressive cooling of the system resulted in a transition from vapor-/steam-dominated fluid to mixed two-phase vapor-liquid dominated fluid at temperatures from 300 to 150 (100) °C. This stage is probably associated with the most intensive chloritization, followed by precipitation of euhedral microcrystalline K-feldspar and quartz in remaining fractures and cavities.

The third stage of mineralization was characterized by the successive precipitation of carbonate minerals, Fe-oxyhydrates, and/or sulfides. The precipitation of calcite/dolomite was controlled by the availability of Ca and Mg ions in fluids convecting in the system, whereas formation of either calcite or dolomite depends on Ca/Mg ratio in the solutions (Reeder 1983). Both Ca and Mg ions were probably supplied by hydrothermal chloritization of amphibole minerals when Ca and some Mg ions were released into the solution by:

$$\mathrm{NaCa_2(Mg, Fe)_5Si_6Al_2O_{22}(OH)_2}\text{ [hastingsite, hornblende]} + 3\mathrm{H_2O} \rightarrow \mathrm{Fe_3(Al_2Si_2O_{10}) \cdot OH_2} \\ \cdot\, \mathrm{(Mg, Fe)_3(O, OH)_6}\text{ [Fe-chlorite]} + 2\mathrm{Ca^{2+}} + 3.5\mathrm{Mg^{2+}} + \mathrm{Na^+} + 0.5\mathrm{Fe^{2+,\,3+}} + 4\mathrm{Si^{4+}} \quad (1)$$

The importance of the amphibole chloritization as the main source for calcium and magnesium ions for carbonate precipitation is also supported by the close spatial relationship between calcite/dolomite veins and amphibolitic rocks. In addition, some calcium ions would have been released by the transformation of plagioclase (An 10–30; Koppelmaa et al. 1996; Puura et al. 2004) into K-feldspar:

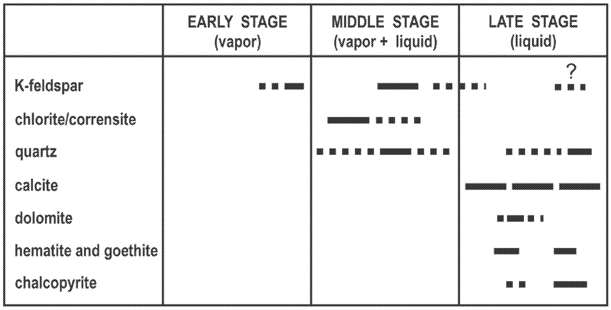

Fig. 12. The post-impact hydrothermal mineralization paragenetic sequence in the Kärdla crater.

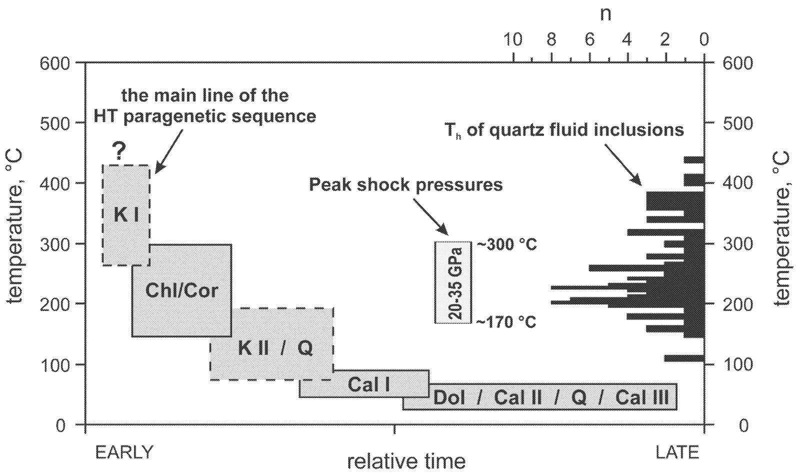

Fig. 13. Decreasing formation temperatures for major post-impact hydrothermal alteration minerals in Kärdla crater. Peak shock pressures (20–35 GPa) after PDF orientations in shocked quartz (Puura et al. 2004) and histogram of quartz aqueous (H_2O-NaCl) fluid inclusion homogenization temperatures (Th) (Kirsimäe et al. 2002) are shown at the right-hand side; K = K-feldspar, Chl/Cor = chlorite/corrensite, Cal = calcite, Dol = dolomite; I, II, III = 1st, 2nd, and 3rd generation, respectively. Formation temperatures are estimated form the chlorite-corrensite geothermometry results (Kirsimäe et al. 2002) and the carbonate minerals stable isotope compositions (Fig. 11).

$$0.8NaAlSi_3O_8{}^*0.2CaAl_2Si_2O_8 \text{ [oligoclase]} + K^+ \rightarrow KAlSi_3O_8 \text{ [K-feldspar]} + 0.8Na^+ + 0.2Ca^{2+} + 0.2Al^{3+} + 0.2Si^{4+} \quad (2)$$

The different morphological and structural generations of calcite reflect the thermal and chemical evolution of the fluids. According to XRD structural refinement, the first two calcite generations are close to pure end member of calcite with less than 5 mol% of Mg, wherein calcite I is practically stoichiometric. Calcite III is remarkably enriched with respect to Mg and represents a Mg-calcite phase. The sequence of carbonate mineral precipitation suggests that calcite I formed in a solution supersaturated with respect to calcite, which resulted in an efficient removal of Ca from the solution, thus, allowing the precipitation of dolomite as the next carbonate phase. Conditions favorable for calcite II precipitation were achieved after Mg removal by dolomite formation. The calcite II generation has abnormally shifted lattice parameters, which suggest involvement of Mn or Fe. The formation of calcite II was followed by precipitation of sulfides and Fe-oxyhydrates, probably at the expense of Fe released by hornblende chloritization (see Reaction 2). In places, goethite spherule intergrowth with calcite I scalenohedral crystals suggests that occasionally the goethite precipitation started shortly before the calcite I ended. Calcite III was the last mineral precipitated in this system, probably at temperatures close to ambient conditions.

The alteration intensity (i.e., abundance of the authigenic phases) varies with location within the structure. At the rim wall, hydrothermal alteration is localized along fractures and impact-injected breccia lenses where the carbonate and sulfide/Fe-oxyhydrate assemblages dominate over the authigenic feldspar-chlorite-quartz minerals. In this zone, the plagioclase K-alteration and hornblende chloritization is restricted to fracture planes and grain boundaries and probably also to metastable impact melt glass/diaplectic glass fragments within the breccia lenses. More prolonged and intense alteration is evident within the crater depression (drill core K-12 and lower part of the K-1 section) where the silicate-clay alteration is dominant. In this area the alteration zones reach progressively outward from the fractures into the host rock, and up to one-third of the plagioclase and hornblende volume is replaced with the authigenic minerals.

Post-impact hydrothermal alteration was most widespread and complete in the upper portion of the allochthonous breccias within and around the central peak. In this area practically all hornblende and plagioclase, along with the impact glass, is replaced mainly by clay (chlorite/corrensite) and K-feldspar minerals.

The variation in alteration intensity is also reflected by the style of the alteration which changes from open-space fracture fillings to a replacement-type of mineralization from the rim walls and deeper parts of the crater toward the upper central areas.

Preliminary heat and fluid transfer simulations in the Kärdla impact structure suggest that the post-impact cooling was rapid (Jõeleht et al. 2005). The highest initial temperatures decreased by 50% from their initial values in 1200–1500 years and by 80% in less than 4000 years after the impact. Initially, the highest temperatures occurred in allochthonous breccias at the central peak, but in a few hundred years the area with the highest temperatures deepened. Comparison of these simulations with the data obtained by this study (Fig. 13) suggests that the main stage of feldspar-chlorite-quartz assemblage formation in Kärdla occurred during a relatively short time, within the maximum of 4000–5000 years after the impact. In the central area of the crater, the last hydrothermal minerals (calcite III, etc.) precipitated probably as late as 10,000 years after the impact, before the ambient conditions were reached.

CONCLUSIONS

In the Kärdla meteorite impact structure, a hydrothermal system was generated by the interaction of impact-heated rocks and intruding seawater. Fluid inclusion studies (Kirsimäe et al. 2002) have shown that the temperatures reached as high as 400–500 °C. Our study demonstrates that the sequence of hydrothermal mineralization with falling temperatures started with precipitation of submicroscopic adularia from vapor-dominated hydrothermal fluids at temperatures greater than 300 °C. This stage was followed by hornblende chloritization during the transition from a vapor- to a liquid-dominated system at temperatures of 300 to 150/100 °C. The second chlorite-feldspar-quartz stage of hydrothermal mineralization was completed by precipitation of microscopic idiomorphic (euhedral) K-feldspar in fractures and cavities in the impact breccia. The final stage was characterized by the sequence of calcite I, dolomite, quartz, calcite II, chalcopyrite/pyrite, Fe-oxyhydrate, and calcite III precipitation at temperatures <100 °C.

The post-impact hydrothermal system studied at Kärdla can be considered as a model for medium to small size impact structures. Its architecture is characterized by pervasive alteration in the upper central area of the crater and by the fracture limited fluid-rock interaction at the rim and in the deeper central portion of the crater depression. The hydrothermal system in Kärdla represents a single thermal event which displays an irreversible cooling path that has resulted in a series of alteration products. The character and the spatial position of the hydrothermal mineralization suggest that geochemical transport was restricted in a "semi-closed" system of fluid-rock interactions.

Acknowledgments–We are grateful to J. Aruväli and T. Martma for their help in carrying out XRD and stable isotope analyses. K. Suuroja and V. Puura are thanked for providing samples, their helpful discussions, and support during the preparation of this paper. D. Stöffler, T. Kenkmann, L. Hecht, R. Tagle, and T. Salge are thanked for many-sided technical support in carrying out EPMA and SEM studies, fruitful and instructive discussions, helpful remarks, and warm hospitality. The Lunar and Planetary Institute and The Barringer Crater Company are thanked for student travel grant awards to Evelin Versh. This work was financially supported by Estonian Science Foundation (grants No. 4541, 5372, 5851); and a DAAD (Deutscher Akademischer Austausch Dienst) research scholarship given to Evelin Versh. We acknowledge the critical reading of the manuscript and numerous suggestions by Drs. L. Hecht, G. Osinski and T. Hode, which significantly improved the manuscript.

Editorial Handling—Dr. Elisabetta Pierazzo

REFERENCES

Ainsaar L., Meidla T., and Martma T. 1999. Evidence for a widespread carbon isotopic event associated with late Middle Ordovician sedimentological and faunal changes in Estonia. *Geological Magazine* 136:49–62.

Ainsaar L., Suuroja K., and Semidor M. 2002. Long-term effects of the Kärdla crater (Hiiumaa, Estonia) on Late Ordovician

carbonate sedimentation. *Deep-Sea Research II* 49:1145–1155.
Allen C. G., Gooding J. L., and Keil K. 1982. Hydrothermally altered impact melt rock and breccia: Contributions to the soil of Mars. *Journal of Geophysical Research* 87:10,083–10,101.
Ames D. E., Watkinson D. H., and Parrish R. R. 1998. Dating of a hydrothermal system induced by the 1850 Ma Sudbury impact event. *Geology* 26:447–450.
Ames D. E., Pope K. O., Jonasson I. R., and Hofmann B. 2002. Chemical sediments associated with the impact-generated hydrothermal system, Vermilion formation, Sudbury structure. *Abstracts with Programs* 34:544.
Cockell C. S. and Lee P. 2002. The biology of impact craters: A review. *Biological Reviews* 77:279–310.
French B. M. 1998. *Traces of catastrophe: A handbook of shock-metamorphic effects in terrestrial meteorite impact structures.* Houston: Lunar and Planetary Institute. 120 p.
Goldsmith J. R., Graf D. L., and Heard H. C. 1961. Lattice constants of the calcium-magnesium carbonates. *American Mineralogist* 46:453–457.
Grahn Y., Nõlvak J., and Paris F. 1996. Precise chitinozoan dating of Ordovician impact events in Baltoscandia. *Journal of Micropaleontology* 15:21–25.
Grieve R. A. F., Langenhorst F., and Stöffler D. 1996. Shock metamorphism of quartz in nature and experiment: II. Significance in geoscience. *Meteoritics & Planetary Science* 31: 6–35.
Hagerty J. J. and Newsom H. E. 2003. Hydrothermal alteration at the Lonar Lake impact structure, India: Implications for impact cratering on Mars. *Meteoritics & Planetary Science* 38:365–381.
Hode T., von Dalwigk I., and Broman C. 2003. A hydrothermal system associated with the Siljan impact structure, Sweden: Implications for the search for fossil life on Mars. *Astrobiology* 3:271–289.
Jõeleht A., Kirsimäe K., Plado J., Versh E., and Ivanov B. 2005. Cooling of the Kärdla impact crater: II. Impact and geothermal modeling. *Meteoritics & Planetary Science*. This issue.
Kirsimäe K., Suuroja S., Kirs J., Kärki A., Polikarpus M., Puura V., and Suuroja K. 2002. Hornblende alteration and fluid inclusions in Kärdla impact crater, Estonia: Evidence for impact-induced hydrothermal activity. *Meteoritics & Planetary Science* 37:449–457.
Komor S. C., Valley J. W., and Brown P. E. 1988. Fluid inclusion evidence for impact heating at the Siljan Ring, Sweden. *Geology* 16:711–715.
Koppelmaa H., Niin M., and Kivisilla J. 1996. About the petrography and mineralogy of the crystalline basement rocks in the Kärdla crater area, Hiiumaa Island, Estonia. *Bulletin of the Geological Survey of Estonia* 6:4–24.
Kraus W. and Nolze G. 1996. POWDER CELL: A program for the representation and manipulation of crystal structures and calculation of the resulting X-ray powder patterns. *Journal of Applied Crystallography* 29:301–303.
Land L. S. 1985. The origin of massive dolomite. *Journal of Geological Education* 33:112–125.
McCarville P. and Crossey L. J. 1996. Post-impact hydrothermal alteration of the Manson impact structure. In *The Manson impact structure, Iowa: Anatomy of an impact crater,* edited by Koeberl C. and Anderson R. R. GSA Special Paper 302. Boulder: Geological Society of America. pp. 347–376.
Mändar H., Vajakas T., Felche J., and Dinnebier R. 1996. AXES: A program for preparation of parameter input files for FULLPROF. *Journal of Applied Crystallography* 29:304.
Naumov M. V. 2002. Impact-generated hydrothermal systems: Data from Popigai, Kara, and Puchezh-Katunki impact structures. In *Impacts in Precambrian shields,* edited by Plado J. and Pesonen L. J. Berlin: Springer. pp. 117–171.
Newsom H. E. 1980. Hydrothermal alteration of impact melt sheets with implications for Mars. *Icarus* 44:207–216.
Newsom H. E., Brittelle G. E., Hibbitts C. A., Crossey L. J., and Kudo A. M. 1996. Impact crater lakes on Mars. *Journal of Geophysical Research* 101:14,951–14,956.
O'Neil J. R., Clayton R. N., and Mayeda T. K. 1969. Oxygen isotope fractionation between divalent metal carbonates. *Journal of Chemical Physics* 51:5547–5558.
Osinski G. R., Spray J. G., and Lee P. 2001. Impact-induced hydrothermal activity within the Haughton impact structure, arctic Canada: Generation of a transient, warm, wet oasis. *Meteoritics & Planetary Science* 36:731–745.
Puura V. and Huhma H. 1993. Paleoproterozoic age of the East Baltic granulitic crust. *Precambrian Research* 64:289–294.
Puura V. and Suuroja K. 1992. Ordovician impact crater at Kärdla, Hiiumaa Island, Estonia. *Tectonophysics* 216:143–156.
Puura V., Kärki A., Kirs J., Kirsimäe K., Kleesment A., Konsa M., Niin M., Plado J., Suuroja K., and Suuroja S. 2000. Impact-induced replacement of plagioclase by K-feldspar in granitoids and amphibolites at the Kärdla crater, Estonia. In *Impacts and the early Earth,* edited by Gilmour I. and Koeberl C. Berlin: Springer. pp. 417–445.
Puura V., Huber H., Kirs J., Kärki A., Suuroja K., Kirsimäe K., Kivisilla J., Kleesment A., Konsa M., Preeden U., Suuroja S., and Koeberl C. 2004. Geology, petrography, shock petrography, and geochemistry of impactites and target rocks from the Kärdla crater, Estonia. *Meteoritics & Planetary Science* 39:425–451.
Rye R. O. and Ohmoto H. 1974. Sulfur and carbon isotopes and ore genesis: A review. *Economic Geology* 69:826–842.
Reeder J. R., ed. 1983. *Carbonates: Mineralogy and chemistry.* Washington D.C.: Mineralogical Society of America. 394 p.
Sturkell E. F. F., Broman C., Forsberg P., and Torssander P. 1998. Impact-related hydrothermal activity in the Lockne impact structure, Jämtland, Sweden. *European Journal of Mineralogy* 10:589–606.
Suuroja K. 2002. Natural Resources of the Kärdla impact structure, Hiiumaa Island, Estonia. In *Impacts in Precambrian shields,* edited by Plado J. and Pesonen L. J. Berlin: Springer. pp. 295–306.
Suuroja K., Suuroja S., All T., and Floden T. 2002. Kärdla (Hiiumaa Island, Estonia): The buried and well-preserved Ordovician marine impact structure. *Deep-Sea Research II* 49:1121–1144.
Suuroja K., Kadastik E., and Mardim T. 1994. *Report of the complex geological mapping in scale 1:50,000 in Hiiumaa Island.* Report No. 4696. Tallinn: Geological Survey of Estonia. In Estonian.
Taylor J. C. 1991. Computer programs for standardless quantitative analysis of minerals using the full powder diffraction profile. *Powder Diffraction* 6:2–9.
Taylor H. P., Jr. 1974. The application of oxygen and hydrogen isotope studies to problems of hydrothermal alteration and ore deposits. *Economic Geology* 69:843–883.
Tobin K. J. and Walker K. R. 1997. Ordovician oxygen isotopes and paleotemperatures. *Palaeogeography, Palaeoclimatology, Palaeoecology* 129:269–290.
Worden R. H. and Rushton J. C. 1992. Digenetic K-feldspar textures: A TEM study and model for diagenetic feldspar growth. *Journal of Sedimentary Petrology* 62:779–789.

Meteoritics & Planetary Science 40, Nr 1, 21–33 (2005)
Abstract available online at http://meteoritics.org

Cooling of the Kärdla impact crater: II. Impact and geothermal modeling

Argo JÕELEHT[1], Kalle KIRSIMÄE[1], Jüri PLADO[1], Evelin VERSH[1], and Boris IVANOV[2]

[1]Institute of Geology, University of Tartu, Vanemuise 46, Tartu 51014, Estonia
[2]Institute of Dynamics of Geospheres, Russian Academy of Sciences, Leninsky Prospect 38/6, Moscow, Russia 117939
*Corresponding author. E-mail: argo.joeleht@ut.ee

(Received 1 June 2004; revision accepted 8 December 2004)

Abstract–Impact and geothermal modeling was performed to explain hydrothermal alteration in a 4 km marine complex crater at Kärdla, Estonia. The impact modeling was used to simulate the formation of the crater and the post-impact temperature distribution in crater environment. The geothermal modeling accounted for coupled heat transfer and multi-phase fluid flow in a variably saturated medium. The modeling results suggest that strong convective fluid flow was initiated. During the first stage, the cooling was rapid due to the effect of the latent heat of vaporization, which efficiently decreased the temperature to the boiling point. The modeling results are consistent with geological observations.

INTRODUCTION

Meteorite impacts and nuclear explosion cratering are events with large amounts of energy being transformed into heat. The physics of the energy release during the formation of these two types of craters are similar. Because military studies of the cratering process were started about 60 years ago, advances in understanding its mechanisms have been considerable. As a result, numerical elastic-plastic modeling tools, which are also applicable in meteorite impact cratering studies, have been developed (e.g., Amsden et al. 1980; Thomson 1979). In recent years, interest in the thermal aspect of cratering has been growing. Temperature is one of the key parameters in equations of state (EOS) and thus also in impact modeling. Although a lot of work is still needed, especially experimental work on the behavior of porous materials, new EOS for different materials allow, for example, estimates of melt production in large craters (O'Keefe and Ahrens 1977; Pierazzo et al. 1997). However, much less attention has been paid to dissipation of heat in craters. A proper understanding of processes in the cooling crater contributes to our knowledge of how ores formed (e.g., in Sudbury, Ivanov and Deutsch 1999a) and hypotheses on the origin and early evolution of life (e.g., Cockell and Lee 2002).

Most of the early attempts to estimate thermal history of craters or the lifetime of possible impact-induced hydrothermal systems used the approximation of a laterally infinite sheet representing a melt or hot suevite layer. Usually, the upper and lower boundaries of the sheet are kept at a constant temperature, allowing diffusion of heat both upward and downward. Naturally, this only provides a rough approximation that holds for the outer part of the crater, where during crater modification hot material is emplaced on top of rocks that have not been heated much by the shock wave. Such an assumption is oversimplified because it describes cooling only in a limited area. In the central part of the crater, the rocks underneath the melt/suevite layer are also heated and, consequently, the cold lower boundary condition is obviously not valid. In addition, even if the heat diffuses downward, which it certainly does, it accumulates at greater depths and it still has to pass the upper layers and escape from the system through the surface at a later time, thus extending the cooling time.

Turtle et al. (2003) made an integrated model for the Vredefort structure, South Africa. As first step, the impact heating was numerically simulated to get the post-impact temperature distribution within the crater. These temperatures were then used as a basis for conductive heat transfer modeling. Unfortunately, the authors provide only a few details on the course of cooling by presenting temperatures immediately after collapse, 0.3 Ma after the impact, at which point the highest temperatures near the surface have disappeared, and 30 Ma years after the collapse, when an equilibrium temperature profile has been achieved. It is difficult to evaluate the time of equilibration because it has not been defined. It could be a few percent of the initial heating (tens of degrees) or equilibrium in the numerical sense, meaning, for example, a small change in temperature during each transient time-step (e.g. 1 µK over 100,000 years). Due to the diffusive nature of conductive heat transfer,

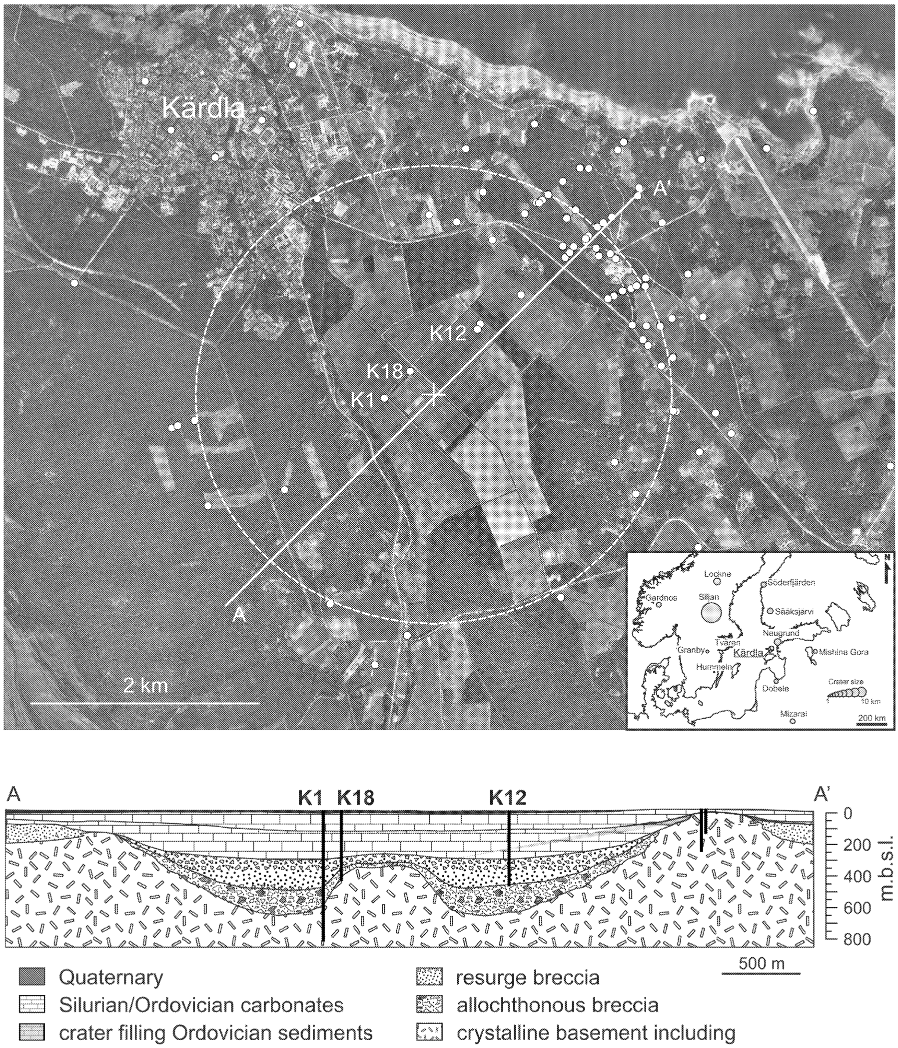

Fig. 1. Location and cross section of the Kärdla structure. White dots on the map denote locations of boreholes. Dashed line and white cross indicate locations of the crater's rim and center, respectively. The white line A-A' indicates the location of the cross section.

the cooling rate becomes smaller and smaller with time and different definitions of thermal equilibrium may be achieved over a very long period of time. Nevertheless, the assumption of conduction as the only heat transfer type is likely to be valid for a crustal-scale thermal model because convection at great depth is probably inhibited due to the low permeability of rocks. Furthermore, radiative heat transfer can be easily masked by uncertainty in thermal conductivity and its pressure-temperature dependencies.

Although convection is suppressed at great depth, geological evidence indicates that hydrothermal systems have developed in many terrestrial craters that vary in size from large (Sudbury, diameter D = 250 km; Allen et al. 1982) to relatively small (Lonar, D = 1.8 km; Hagerty and Newsom 2003). A recent paper by Abramov and Kring (2004) presents the results of numerical modeling of impact-induced hydrothermal convection at Sudbury. The model takes into account the heat of crystallization for the melt layer, heat transfer by conduction, and convective heat transfer by single- or two-phase fluid flow in the saturated porous medium. It also takes into account the reduction of permeability at temperatures above the brittle/ductile transition (360 °C). Indeed, the transition from convective to conductive heat transfer has been observed in present-day geothermal fields (e.g. Muroka et al. 1998), but further investigation is needed to determine whether these conditions (collapse of pores and fractures) are applicable to impactites, which often still preserve shock-produced large cavities and caverns. The permeability value of 10^{-11} darcies (10^{-23} m^2) assumed by Abramov and Kring (2004) for rocks at temperatures above 500 °C is at least two to three orders of magnitude lower than those usually reported for ductile crustal rocks (Manning and Ingebritsen 1999; Ingebritsen and Manning 1999).

Their model results might suffer from poor resolution, which is well demonstrated for the case of reduced breccia thickness. If the thickness of the high-permeability layer equals a single grid cell, then it cannot properly accommodate both the basal thermal boundary layer and the vertical flow part of the convection cell. As a result, the heat removal from the top might be underestimated because of numerical reasons. Nevertheless, Abramov and Kring (2004) demonstrate convincingly that convective heat transfer plays an important role in the cooling of the Sudbury impact crater, and the long-lived hydrothermal system causes hot upwellings and overall cooling from the outside inward.

Rathbun and Squyres (2002) attempted to model impact-induced hydrothermal systems in hypothetical Martian craters where environmental conditions differ from conditions on Earth because the availability of water for maintaining long-period hydrothermal circulation systems is questionable on Mars. Nevertheless, their models might have underestimated the post-impact temperatures, as it is difficult to agree with their assumption of impact heating of only about few tens of degrees at the center of a 7 km diameter crater. Low heating might also be the likely reason why the simulated flow rates of free convection in case of simple crater are about 4 orders of magnitude lower than those of forced convection.

Geological evidence of hydrothermal alteration is observed in the Kärdla impact crater, Estonia (Kirsimäe et al. 2002, Versh et al. 2005). The aims of this paper are to study the time scale and contribution of different thermal processes involved in the cooling of the Kärdla crater by means of numerical heat and multi-phase fluid transfer modeling. In order to estimate heating by the impact and the post-impact temperature distribution, numerical impact modeling of the Kärdla crater has been performed.

GEOLOGICAL SETTINGS

The Kärdla meteorite impact structure, 4 km in diameter, formed in an Ordovician shallow sea shelf about 455 million years ago. The target was composed of granitic basement overlain by 120 m of Cambrian porous siliciclastic rocks and 20 m of Ordovician limestones. The structure is practically uneroded and hosts a complete sequence of impactites and post-impact sediments in an annular trough. Although extensively drilled at the NE rim, the inner structure of the crater is based on only three deep boreholes, which extend to the allochthonous breccia layer (Fig. 1). Two of them (K-18 and K-1 at crater radial distances of 250 and 450 m, respectively) prove the existence of a central uplift and, thus, the complex nature of the crater. The seawater backsurge created at least two gullies (Suuroja et al. 2002) and deposited a sediment layer at least 150 m thick (previously partially interpreted as slumped breccia) that primarily consists of redeposited sedimentary rocks originating outside of the crater. It also contains blocks of allochthonous breccia and fractured basement, which were derived from the rim and probably from the central uplift as well.

Impact-heated rocks in Kärdla were hydrothermally altered as described by Versh et al. (2005) in detail. A parasequence of at least eight hydrothermal phases has been recognized that covers a full range from initial high-temperature to late stage low-temperature associations. The alteration sequence includes secondary K-feldspar, occurring in two morphological generations; Fe-chlorite/corrensite; secondary quartz; three morphologically, chemically, and structurally distinctive generations of calcite; dolomite; chalcopyrite/pyrite; hematite and goethite.

Mineralogical data allow for estimates of the post-impact temperatures. The data, however, are limited because there are only three boreholes inside of the crater that extend to allochthonous breccia layer or deeper. The post-impact temperature estimates are therefore available only for radial distances of 250, 450, and 700 m (boreholes K-18, K-1, and K-12, respectively). They show both vertical and lateral variations. Vertically the highest concentration of hydrothermal minerals is found in the allochthonous breccias in the upper part of the structure, whereas radially the alteration intensity decreases away from the center. In general, the main alumosilicate phase of the hydrothermal alteration (chloritization) occurred at temperatures from 150 to 300 °C (Kirsimäe et al. 2002). It was probably preceded by a precipitation of cryptocrystalline K-feldspar I at somewhat higher temperatures and followed a K-feldspar II at temperatures below 150 °C. The homogenization temperatures of fluid inclusions in the quartz fall into the

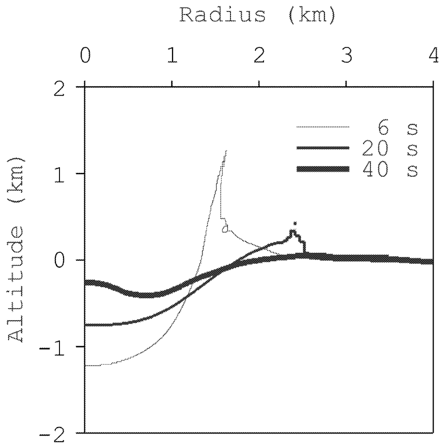

Fig. 2. The simulated shape of the Kärdla crater at the time when maximum depth has been reached (6 s), when excavation in lateral direction stopped (20 s), and when all movement ceased after a slight collapse of the central uplift (40 s).

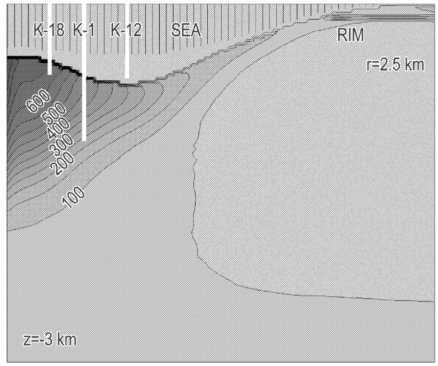

Fig. 3. Post-impact temperature distribution as the basis point for thermal modeling. White lines indicate the approximate location and depth of boreholes K18, K1, and K12. The sea is indicated with hatching; r and z indicate radial and vertical dimensions of the model space, respectively.

same range with the chloritization, but also show temperatures in excess of 400 °C. At later times of hydrothermal circulation, calcite/dolomite and sulfide/Fe-oxyhydrates precipitated at temperatures below 75 °C down to ambient conditions (Versh et al. 2005).

IMPACT MODELING

The formation and modification of the Kärdla impact crater was numerically simulated using the modified version (Ivanov et al. 1997; Ivanov and Deutch 1999b) of the two-dimensional hydrocode SALE (Amsden et al. 1980). The target in Kärdla consisted of four layers as described above, but in the simulations we assumed only a non-layered granite target because 1) no usable equation of state exists for high-porosity sandstone and/or siltstone, and 2) the limestone layer (about 20 m) and water layer (about 100 m) were too thin to essentially affect the simulation results. An analytical equation of state (ANEOS; Thompson and Lauson 1972) for granite was used to describe the pressure and temperature versus density and internal energy of the projectile and the target over a wide range of parameter values. In its central part, the model was discretized to a 10 × 10 m grid.

The size of the projectile and the acoustic fluidization (AF) parameters were determined by trial-and-error to fit the simulated crater diameter and central uplift height to the observed features of the Kärdla structure. A granite projectile of 300 m diameter with vertical velocity of 15 km s^{-1} was assumed. This vertical velocity corresponds to an actual velocity of 21.2 km s^{-1} at the statistically most probable impact angle of 45°. In order to simulate the formation of a central peak by vertical uplift of basement rocks, a relatively low effective kinematic viscosity (lim = 1.6×10^4 m^2 s^{-1}) and decay time of the block oscillations (T_{dec} = 8 s) were required. An oscillation period of 0.1 s was used. More details about scaling of the AF model parameters are presented in Melosh and Ivanov (1999), and in Wünnemann and Ivanov (2003).

According to the modeling results, the maximum crater depth (1.2 km) was reached in 6–7 s, after which the central uplift started to rise (Fig. 2). However, at the same time the excavation in the radial direction continued, and the final crater diameter was achieved about 20 s after the impact. The central uplift continued to rise until 30–35 s after the impact and then collapsed to some extent.

The simulation results suggest that impact-heated rocks are found at two positions. First, a hot layer of brecciated and probably partly melted rocks that are influenced by impact to different degrees. It is formed near the free surface during the crater excavation and modification stages and it extends outside the crater as ejecta blanket. In Kärdla, this layer corresponds to allochthonous breccias lying directly on top of autochthonous breccia. This allochthonous breccia layer is the only location where PDFs in quartz have been found so far (Suuroja 1999; Preeden 2002; Puura et al. 2004). Second, material of the central mound and its closest neighborhood are heated up during shock wave passage and subsequent decompression.

During the first 1/1000th of a second after the impact, pressures up to 200 MPa and temperatures of 14,000–15,000 K occurred at the projectile-target contact. Such extreme conditions were very limited both in space and time. Most of the rocks in the crater area experienced more moderate conditions. The highest simulated post-impact temperatures, which slightly exceed 800 °C, were found in the near-surface part at the center of the uplift (Fig. 3). However, at a radial distance of only 250 m, the temperatures in the uppermost 80 m (corresponding to present day depths of 350–430 m in the borehole K-18) are in the range of 630–650 °C. At a distance of 450 m, temperatures decrease from 480 °C near the surface to about 250 °C at a depth corresponding to the lowermost part of borehole K-1. Temperatures of about 300 °C were simulated at the location of borehole K-12, which penetrates only about 20 m to allochthonous breccias. At the rim the near-surface temperatures were about 100 °C, but further away from the crater temperatures up to 200 °C may have existed in the shocked ejecta fragments and the corresponding deposits.

HEAT AND MASS TRANSFER SIMULATIONS

Governing Equations and Numerical Procedure

Coupled multi-phase flow and heat transfer were solved using a fully implicit 2D axi-symmetric finite difference code. For each component κ (water, air) in phase ψ (liquid, gas) the Darcy flow U (m s^{-1}) is described by (de Marsily 1986; Pruess et al. 1999):

$$U_\psi = -\frac{kk_{r\psi}}{\mu_\psi}(\nabla P_\psi + \rho_\psi g \nabla z) = -\frac{kk_{r\psi}\rho_0 g}{\mu_\psi}(\nabla h_\psi + \rho_r \nabla z) \quad (1)$$

where k is permeability (m^2), k_r is the unitless relative permeability, μ is viscosity (Pa s), P is pressure (Pa), ρ is density (kg m^{-3}), g is the acceleration of gravity (m s^{-2}), z is the elevation above datum (m), $h_\psi = P_\psi/(\rho_0 g) + z$ is hydraulic head (m) of reference density fluid ρ_0, and $\rho_r = (\rho_\psi - \rho_0)/\rho_0$. The mass flux q (kg m^{-2} s^{-1}) is:

$$q_\psi = \rho_\psi U_\psi = -\rho_0 K_\psi(\nabla h_\psi + \rho_r \nabla z) \quad (2)$$

with $K_\psi = kk_{r\psi}\rho_\psi g/\mu_\psi$ as a hydraulic conductivity tensor (m s^{-1}). The mass accumulation term in a compressible porous medium is

$$\rho_0 S_{s\psi} X_\psi^\kappa s_\psi \frac{\partial h_\psi}{\partial t} = -\nabla q_\psi X_\psi^\kappa \quad (3)$$

where

$$S_{s\psi} = \rho_\psi g(\alpha + \varphi\beta_\psi) \quad (4)$$

is the specific storage coefficient (m^{-1}), t is time (s), X is a unitless mass fraction of fluid phase ψ, s is a unitless fraction of porosity occupied by fluid, φ is unitless porosity, and α and β are compressibilities (Pa^{-1}) of rock and fluid, respectively.

After defining fluid pressure head in phase ψ as $h_\psi = h_0 + h_{c\psi}$ with h_0 and $h_{c\psi}$ as the pressure heads of reference fluid and the capillary pressure head, respectively, the total mass balance is obtained by summing accumulations over all components and phases. The capillary pressure head of the water phase is calculated using the van Genuchten function (van Genuchten 1980; Pruess and Garcia 2002):

$$h_c = -\frac{1}{\alpha_{vG}}(s^{-1/\lambda}vG - 1)^{1-\lambda_{vG}} \quad (5)$$

where s is taken equal to water saturation by assuming full and irreducible saturations of 1 and 0, respectively. The fitting parameters of the van Genuchten function $\lambda_{vG} = 0.55$ and α_{vG} = 2.5 have been assumed. The relative permeability is dependent on saturation of phases and was calculated using the Brooks-Corey-Burdine model (Chen et al. 1999).

The change in saturation accounting for accumulations of all phases is:

$$\varphi\rho_0\frac{\partial s_\psi}{\partial t} = -\nabla q_\psi X_\psi^\kappa, \sum_{\psi,\kappa} s = 1 \quad (6)$$

Thermal equilibrium is described by

$$\frac{\partial Q}{\partial t} = \nabla[\lambda\nabla T - (\sum c_\psi q_\psi X_\psi s_\psi)T + L_h(q_l s_l + q_g s_g)X_l] + H \quad (7)$$

where λ is thermal conductivity tensor (W m^{-1} K^{-1}), T is temperature (°C), c is specific heat capacity (J kg^{-1}), L_h is pressure-dependent latent heat of vaporization (J kg^{-1}), and H is radiogenic heat production (W m^{-3}). Subscripts l and g denote liquid and gas phases, respectively. The amount of energy per unit volume (J m^{-3}) is

$$Q = [\sum(\varphi\rho_\psi c_\psi X_\psi) + (1-\varphi)\rho_s c_s]T \quad (8)$$

with subscript s standing for solid rock. If phase change of the fluid in a grid cell occurs, the temperature in this cell is forced to the boiling point temperature until a single phase remains.

Water and steam properties (density, viscosity, compressibility, thermal conductivity, heat capacity, and enthalpy) were calculated as functions of pressure and temperature using “IAPWS Industrial Formulation 1997 for the Thermodynamic Properties of Water and Steam.” Thermal conductivity is the porosity-weighted arithmetic mean of that of rock matrix and fluid. In addition, the thermal conductivity of rock matrix is assumed to be temperature-dependent (Kukkonen and Jõeleht 1996):

$$\lambda_m = \frac{\lambda_r}{1 + B(T - T_r)} + C(T + 273.15)^3 \quad (9)$$

where λ_r is matrix thermal conductivity at room temperature

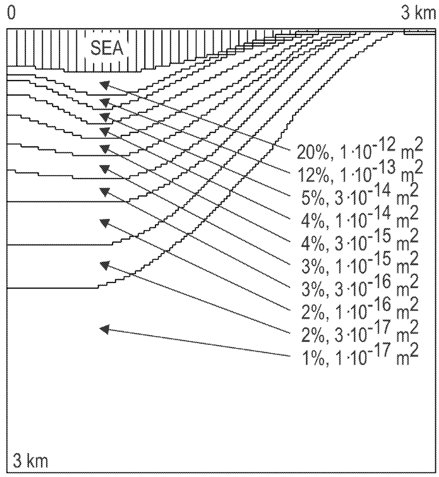

Fig. 4. The porosity and permeability values of the thermal model. The highest porosity and permeability values were applied to resurge deposits (20%, 10^{-12} m^2), whereas the allochthonous breccia and fractured basement were assumed to have gradual decrease of permeability and porosity with depth to 1% and to 10^{-17} m^2.

(T_r = 20 °C). Parameter B = 0.0015 accounts for the decrease of lattice conductivity with an increase of temperature due to thermal expansion. Parameter $C = 5 \times 10^{-11}$ K^{-3} accounts for the radiative heat transfer component, which starts to contribute significantly at temperatures exceeding 800 °C.

To avoid numerical instability, the Il'in scheme (Clauser and Kiesner 1987; Clauser 2003) was applied to the diffusion-convection Equation 7. The Il'in scheme uses local upwinding and is second-order accurate and unconditionally stable.

The fluid flow and heat transport equations are solved in a double-iterative manner. First, a solution of the fluid flow is iteratively obtained. Then, the updated hydraulic head and fluid flow values are used in solving the heat transfer. Updated temperature values are used in the next cycle for updating hydraulic parameters. For steady-state calculations, the hydraulic-thermal cycle is repeated until the maximum temperature change during the cycle is below 1 mK. The convergence criteria for head and temperature fields are 10 μm and 10 μK, respectively. For transient calculations these convergence criteria are 1 μm and 1 μK, respectively. Both fluid flow and heat transfer equations are solved using the "strongly implicit procedure" (Stone 1968). The length of the following time step in the transient calculations is adjusted automatically similarly to the HST3D code (Kipp 1987), so that the maximum change of head, temperature or fluid phase would not exceed 0.1 m, 0.1 K, and 5%, respectively.

Model Space

The model space, 3.0 km in radius and 3.08 km in depth, was discretized with a 20 × 20 m grid and assumed axial symmetry. For each grid cell porosity, permeability, thermal conductivity, and radiogenic heat production values were applied. Porosity and permeability distributions (Fig. 4) are based on available petrophysical data (Plado et al. 1996; 2002; Jõeleht 1995). Relatively high porosity (12%) was assumed for the allochthonous breccia layer. In the deeper, autochthonous part, the porosity decreases gradually from 5% underneath the allochthonous breccia layer to 1% in more distant areas.

The post-impact water saturation in the breccia layers and fractured basement is linked to porosity. The impact process causes fracturing and enhances porosity, but in our view, it does not bring additional water to the rocks either during the shock wave passage or the excavation stage. Thus, rocks have the amount of water corresponding to pre-impact porosity of crystalline rocks (here assumed to be 1%) and the saturation in impactites is inversely proportional to the post-impact porosity (up to 12%). The rest of the pore space is filled by air. The resurge sediments are assumed fully saturated. The post-impact steady-state hydrostatic hydraulic head was used at the start of transient heat and mass transfer modeling.

Compared to porosity, the permeability of the impacted rock units is less well constrained, as there are only a few pumping test data available for Kärdla. The tests in the fractured basement rocks in the north-eastern rim (Kala et al. 1976) yielded permeabilities in the range of 10^{-13}–10^{-12} m^2, which is less than an order of magnitude lower than that of overlaying Cambrian siliciclastic rocks. Pumping in the allochthonous and autochthonous part of the borehole K-18 (at depths of 350–430 m) gave similar results (10^{-12} m^2, Tassa and Perens 1984). Because other deep permeability data are not available, we assumed that permeability decreases gradually with depth similarly to porosity, from 1×10^{-13} m^2 at the allochthonous breccia to background values of the basement (1×10^{-17} m^2) in the more distant areas.

The impact modeling code is not able to account for the resurge flow, yet. The flow, however, did take place and eroded the crater rim and seabed outside of the crater. Resurge sediments are at least 170 m thick (in borehole K-1) and are mainly composed of sedimentary rocks with blocks of allochthonous breccia from the rim and central uplift. Resurge deposits were included in the model by assuming their initial post-impact temperature to be that of seawater (20 °C) and assigning a permeability of 1×10^{-12} m^2, which is typical for the Cambrian sedimentary rocks in the surrounding area.

The thermal conductivity of the allochthonous breccia (2.6 W m^{-1} K^{-1}) is lower than that of the autochthonous breccia and basement (3 W m^{-1} K^{-1}) due to increased porosity (Jõeleht and Kukkonen 1996; Plado et al. 2002). A radiogenic

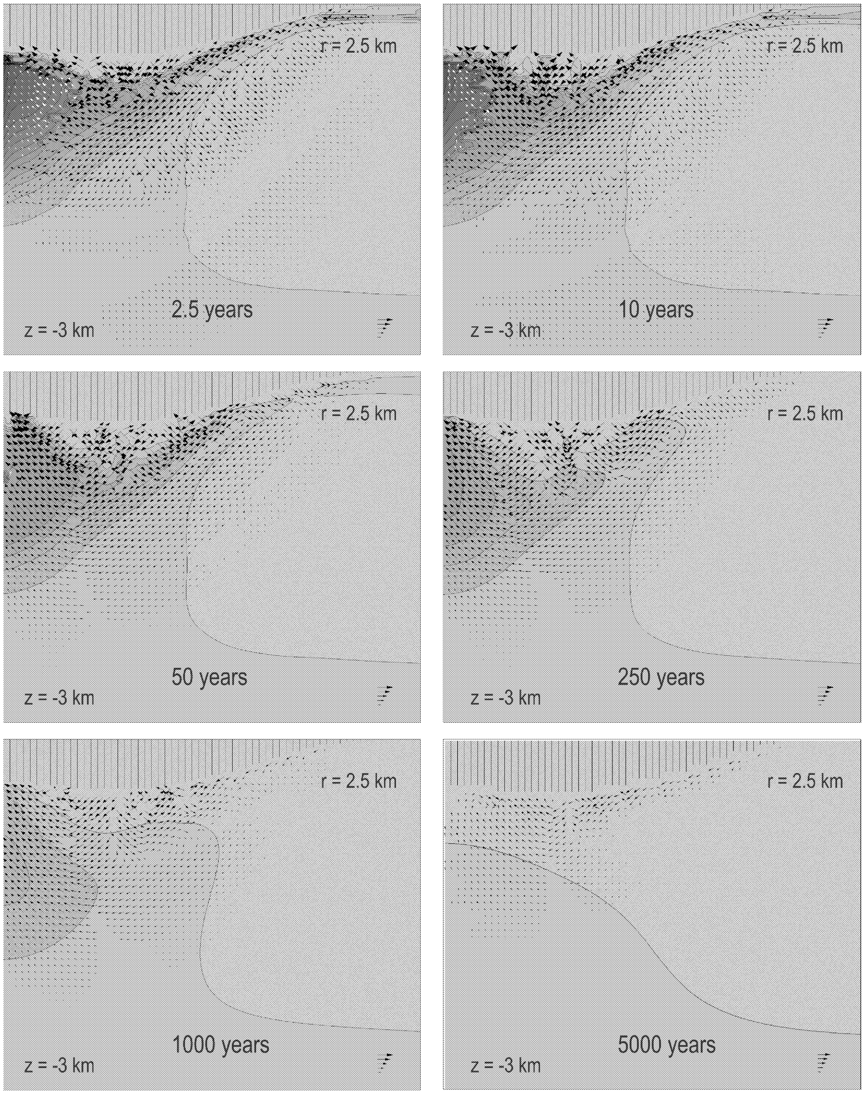

Fig. 5. Simulations suggest that the borehole sites were dominated by liquid water already during the first decade after the impact, but at the central uplift above, boiling point temperatures existed for almost 100 years. The hydrothermal flow continued for several thousands of years and began to cease 9,000–10,000 years after the impact. Temperature isolines are drawn every 50 K, with the outermost contour of 50 °C. Mass flow rates of liquid water (black arrows) and vapor (white arrows) are drawn at the same lognormal scale (bottom right of each figure), with the largest arrow corresponding to 10^{-3} kg m^{-2} s^{-1} and the shortest to 10^{-7} kg m^{-2} s^{-1}; r and z indicate radial and vertical dimensions of the model space, respectively.

heat production of 1 μW m^{-3} was assumed for all rock units (Jõeleht 1995).

A constant temperature (20 °C) and hydraulic head (100 m above the pre-impact seabed) were applied to grid cells corresponding to the seabed. A constant heat flow density (50 μW m^{-2}) was applied to the lower boundary and a no-flow condition was used at lateral sides.

Cooling History

The cooling history of the Kärdla crater can be divided into three periods that were successively dominated by 1) boiling heat effects, 2) convection, and 3) conduction.

The first and the shortest period of cooling was strongly influenced by convective heat transfer with boiling heat effect. The diameter of the vapor-dominated zone decreased to half of its initial 1.6 km size in about 5 years (Fig. 5). The drop of temperature to the boiling point (250–290 °C depending on hydrostatic pressure) took place in a few tens of years in the upper part of the central uplift (permeable allochthonous breccia and upper portion of autochthonous breccia) and lasted for less than a hundred years in the deeper part.

During the first period, the driving force of the convective flow is the large density contrast between liquid water and air/vapor. The simulated mass flow rates of liquid water in the upper part of the section are as high as 10^{-3}–10^{-5} kg m^{-2} s^{-1}. Although these flow rates indicate a strongly convecting environment, the effect of boiling heat overrides all other thermal effects. The latent heat of vaporization of fresh water at hydraulic pressure conditions in Kärdla is 1.3–1.7 MJ kg^{-3}, which corresponds to about 500 K temperature change in the same volume of typical rocks. As a rough estimate, for a rock with 5% porosity that is initially filled with dry air, only the amount of about three pore volumes of water is required to be vaporized in order to decrease the bulk temperature by 100 K. However, in rocks with 12% porosity (such as the allochthonous breccia), only about 1.2 pore volumes of water is needed to be vaporized for the same change in temperature. The high-enthalpy steam flows upwards and discharges energy to the near-surface layers and sea. Since relatively small flow rates can move the vaporization front, the gas phase in the central part of the crater remains poorly saturated with respect to water vapor and thus the rocks were probably not much affected by alteration.

The second period, which started after the most efficient heat removal process has stopped, lasted considerably longer. Nevertheless, heat transfer in the central part of the crater is still dominated by convection. Flow rates continued to remain high because the crater rocks were not fully saturated yet and there was much trapped air that flowed buoyantly toward the surface. Even in the liquid phase saturated medium, the 20% density difference between the recharging cold water and hot water that is close to boiling point causes strong convection as well. The influence of relative permeability, which reduces flow rates in partially saturated media, decreased gradually with time as rocks became more and more saturated with liquid water.

The transition from a system dominated by convective heat transfer to a conduction-dominated system took place 3000–4000 years after the impact. This transition occurs when the flow system Peclet number (the ratio of heat transferred convectively over that transferred conductively) decreases below 1. From a numerical point of view, this means that the sum of the vertical grid Peclet numbers (Clauser and Kiesner 1987) decreases below 1. Although convective heat transfer stops dominating at this point, groundwater flow still continues for a long time and thus may produce low-temperature hydrothermal mineralization.

After some 9000–10,000 years, the impact-induced flow system has ceased. However, thermal equilibration takes a much longer time. Even though the maximum temperature disturbance after 10,000 years is only about 15 K, the heat flow density is two times higher than in surrounding areas and the anomaly could have been easily detected with modern geothermal techniques. The heat flow density anomaly becomes instrumentally undetectable 40,000–50,000 years after the impact.

The above results mainly describe the cooling of the central uplift and its vicinity. The cooling rates and the lengths of respective periods, however, vary in different parts of the crater. Figure 6 shows a family of curves representing the temperature above steady state versus time in grid cells of the topmost one kilometer of the model at different radial distances. At these distances (excluding 0-distance i.e., the crater's center) borehole data are available for comparison. It is evident that cooling to ambient temperatures at the radius of the crater depression (r = 700 m), which in Kärdla has been the main recharge area for the hydrothermal system, was very rapid (Fig. 6). At the slope of the central uplift (the approximate locations of boreholes K-18 [r = 250 m] and K-1 [r = 450 m]) cooling to the boiling point was also very quick (a few years to a few tens of years), but then the temperatures remained more or less constant for a while. This can be attributed to strong convective upward flow of fluids. The flow velocity is so high that partial boiling may occasionally occur as the pressure and boiling point temperature decrease upwards. At the crater's rim (r = 2000 m), the bulk temperatures have not been high, but cooling to ambient conditions took at least few hundred years.

DISCUSSION AND CONCLUSIONS

Numerical models are only approximations due to ambiguity in the parameters and processes involved. These uncertainties exist both in impact and thermal models. In impact modeling, for example, we were not able to incorporate water and sediment layers. Possibly, addition of

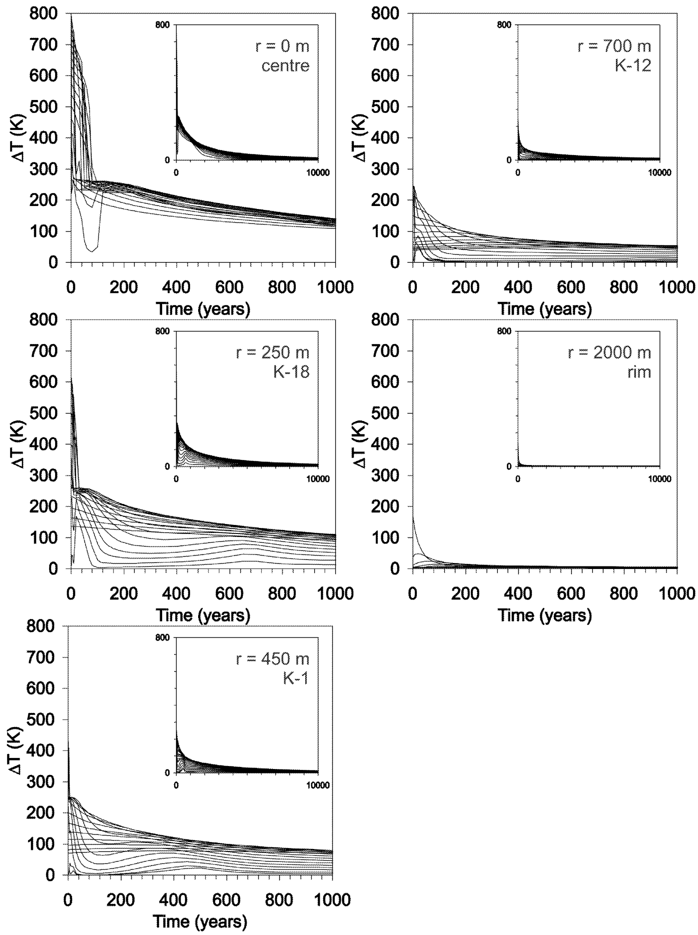

Fig. 6. Temperature above steady state versus time. Each line shows the change of temperature in grid cells of the uppermost 1000 m. The data represents the uppermost 1000 m of the model at radial distances of 0, 250, 450, 700, and 2000 m.

the water layer to the model will not change the post-impact temperature distribution much. However, there is no consensus on the sea depth at the crater site at the time of impact. Different authors estimate sea depth ranging from 20 m (Puura and Suuroja 1992; Ormö and Lindström 2000), to over 50 m (Ainsaar et al. 2002; Suuroja et al. 2002), and up to 100 m (Lindström et al. 1992; Suuroja 1996). Suuroja et al. (2002) admit that the particular type of bioclastic argillaceous-calcareous sedimentation that occurred before and continued after the impact might have taken place at a depth interval from tens to about 200 m. Nevertheless, even in the latter case, the sea depth was less than the size of the projectile, and thus it was not capable to decrease the velocity of the projectile significantly (Shuvalov 2002).

According to laboratory experiments, the impact heating of dry porous sandstones is usually higher than that of non-porous rocks due to compaction-related frictional heating (Ahrens and Gregson 1962; Kieffer et al. 1976). However, it is difficult to predict the thermal behavior of water-saturated porous rock because of massive pore-water vaporization. A

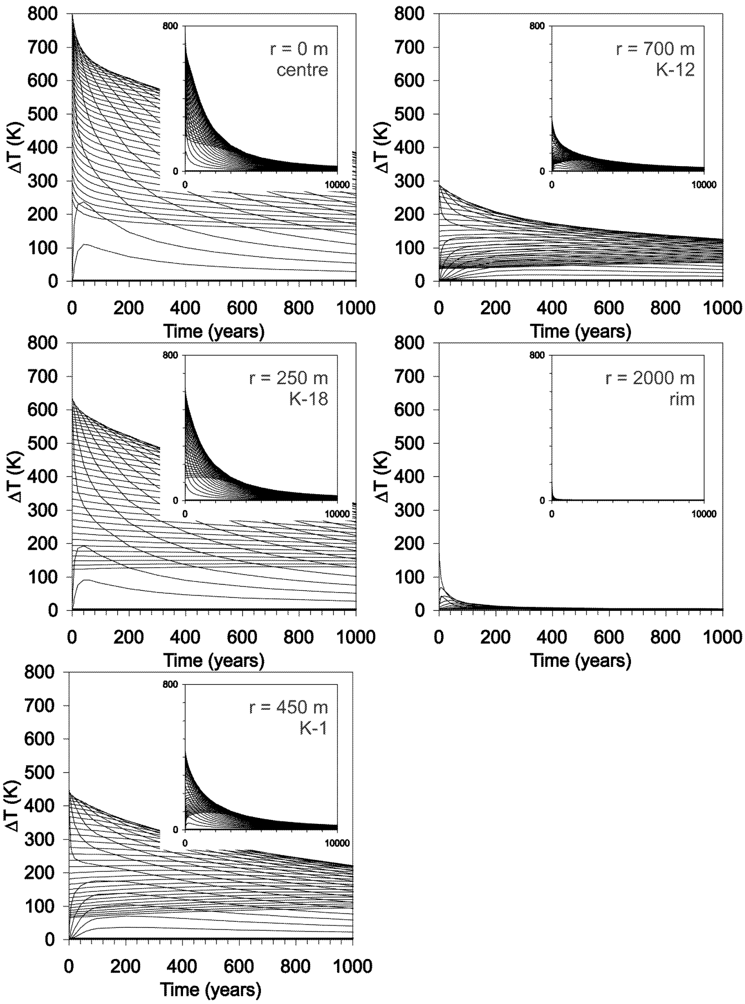

Fig. 7. The same as in Fig. 6, but for the model without convection.

better post-impact temperature estimate requires 3D modeling with proper EOSs and the resurge flow included. This task extends beyond the aims and capabilities of this work.

The seawater depth has only a small effect on thermal modeling. Even for the shallowest estimates, there was still at least 200 m of water column inside of the crater. Compared to the obtained results above, a 100 m lower water column decreases the boiling temperature by a few tens of degrees and the latent heat of vaporization increases by about 10%, whereas the effects due to a 100 m higher water column are even smaller. Although sea depth variations have a minor effect inside the crater, they might be more important at the rim. If the highest parts/peaks of the rim rose above sea level, they became groundwater recharge areas instead of being places where hot water discharged to the sea. However, there is no evidence to either support or reject the hypothesis of flow direction reversal.

Permeability is the key parameter in hydrothermal convection systems because it controls fluid flow rates in the rocks. In Kärdla, the permeability data are insufficient for a full description of the crater rocks. The values we have used provide only a qualitative picture of the actual system. Furthermore, permeabilities used in the model characterize the present-day situation, which incorporates permeability reduction due to compaction and closure of pores/fractures by mineral precipitation. We, however, do not account for a temporary decrease of permeability at temperatures above brittle/ductile transition as it is described by Abramov and Kring (2004), because the main part of the pores/caverns and fractures of the allochthonous and autochthonous breccias are due to impact deformation of the rocks and have not been erased by the ductile behavior of rocks. This ambiguity in permeability is still great due to the relative permeability that reflects obstructed flow conditions in an air/liquid-saturated medium. Consequently, the flow rate depends on the initial post-impact pore pressure and water saturation of the rocks, factors that we could only guess. The modeling, however, suggests that an exact knowledge of the initial saturation is not crucial to the final results. Initially, the highest liquid water flow rates occur at the hydrothermal systems' recharge area in the upper part of the section, where the intrinsic permeability and water saturation are also highest. Although the suction due to the air/water density contrast is large, the relative permeability forces the liquid water flow to be more intrusion-like because the flow rates within the intrusion are larger than at its edges. From the thermal point of view, the permeability variation can change the timing of transitions from the vaporization-dominated stage to convection-dominated, and to conduction-dominated stages, but it cannot cancel the existence of these stages.

Nevertheless, a proper knowledge of the permeability structure is important because it can modify the shape of the entire flow system. The present results are based on the assumption that there is a quite strong gradual decrease of permeability with depth (Fig. 4). Therefore, the upper part of the section cools down faster than the deeper section. However, additional test models suggest that if the decrease of permeability with depth is smaller, then the flow system becomes deeper. This implies that the deeper part of the central uplift becomes vapor-free earlier than the upper part, which is heated by rising steam. Supposedly, these two cases should be mirrored by differences in the intensity of hydrothermal alteration and the isotopic composition of the precipitates, but the geological information gathered so far is insufficient to prove it.

Two initial conditions in the cooling modeling, the water saturation and hydraulic head, have been guessed. The water saturation is based on an assumption that no additional water is brought into the impact-created pores during the crater formation and the rocks contain the same amount of water that existed in the rocks before the impact. In our view, it is unlikely that water enters into the pores not only during the shock wave passage but also during the excavation stage because, according to impact modeling in shallow marine conditions, the cavity expands faster in water than in rocks (Shuvalov 2002) and no source for additional water exists. We assumed that the rest of the pore space is filled by air. Although the latter is probably true for the near-surface layers, it is questionable for the deeper part of the crater because there might not have been enough time for air to flow to the deeper sections during the craters' formation and modification stages. It could mean that a limited amount of air still existed in pores of the deeper part of the structure but pore fluids were in underpressure conditions. This is the opposite of our transient modeling assumption of hydrostatic hydraulic head as a starting condition that more likely suggests overpressure conditions in the impactites. The hydrostatic pressure is, however, valid for the laterally distant areas and probably also for the deep sections that were not affected by the impact.

The modeling results indicate that the hydraulic quasi-equilibrium in the deeper part of the model is achieved in about 1–1.5 years. This is the time required to get the excess air out of the model and represent the uncertainty associated with the saturation process. Although there might not be air that must escape from the pores before water can intrude, the water phase is discontinuous and a relative permeability effect is applicable to such an environment. We estimate that the error due to an improper hydraulic starting condition is much smaller than the ambiguity due to other parameters such as permeability or relative permeability.

In order to demonstrate the importance of convective heat transfer, a model with only conductive heat transfer (Fig. 7) has been carried out. In this case, the simulated cooling period is much longer, and within the depth range of the autochthonous breccias temperatures above 300 °C could have lasted for thousands of years. It is, however, noticeable that the initially hottest part of the section (corresponding to the allochthonous breccia) cooled by several hundreds of degrees during the first century. The cooling of the allochthonous layers would be even more rapid if resurge deposits did not cover them.

Regardless of the ambiguity in parameters, the model results are broadly consistent with mineralogical observations (Versh et al. 2005), although, at the first sight, the simulated post-impact temperatures are too high at the center. At the radial distance of 250–450 m, simulated temperatures of up to 500–650 °C would allow formation of a high-temperature hydrothermal mineral assemblage made of garnet, actinolite and/or epidote, but so far, these minerals have not been identified in drill cores K-18 or K-1. Kirsimäe et al. (2002) proposed that the absence of these mineral assemblages is because the initial high-temperature stage (>300 °C) was too short for alteration to achieve equilibrium for high temperature phases. Numerical simulations support this hypothesis, but also suggest that the low water saturation of the air phase may have played an important role. Initially, the rocks were filled with dry air, which probably inhibited the hydrothermal alteration until the air became more saturated by water vapor. This happened only in the vicinity of the boiling front, which moved quickly towards the center and also caused a rapid drop in temperature. Even near the boiling front, the air tends to be undersaturated because the steam is mixed with dry air that escapes from greater depths.

Based on the impact simulations, the rim is relatively unaffected thermally, and post-impact temperatures reaching the boiling point can be associated only with the allochthonous breccia either in the form of injection dikes or the ejecta layer. These results are in agreement with mineralogical observations indicating that, for example, the K-feldspar I that might be related to the near-boiling conditions occurs only in allochthonous injection dikes, whereas the rest of the rock is barely affected by any hydrothermal alteration. Moreover, high temperature mineral alteration at the rim is restricted to fracture planes and grain boundaries, which also implies a very short duration of these processes. However, it is obvious that mineralogical observations at individual locations may reveal much higher (maximum) temperature estimates compared to the numerical modeling, which produces only bulk average estimates over the 20 × 20 m grid spacing used.

The cooling of crater rocks is site-specific, depending on distance from the center and depth. The fastest cooling occurs at the groundwater recharge area, which in the case of Kärdla is at the crater depression. The central uplift works like a chimney that keeps the fluid flowing toward the center and upward. This also implies that the precipitation of different hydrothermal minerals/generations occurs simultaneously at different locations. At the time when Fe oxyhydrates, calcite, or other low-temperature alteration products are formed at the crater depression area, the central part may still be at vapor-dominated conditions with high-temperature alteration products.

In conclusion, we suggest that post-impact cooling of the Kärdla crater was rapid and driven by convective heat transfer during the early phases of the development. The highest post-shock temperatures in the central area of the structure decreased by 50% from their initial values in 1200–1500 years and by 80% in less than 4000 years after the impact. The transition from a system dominated by convective heat transfer a conduction-dominated system took place about 3000–4000 years after the impact, whereas it took about 9000–10,000 years for the impact-induced hydrothermal flow system to cease. However, the thermal equilibration of the impact-heated rocks took a much longer time and the heat flow density anomaly became instrumentally undetectable only 40,000–50,000 years after the impact.

The validity of the numerical heating-cooling model for Kärdla structure is supported by geological observations, which are well constrained both for maximum temperature and temperature field distribution. This emphasizes the strong need for linking between complex numerical modeling and geological studies.

The numerical modeling example of the Kärdla structure demonstrates the importance of convective heat transfer in the development of Earth and probably also Mars-based impact structures. The cooling rates of impact-heated rocks in a water-saturated environment can be much higher than believed so far.

Acknowledgments–We appreciate comments and suggestions by J. Melosh, H. Henkel, and an anonymous reviewer. This study has been supported by the Estonian Science Foundation through grants 4541 and 5851. For the orthophoto in Fig. 1, the Estonian Land Board is acknowledged.

Editorial Handling—Dr. Elisabetta Pierazzo

REFERENCES

Abramov O. and Kring D. A. 2004. Numerical modeling of an impact-induced hydrothermal system at the Sudbury crater. *Journal of Geophysical Research* 109, doi:10.1029/2003JE002213.

Ahrens T. J. and Gregson V. G. 1962. Shock compression of crustal rocks: Data for quartz, calcite and plagioclase rocks. *Journal of Geophysical Research* 69:4839–4874.

Ainsaar L., Suuroja K., and Semidor M. 2002. Long-term effect of the Kärdla crater (Hiiumaa, Estonia) on Late Ordovician carbonate sedimentation. *Deep-Sea Research Part II* 49:1145–1155.

Allen C. G., Gooding J. L., and Keil K. 1982. Hydrothermally altered impact melt rock and breccia: Contributions to the soil of Mars. *Journal of Geophysical Research* 87:10,083–10,101.

Amsden A. A., Ruppel H. M., and Hirt C. W. 1980. SALE: A simplified ALE computer program for fluid flow at all speeds. Los Alamos National Laboratory Report LA-8095. 101 p.

Chen J., Hopmans J. W., and Grismer M. E. 1999. Parameter estimation of two-fluid capillary pressure saturation and permeability functions. *Advances in Water Resources* 22:479–493.

Clauser C., ed. 2003. *Numerical simulation of reactive flow in hot aquifers.* Berlin-Heidelberg: Springer Verlag. 332 p.

Clauser C. and Kiesner S. 1987. A conservative, unconditionally stable, second-order three-point differencing scheme for the diffusion-convection equation. *Geophysical Journal of Royal Astronomical Society* 91:557–568.

Cockell C. S. and Lee P. 2002. The biology of impact craters–A review. *Biological Reviews* 77:279–310.

Hagerty J. J. and Newsom H. E. 2003. Hydrothermal alteration at the Lonar Lake impact structure, India: Implications for impact cratering on Mars. *Meteoritics & Planetary Science* 38:365–381.

Ingebritsen S. E. and Manning C. E. 1999. Geological implications of a permeability-depth curve for the continental crust. *Geology* 27:1107–1110.

Ivanov B. A., DeNiem D., and Neukum G. 1997. Implementation of dynamic strength models into 2D hydrocodes: Applications for

atmospheric breakup and impact cratering. *International Journal of Impact Engineering* 20:411–430.
Ivanov B. A. and Deutsch A. 1999a. Sudbury impact event: Cratering mechanics and thermal history. In *Large meteorite impacts and planetary evolution II,* edited by Dressler B. and Grieve R. A. F. Boulder, Colorado: Geological Society of America. pp. 389–397.
Ivanov B. A. and Deutsch A. 1999b. The phase diagram of $CaCO_3$ in relation to shock compression and decomposition. *Physics of the Earth and Planetary Interiors* 129:131–143.
Jõeleht A. 1995. Petrophysical properties of Estonian bedrock. Tallinn, Estonia: Geological Survey of Estonia.
Jõeleht A. and Kukkonen I. T. 1996. Heat flow density in Estonia–Assessment of palaeoclimatic and hydrogeological effects. *Geophysica* 32:291–317.
Kala E., Suuroja K., and Tassa V. 1976. Ottshot o predvaritelnoi razvedke granitoidov mestorozhdenija Palukjula. Tallinn, Estonia: Estonian Geological Survey. In Russian.
Kieffer S. W., Phakey P. P., and Christie J. M. 1976. Shock processes in porous quartzite: Transmission electron microscope observations and theory. *Contributions to Mineralogy and Petrology* 59:41–93.
Kipp K. L. 1987. HST3D: A computer code for simulation of heat and solute transport in three-dimensional ground-water flow systems. Denver: U.S. Geological Survey.
Kirsimäe K., Suuroja S., Kirs J., Kärki A., Polikarpus M., Puura V., and Suuroja K. 2002. Hornblende alteration and fluid inclusions in Kärdla impact crater, Estonia: Evidence for impact-induced hydrothermal activity. *Meteoritics & Planetary Science* 37:449–457.
Kukkonen I. T. and Jõeleht A. 1996. Geothermal modelling of the lithosphere in the central Baltic shield and its southern slope. *Tectonophysics* 255:25–45.
Lindström M., Flodén T., Puura V., and Suuroja K. 1992. The Kärdla, Tvären and Lockne craters–Possible evidences of an Ordovician asteroid swarm. *Eesti Teaduste Akadeemia Toimetised* 41:45–53.
Manning C. E. and Ingebritsen S. E. 1999. Permeability of the continental crust: Implications of the geothermal data and metamorphic systems. *Reviews of Geophysics* 37:127–150.
Melosh H. J. and Ivanov B. A. 1999. Impact crater collapse. *Annual Review of Earth and Planetary Sciences* 27:385–415.
Muraoka H., Uchida T., Sasada M., Yagi M., Akaku K., Sasaki M., Doi N., Saito S., Sato K., and Tanaka S. 1998. Deep geothermal resources survey program: Igneous, metamorphic and hydrothermal processes in a well encountering 500 °C at 3729 m depth, Kakkonda, Japan. *Geothermics* 27:507–534.
O'Keefe J. D. and Ahrens T. J. 1977. Impact-induced energy partitioning, melting, and vaporization on terrestrial planets. Proceedings, 8th Lunar Science Conference. pp. 3357–3374.
Ormö J. and Lindström M. 2000. When a cosmic impact strikes the seabed. *Geological Magazine* 137:67–80.
Pierazzo E., Vickery A. M., and Melosh H. J. 1997. A reevaluation of impact melt production. *Icarus* 127:408–423.
Plado J., Pesonen L., Elo S., Puura V., and Suuroja K. 1996. Geophysical research on the Kärdla impact structure, Hiiumaa Island, Estonia. *Meteoritics & Planetary Science* 31:289–298.
Plado J., Jõeleht A., and Šogenova A. 2002. Physical properties. In: *Soovälja (K-1) drill core,* edited by Põldvere A. *Estonian Geological Sections* 4:21–24.
Pruess K. and Garcia J. 2002. Multiphase flow dynamics during CO_2 disposal into saline aquifers. *Environmental Geology* 42:282–295.
Pruess K., Oldenburg C., and Moridis G. 1999. TOUGH2 user's guide. Version 2.0. Report LBNL-43134. Berkeley, California: Lawrence Berkeley National Laboratory.
Preeden U. 2002. Löögimoonde jälgedega kvarts ja selle asend Kärdla meteoriidikraatris. Bachelor's thesis, University of Tartu, Tartu, Estonia. In Estonian.
Puura V. and Suuroja K. 1992. Ordovician impact crater at Kärdla, Hiiumaa Island, Estonia. *Tectonophysics* 216:143–156.
Puura V., Huber H., Kirs J., Kärki A., Suuroja K., Kirsimäe K., Kivisilla J., Kleesment A., Konsa M., Preeden U., Suuroja S., and Koeberl C. 2004. Geology, petrography, shock petrography, and geochemistry of impactites and target rocks from the Kärdla crater, Estonia. *Meteoritics & Planetary Science* 39:425–451.
Rathbun S. W. and Squyres J. A. 2002. Hydrothermal systems associated with Martian impact craters. *Icarus* 157:362–372.
Shuvalov V. 2002. Numerical modeling of impacts into shallow sea. In *Impacts in precambrian shields,* edited by Plado J. and Pesonen L. J. Berlin-Heidelberg: Springer Verlag. pp. 323–336.
Stone H. L. 1968. Iterative solution of implicit approximations of multidimensional partial differential equations. *SIAM Journal on Numerical Analysis* 5:530–558.
Suuroja K. 1996. Formation and development of the Kärdla impact structure. M.Sc. thesis, University of Tartu, Estonia.
Suuroja S. 1999. Kärdla kraatri bretšade litoloogia. Master's thesis, University of Tartu, Estonia. In Estonian.
Suuroja K., Suuroja S., All T. and Flodén T., 2002. Kärdla (Hiiumaa Island, Estonia)—The buried and well-preserved Ordovician marine impact structure. *Deep-Sea Research Part II* 49:1121–1144.
Tassa V. and Perens R. 1984. Ottshot o poiskah mineralnyh vod dlja mezhkolhoznogo sanatorija na o. Hiiumaa. Tallinn, Estonia: Estonian Geological Survey. In Russian.
Thomson S. L. 1979. CSQIII: An Eulerian finite difference program for two-dimensional material response: users manual. Albuquerque, New Mexico: Sandia National Laboratories.
Thompson S. L. and Lauson H. S. 1972. Improvements in the chart D radiation-hydrodynamic code III: Revised analytical equation of state. Albuquerque, New Mexico: Sandia National Laboratories.
Turtle E. P., Pierazzo E., and O'Brien D. 2003. Numerical modelling of impact heating and cooling of the Vredefort impact structure. *Meteoritics & Planetary Science* 38:293–303.
van Genuchten M. Th. 1980. A closed-form equation for predicting the hydraulic conductivity of unsaturated soils. *Soil Science Society of America Journal* 44:892–898.
Versh E., Kirsimäe K., Jõeleht A., and Plado J. 2005. Cooling of the Kärdla impact crater: I. The mineral parasequence observations. *Meteoritics & Planetary Science*. This issue.
Wünnemann K. and Ivanov B. A. 2003. Numerical modeling of the impact crater depth-diameter dependence in an acoustically fluidized target. *Planetary Space Science* 51:831–845.

ARTICLE IN PRESS

ELSEVIER

Available online at www.sciencedirect.com

ScienceDirect

Planetary and Space Science ▮ (▮▮▮▮) ▮▮▮–▮▮▮

Planetary and Space Science

www.elsevier.com/locate/pss

Development of potential ecological niches in impact-induced hydrothermal systems: The small-to-medium size impacts

Evelin Versh, Kalle Kirsimäe*, Argo Jõeleht

Institute of Geology, University of Tartu, Vanemuise 46, 51014 Tartu, Estonia

Accepted 2 December 2005

Abstract

Effect of meteorite impact on the biological evolution is usually considered by its catastrophic consequences. However, the impacts can create opportunity for other organisms and the structures themselves can serve as suitable ecological niches (oases) for life. In this contribution we present results of modeling of an impact-induced hydrothermal (IHT) system in a small-to-medium sized impact crater, where the development of zones habitable for primitive hydrothermal thermophilic and hypethermophilic microorganisms was studied. The impact and geothermal modeling was verified against the 4-km diameter Kärdla complex structure, Hiiumaa Island, Estonia. If there is an sufficient amount of water present in the target (e.g., sea cover, groundwater or permafrost resources) then the differential temperature fields created by the impact initiate a hydrothermal circulation system within the crater. The results of transient fluid flow and heat transfer simulations in Kärdla suggest that immediately after impact the temperatures in the central area, which contains the most hydrothermal alteration, were well above the boiling point. However, due to efficient heat loss at the groundwater vaporization front, the vapor-dominated area disappears within a few decades. In the central uplift area, the conditions favorable for thermophilic microorganisms (temperatures $<100\,^{\circ}$C) were reached in 500–1000 years after the impact. The overall cooling to ambient temperatures in the deeper parts of the central uplift lasted for thousands of years. In the crater depression and rim area the initial temperatures, suggested by the impact modeling, were much lower—from 150 °C to ambient temperatures, except locally in fracture zones and suevite pockets. Our data suggest that in small-to-medium size impact craters with insignificant melting, the suitable conditions for hydrothermal microbial communities are established shortly (tens to few hundreds of years as maximum) after the impact in most parts of the crater. In the central uplift area the microbial colonization is inhibited for about a thousand years. However, this is the area, which afterwards retains the optimum temperatures (45–120 °C) needed for hydrothermal microorganisms for the longest period. Geochemical and mineralogical data suggest, in general, neutral pH 7($\pm$1) fluid of the IHT system, which is, when compared to volcanic hydrotherms, richer in dissolved oxygen and poor in reduced compounds. This suggests the preference for sulfur-reducing microorganisms in the possible impact-induced hydrothermal communities.

Keywords: Meteorite crater; Hydrothermal systems; Geothermics; Habitat; Microorganisms

1. Introduction

Meteorite impact events are mostly known to public by their catastrophic consequences. Impact heating and the super-high pressures wipe out all living matter at the immediate vicinity of the impact site, and in the case of large-scale impacts, the biological devastation may obtain a global scale. At the same time, the cooling impact structures may have served as suitable ecological niches for life (e.g., Cockell and Lee, 2002). This is the case particularly for present day preferential microbial colonization of the shocked rocks compared to the unshocked or low-shocked rocks in the ~23 Ma Haughton crater, Arctic Canada (Cockell et al., 2002). Furthermore, the impact-induced endolithic habitats (pores and fractures) would have served as potential refuges from ultraviolet radiation already for earliest Archean microorganisms (Cockell, 2004).

*Corresponding author. Tel.: +372 7375 894; fax: +372 7375 836.
E-mail addresses: evelin.versh@ut.ee (E. Versh), kalle.kirsimae@ut.ee (K. Kirsimäe), argo.joeleht@ut.ee (A. Jõeleht).

0032-0633/$ - see front matter © 2006 Elsevier Ltd. All rights reserved.
doi:10.1016/j.pss.2005.12.022

Please cite this article as: Evelin Versh et al., Development of potential ecological niches in impact-induced hydrothermal systems: The small-to-medium size impacts, Planetary and Space Science (2006), doi:10.1016/j.pss.2005.12.022.

If there is sufficient amount of water present in the target (e.g., impacts into sea, groundwater or permafrost resources) the differential temperature fields created by the impact can initiate a hydrothermal circulation system within the crater. Evidences of impact-induced hydrothermal (IHT) activity have been found at a number of terrestrial impact structures (e.g., Naumov, 2002), this phenomenon is also suggested for extraterrestrial craters (Newsom, 1980; Newsom et al., 1996). While volcanic hydrothermal systems have been found to support life on Earth (Corliss et al., 1979) there is no well-documented evidence for life at IHT systems yet (Cockell and Lee, 2002). There are several possible reasons. Firstly, the cooling of an impact crater occurs geologically in a short period of time and suitable temperature zones (ecological niches) may change too rapidly in time and space, thus preventing a stable colonization. Secondly, activity of microbial organisms, which are most adaptive for hydrothermal conditions, is not easy to recognize in a fossil IHT system. Thirdly, there is yet a need for detailed studies of these IHT systems. The latter are interesting to study also in respect to early life as they could well have provided conditions supportive for the development of life on the Archean Earth, which cannot be excluded for other planetary bodies as well (Kring, 2000; Mojzsis and Harrison, 2000).

IHT systems may persist for extended periods of time; however, their size and life time will critically depend on the magnitude of the impact event, the composition and structure of the target, and the prevailing cooling mechanism. In this contribution, we study the evolution of potentially suitable habitats for high-temperature (hyperthermophilic and thermophilic) microorganisms in an IHT system at a small-to-medium sized impact crater by complex numerical modeling. The impact and geothermal transient fluid modeling was scaled and verified against the 4-km diameter Kärdla impact structure, Estonia, which structure and development is well constrained (e.g., Puura and Suuroja, 1992; Suuroja et al., 2002; Kirsimäe et al., 2002; Puura et al., 2004; Versh et al., 2005; Jõeleht et al., 2005).

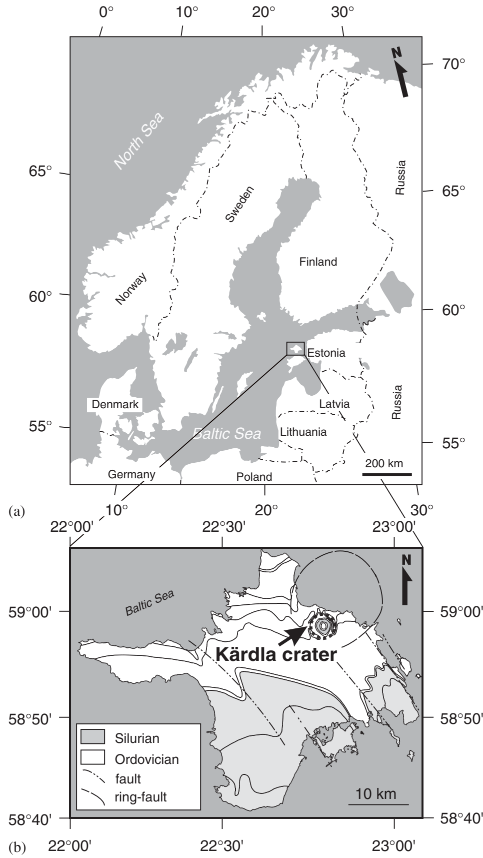

Fig. 1. (a) Location of the Kärdla structure in northern Europe, at the west coast of the Baltic Sea. (b) Location of the crater and its surrounding ring-fault at the bedrock map of the Hiiumaa Island.

2. Geological setting of the Kärdla structure

The Kärdla structure is located on the Island of Hiiumaa (58°58′40″N, 22°46′45″E), 25 km off the northwestern coast of Estonia (Fig. 1). The structurally complex (Puura and Suuroja, 1992) impact structure is 4 km in diameter and ~540 m deep with a central uplift exceeding 100 m. The crater formed in a shallow (~100 m deep) epicontinental Ordovician sea about 455 Ma ago (Grahn et al., 1996) into a target composed of a 150 m-thick Early Paleozoic siliciclastic and carbonate sedimentary sequence on top of Paleoproterozoic crystalline basement represented by regionally metamorphosed retrograde amphibolite-facies migmatitic granites and quartz–feldspar gneisses with amphibolites, biotite gneisses, and biotite–amphibole gneisses (Suuroja et al., 2002). The structure is practically uneroded owning to rapid burial after the event and is today covered by post-impact Upper Ordovician, Silurian, and Quaternary deposits, which also compose the upper portion of the crater-filling sediments (Fig. 2). The lower part of the crater depression is filled with complete sequence of authigenic and allogenic (sedimentary and crystalline polymict breccias with suevitic breccia zones) impact breccias covered by resurge breccias (Puura and Suuroja, 1992; Puura et al., 2004). Authigenic breccias are composed of cataclastic crystalline basement rocks that are fractured to different degrees. Fracturing decreases gradually with depth and extends to ~1 km beneath the original surface. No evidence of an impact melt sheet in the crater interior has been found; however, the suevitic breccia units

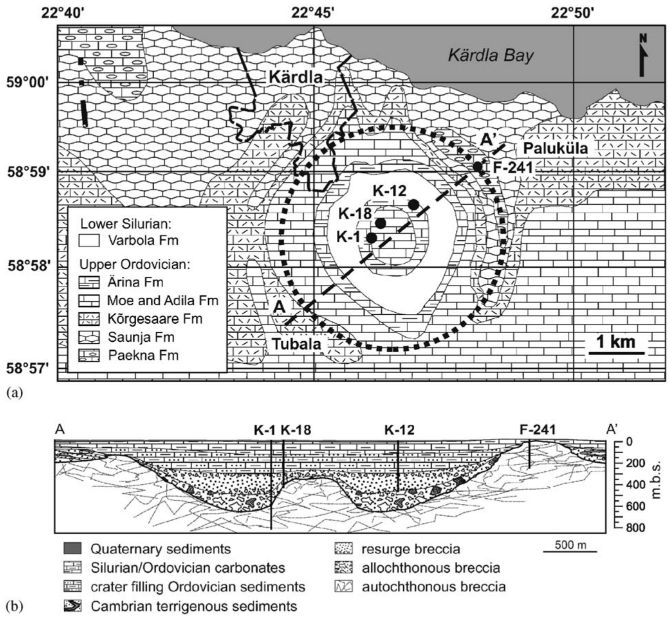

Fig. 2. (a) Geological map of the Kärdla structure area with location of drill-cores referred to in the text. Black dashed lines show the location of the crater rim and the cross-section (A–A′) presented in (b). Black long dashed line marks the border of the town Kärdla in the NW part of the crater. (b) Cross-section of the crater structure in SW–NE direction with locations of drill-cores. Vertical scale indicates meters below surface. Modified after Versh et al. (2005).

were found to contain devitrified melt clasts (Suuroja et al., 2002).

3. Impact and geothermal modeling

Impact and geothermal modeling was applied to study the impact cooling and the space–time development of suitable habitats for high-temperature microbial life colonization in the Kärdla structure. In the first step, the heating by the impact and the post-impact temperature distribution were found by numerical impact modeling using the modified version (Ivanov et al., 1997; Ivanov and Deutsch, 1999) of the two-dimensional hydrocode SALE (Amsden et al., 1980). An analytical equation of state (ANEOS; Thompson and Lauson, 1972) was used to describe the properties of the granitic projectile and the target. The diameter (300 m) and velocity (15 km s^{-1}) of the projectile were found by trial to fit the simulated crater size and shape to the observations in Kärdla.

In the second step, the impact geothermal modeling accounting for coupled heat transfer and multi-phase fluid flow in a variably saturated medium was performed. The distribution of parameters in the two-dimensional axi-symmetric model was partially based on borehole data. The data are limited because there are only three boreholes inside of the crater that extend to at least suevitic breccias (Fig. 2). Nevertheless, they reveal vertical porosity variations in the breccias and fractured basement (Plado et al., 2002) that were used for the post-impact water saturation of rocks assuming that the saturation is a reciprocal of the porosity. The permeability of rocks was also assumed to vary with lithology and depth from 10^{-13} m^2 in the suevitic breccia to 10^{-17} m^2 in the unaffected rocks at greater depth. The resurge of seawater into the crater was not simulated by the impact modeling hydrocode. However, the resurge sediments were added to the model assuming their temperature as that of the seawater (20 °C) and permeability of 10^{-12} m^2, a value that is typical for the sedimentary rocks, which compose the majority of the resurge sediments. More details on the modeling are given in Jõeleht et al. (2005). The impact heating–cooling model was verified against the geological observations and characterization of IHT activity within the Kärdla structure (Versh et al., 2005).

4. Mineralogical characteristics of the Kärdla structure hydrothermal system

In the Kärdla structure an IHT system was generated by the interaction of impact heated rocks and intruding seawater, representing a single thermal event with an irreversible cooling path, resulting in a series of alteration products. The impactites inside and in the vicinity of the crater are characterized by a major HT alteration of authigenic and allogenic breccias. Hornblende and plagioclase, along with impact glass and melt clasts, were replaced mainly by clay (chlorite/corrensite), quartz, and orthoclase-type K-feldspar in impact affected granites and amphibolites, resulting in K-metasomatism and Na and Ca depletion. The aluminosilicate HT alteration took place in circulating vapor- to vapor–liquid-dominated environment in the early and middle stages of the system development at temperatures $>300\,^{\circ}C$ to $150/100\,^{\circ}C$ (Versh et al., 2005). The maximum fluid temperatures at early stages of the IHT fluids circulation reached as high as 400–500 °C as revealed by fluid inclusion studies in quartz (Kirsimäe et al., 2002). The high-temperature stages were followed by quartz–carbonate–sulfide and Fe-oxyhydrates crystallization from liquid-dominating fluids at lower temperatures ($<100\,^{\circ}C$), characterizing the latest cooling phase of the system.

The IHT alteration in Kärdla impactites is mainly located in the upper central area of the crater, but the fracture-limited fluid–rock interaction also occurs at the rim and in the deeper central areas of the crater depression (Versh et al., 2005). It was found that the alteration intensity (i.e., the abundance of the authigenic phases) varies with the location within the structure. At the rim wall, hydrothermal alteration is localized along fractures and impact-injected breccia lenses, where the carbonate and sulfide/Fe-oxyhydrate assemblages dominate over the authigenic feldspar–chlorite–quartz minerals. More prolonged and intense alteration is evident within the crater depression (drill-core K-12 and the lower part of the K-1 section) and around the central uplift (drill-core K-18), where the silicate–clay alteration is dominant. At the rim wall area, the plagioclase K-alteration and hornblende chloritization is restricted to fracture planes and grain boundaries and probably also to metastable impact melt glass/diaplectic glass fragments within the breccia lenses. Conversely, in the central uplift—crater depression area the alteration zones reach progressively outwards from the fractures into the host rock, and up to one-third of the plagioclase and hornblende volume is replaced with the authigenic minerals.

5. Development of IHT system at the Kärdla-sized crater and the distribution of potential hydrothermal ecological niches

During the first thousandth of a second after the impact, pressures up to hundreds of GPa and temperatures up to ten thousands of degrees occur at the immediate projectile—Earth compression zone. However, the impact pressures and temperatures for most parts of the crater area are much less, ranging from 100–50 GPa and ~1200 K in impact melt down to ambient conditions at some radial distances from the impact center. Geological observations and the modeling of the impact suggest that the heated rocks, which can initiate the hydrothermal fluid flow, are found at two positions. First, a layer of melted and/or hot brecciated rocks formed near the free surface during the crater excavation and modification stages. The degree of rock melting as well as the volume and extent of this layer depends on the crater scaling (Ivanov and Deutsch, 1999). Second, the rocks those form in the central uplift and its closest neighborhood, which are heated up during shock-wave passage and decompression. Also, an additional thermal impulse into the crater area can be provided by the stratigraphic uplift and shear heating during the formation of the central peak, and the rapid unloading of the target basement (Masaitis and Naumov, 1993; Crossey et al., 1994).

Spatial configuration of the IHT system(s) depends evidently on the presence and dimensions of the impact melt sheet. In large multi-ring impacts the initially impermeable melt sheet covers the entire peak ring-basin area, as well as in part the space between the peak ring and final crater rim (e.g., Sudbury structure in Ontario, Canada). In that case, the IHT system develops originally in the annular trough between the peak ring and the final crater rim, with the fluid venting through faults in the crater modification zone (Abramov and Kring, 2004). However, in the small-to-medium scale craters without significant melting, the IHT system forms in and around the central high (Jõeleht et al., 2005). Likewise, the life time of the IHT system varies significantly with the crater size depending on the amount of melting and governing mode of heat transport. In large structures, such as Sudbury, the formation of the IHT system is in most part of the crater inhibited for $\sim 10^5$ years by the low permeability of rock and or melt and the first period of cooling is mainly determined by the least effective, i.e. conductive heat removal mechanism. Consequently, Abramov and Kring's (2004) estimate for the life time (defined herein as the time needed for the system to cool below 90 °C within 1 km of the surface everywhere in the model) of the 150-km diameter Sudbury is in the range of 0.22–3.2 Ma, depending on the surface permeability.

In structures with limited melting the IHT system is formed shortly after the impact and the cooling is governed mainly by convective heat transport leading to more rapid temperature decrease. In the 4-km diameter Kärdla structure the cooling to temperatures below 90 °C in the uppermost 1 km takes only 1500–4500 years (Jõeleht et al., 2005), which is two to three orders of magnitude less than in large-scale structures. The modeling results suggest that in similar small-to-medium scale craters the habitable zone for hyperthermophilic and thermophilic organisms is created soon after the impact in most part of the crater. Moreover, the small-to-medium scale structures are the most likely devoid of deep heat sterilization of large rock volumes as in the case of large-scale melting. The organisms, that survive the impact, are readily present in the environment and are capable of colonizing the system

Please cite this article as: Evelin Versh et al., Development of potential ecological niches in impact-induced hydrothermal systems: The small-to-medium size impacts, Planetary and Space Science (2006), doi:10.1016/j.pss.2005.12.022.

in a short time after the impact. Simulated impact experiments suggest that *Bacillus subtilis* spores survive the pressures of 32 GPa and temperatures peaked at 250 °C (Horneck et al., 2001). At the Kärdla-type crater these limits were exceeded only at the centermost area.

The results of transient fluid flow and heat transfer simulations in the Kärdla structure (Fig. 3) suggest that in the most hydrothermally altered central area the temperatures were well above the boiling point (250–290 °C, depending on the hydrostatic pressure) immediately after the impact and a vapor-dominated area formed. However, due to efficient heat removal at the liquid/vapor front (Jõeleht et al., 2005), this area diminishes in a few tens of years in the upper part of the central uplift (the most permeable breccia sequence) and it lasted for less than a hundred years in the deeper part. At the crater depression and rim area the initial temperatures suggested by impact modeling were much lower—from 150 °C to ambient temperatures at the outer rim. However, the mineralogical data (Versh et al., 2005) suggest that the temperatures at the rim might have been locally higher (up to 200–300 °C) in the fracture zones and suevite pockets for few years after the impact. In most areas of the crater the conditions favorable for high-temperature microorganisms (temperatures <100 °C) were reached in less than 500–1000 years. The suitable zones for hyperthermophilic (80–120 °C) and thermophilic (45–80 °C) organisms change significantly in space and volume with time (Fig. 4). As a general consequence, the volume of space that is habitable for hydrothermal microbial communities (temperature range of 45–120 °C) in the Kärdla structure grows rapidly during the first period of the cooling. It reaches the maximum in 1500–2000 years and then fades within 20,000–25,000 years with the gradual decrease and deepening of the habitable zone(s) toward the craters center. The cooling of the rim is quite fast as is demonstrated by the prompt changes of the volume with temperatures 45–80 °C during the first decades after the impact (Fig. 4 inset). Although in the central peak region the possible microbial colonization is inhibited for about a thousand years, this is the rock body that retains the optimum growth temperatures (45–80 °C) needed for thermophiles and/or hyperthermophiles (80–120 °C) for the longest period. The thermal equilibration of the whole impact takes much longer time. Even though the maximum temperature disturbance after 10,000 years is only about 15 K, the heat flow density is two times higher than in the surrounding areas (Jõeleht et al., 2005).

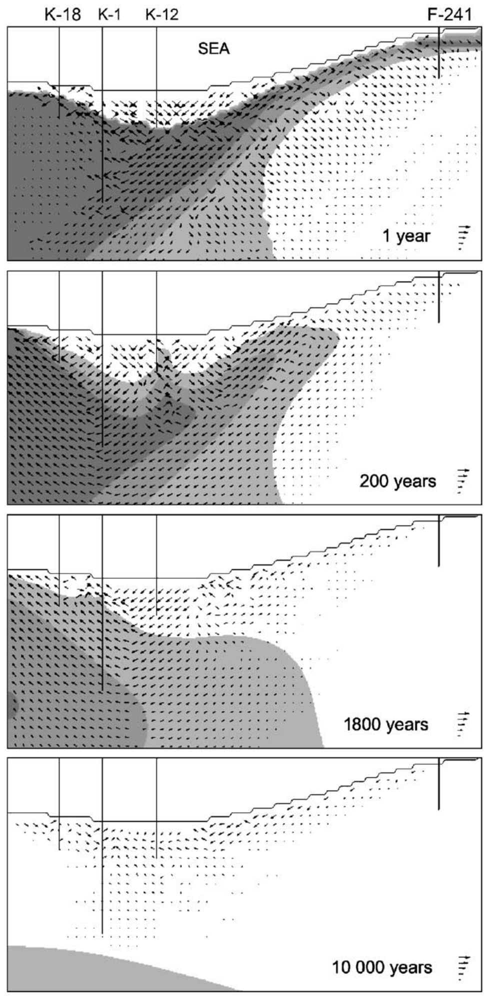

Fig. 3. Geothermal modeling simulations of post-impact temperature distribution at the Kärdla impact site 1, 200, 1800 and 10,000 years after the impact event. The simulation reaches down to 1.0 km in depth and 2.5 km in width. Mass flow rates of liquid water (black arrows) and vapor (white arrows) are drawn in the lognormal scale with the largest arrow corresponding to 10^{-6} and the shortest to 10^{-10} kg m^{-2} s^{-1}. The isotherms represent following: dark gray, >120 °C; gray, 120–80 °C (growth-temperature range of hyperthermophiles), light gray, 80–45 °C (growth-temperature range of thermophiles); white, <45 °C.

6. Potential inhabitants of the IHT systems

Modern hydrothermal systems (including deep-sea hydrothermal vents) support a large variety of microorganisms, including thermophilic and hyperthermophilic forms of both the *Bacteria* and *Archaea* domains (Van Dover, 2000). Most hyperthermophilic organisms are *Archaea*, capable of growing at temperatures as high as 113 °C (nitrate-reducing chemolithoautotroph *Pyrolobus fumarii*; Blöchl et al., 1997) and recently reported 121 °C (Fe^{3+}-reducing chemolithoautotroph *Strain 121*; Kashefi and Lovley, 2003). Yet, culture of the thermophilic aerobe *Thermus aquaticus*, readily isolated from terrestrial HT

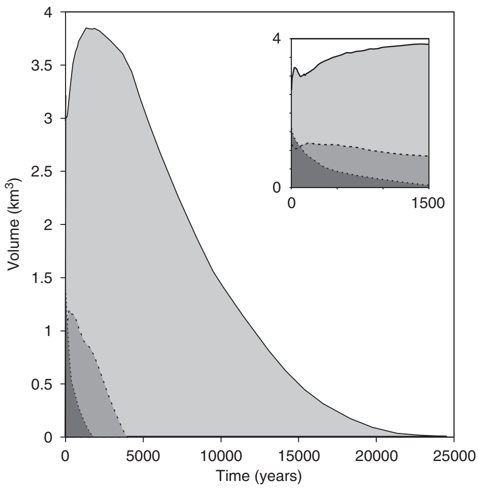

Fig. 4. Simulated volume of rocks with temperature >120°C (dark gray), 80–120 °C (gray) and 45–80 °C within the crater (up to radius 2 km) as a function of time. The inset shows rapid volumetric changes during the first decades that can be attributed to the fast cooling of the rim.

systems of 90–100 °C, do not grow reliably in laboratory conditions at temperatures above 80 °C, the cardinal growth temperatures determined in the laboratory studies might really be underestimates of true in vivo growth temperatures (Cowan, 2004). Apart from these extremes, the optimum temperatures are much lower and in general, the diversity of microbiota increases with the lowering temperature. The optimum growth conditions for most thermophiles is 45–80 °C and 80–107 °C for hyperthermophiles, while the upper limit for eucaryotes is only ~60 °C (Barns and Nierzwicki-Bauer, 1997).

The variety of microfossils associated with ancient hydrothermal deposits reported to date is much less when compared with recent viable systems. They are mostly presented by filamentous and autotrophic, even though the microbial communities of most modern hydrothermal ecosystems also contain mesophilic and thermophilic cocci which, however, are difficult to recognize in the geological record (Reysenbach and Cady, 2001). Reysenbach and Cady (2001) explain the abundance of filamentous and sheathed organisms in terrestrial and marine hydrothermal systems with an advantage of that morphology over cocci, by enabling complex microbial mat formation and retain filaments in a fast-flowing fluid environment. However, this should not be taken as a universal rule. Modeling results suggest in Kärdla the net Darcy velocities are in the order of 10^{-6} m/s at most, which are evidently too low to cause this kind of environmental adaptation in heavily fractured impactites.

The structure of the microbial community at a particular IHT system is primarily defined by the environmental conditions depending on the temperature and geochemical characteristics of the fluid (fluid–rock interaction) within the system, but also the possibility for photosynthesis. In terrestrial hydrotherms (springs) thermophilic photoautotrophs predominate over other groups. At deep sea hydrothermal vents chemosynthetic (chemolithoautotrophic) groups use the energy from the interaction of reduced compounds in the hydrothermal fluid (sulfur, iron, etc.) and surrounding oxidized seawater (Van Dover, 2000). The IHT systems differ from most known volcanic (both terrestrial and deep sea) hydrotherms in many aspects, such as temperature history, fluid flow characteristics and chemistry, size, etc. As an example, at large craters IHT systems can be generated that are volumetrically an order of magnitude larger compared to volcanic hydrotherms (Abramov and Kring, 2004). The assemblage and geochemical characteristics of the hydrothermal minerals in IHT systems vary within a narrow interval of pH and suggest weakly alkaline and near neutral environments (pH 6–8) as the result of anion hydrolysis of mainly the aluminosilicate composition rocks and impact-derived impact melts/glasses. Also, the solutions maintain Eh values of > -0.5 V (at least for a neutral environment) in the course of the hydrothermal process (Naumov, 2002; Koeberl and Reimold, 2004). However, in target rock sediments rich in organic carbon the organics can be degraded/respired at the rate which exceeds oxygen transport and groundwater would be of reducing character. These constrained environmental variables suggest some limitation/specification for possible thermophilic and/or hyperthermophilic microorganisms that could colonize such a system. The ecological analysis of the thermophiles and hyperthermophiles in the IHT system is beyond the scope of this paper. However, if most of the *Archaea* and *Bacteria* are neutrophiles and can easily grow in the slightly acidic-alkaline pH range (6–8) of the impact-induced environment, then, unlike the volcanic environments that are generally low in oxygen and rich in reductants (Barns and Nierzwicki-Bauer, 1997), the impact-induced systems seem to be richer in dissolved oxygen, but not necessarily oxidative, and poor in reduced compounds. This would suggest the preference of sulfur-reducing microorganisms in the marine IHT communities, whereas many sulfate reducers are also able to use molecular H_2, on which most of the chemolithotropic reactions rely in hydrothermal vents (McCollom and Schock, 1997). Furthermore, the microorganisms in impact-induced hydrotherms cannot be/have not been as highly specialized as these hydrotherms, especially in small-scale craters, which change rapidly in the space and environmental quality. This implies that the potential habitats in IHT systems would be occupied by organisms capable of adapting to the changing conditions by applying alternative metabolic processes.

A search was conducted, as part of this investigation, for possible fossil remains of IHT microbial activity in the

Kärdla structure. However, the observations have not revealed any direct in situ evidences of microbial colonization and preservation within these rocks so far, and this question needs further investigation.

7. Conclusions

The role of meteorite impacts in the biological evolution is controversial—large-scale impacts can cause global interruptions in the development of some ecosystems, yet creating opportunities for other organisms/ecosystems. On a smaller scale, the impact structures themselves can serve as suitable ecological niches (oases) for life. In impacts into water-containing targets—planetary surfaces covered with sea, groundwater or permafrost resources—the impact heating of crater rocks can initiate hydrothermal circulation systems. These IHT systems may host the most primitive thermophilic and/or hyperthermophilic microorganisms that are interesting to study in respect to origin of early life on Earth, as well as for exobiological perspectives. The impact modeling at a small-to-medium scale Kärdla structure suggests that the habitable zone for hydrothermal hyperthermophilic and thermophilic organisms is created soon after the impact in most parts of the crater, whereas the small-to-medium scale structures are the most likely to be devoid of deep heat sterilization of large rock volumes as in the large-scale impacts that include significant melt production. The transient fluid flow and heat transfer simulations for Kärdla suggest that the temperatures were above the boiling point immediately after the impact, and the potential colonization was inhibited for about a thousand years in the deeper part. In most parts of the crater the conditions favorable for thermophilic microorganisms (temperatures $<100\,^{\circ}C$) were reached in 500–1000 years. The suitable zones for hyperthermophilic (80–120 °C) and thermophilic (45–80 °C) organisms change significantly in space and volume with time. The space habitable for hydrothermal microbial communities (temperature range 45–120 °C) in Kärdla structure grows rapidly during the first period of the cooling reaching the maximum in 1500–2000 years and then fades within 20,000–25,000 years with gradual decrease and deepening of the habitable zone(s) toward the crater center. The cooling of the rim is quite fast as is demonstrated by prompt changes of the volume with temperatures 45–80 °C during the first decades after the impact. However, the mineralogical data (Versh et al., 2005) suggest that the temperatures at the rim might have been locally higher (up to 200–300 °C) in the fracture zones and suevite pockets for few years after the impact. The geochemical and mineralogical data suggest that the environmental conditions in IHT systems vary within a narrow interval of pH 6–8 as a result of anion hydrolysis of mainly the aluminosilicate composition rocks and impact-derived impact melts/glasses. Unlike volcanic environments the impact-induced systems are apparently richer in dissolved oxygen, and low in reduced compounds. This would suggest a preference for sulfur-reducing microorganisms in the IHT communities, while the organisms in impact-induced hydrotherms cannot be highly specialized owning to rapid changes in the temperature and fluid composition in the course of the impact cooling.

Acknowledgments

The research was financially supported by Estonian Science Foundation (Grants no. 5372, 5851).

References

Abramov, O., Kring, D.A., 2004. Numerical modeling of an impact-induced hydrothermal system at the Sudbury crater. J. Geophys. Res. 109, E10007.

Amsden, A.A., Ruppel, H.M., Hirt, C.W., 1980. SALE: A simplified ALE computer program for fluid flow at all speeds. Los Alamos National Laboratory Report LA-8095. Los Alamos National Laboratory, Los Alamos, NM.

Barns, S.M., Nierzwicki-Bauer, S.A., 1997. Microbial diversity in ocean, surface and subsurface environments. In: Banfield, J.F., Nealson, K.H. (Eds.), Geomicrobiology: Interactions Between Microbes and Minerals. Reviews in Mineralogy, Vol. 35. Mineralogical Society of America, Washington DC, pp. 35–79.

Blöchl, E., Rachel, R., Burggraf, S., Hafenbradl, D., Jannasch, H.W., Stetter, K.O., 1997. Pyrolobus fumarii, gen. and sp. nov., represents a novel group of archaea, extending the upper temperature limit of life to 113 °C. Extremophiles 1, 14–21.

Cockell, C.S., 2004. Impact-shocked rocks—insights into archean and extraterrestrial microbial habitats (and sites for prebiotic chemistry?). Adv. Space Res. 33, 1231–1235.

Cockell, C.S., Lee, P., 2002. The biology of impact craters—a review. Biol. Rev. 77, 279–310.

Cockell, C.S., Lee, P., Osinski, G., Horneck, G., Broady, P., 2002. Impact-induced microbial endolithic habitats. Meteorit. Planet. Sci. 37, 1287–1298.

Corliss, J.B., Dymond, J., Gordon, L.I., Edmond, J.M., Von Herzen, R.P., Ballard, R.D., Green, K.K., Williams, D., Bainbridge, A., Crane, K., Van Andel, T.H., 1979. Submarine thermal springs on the Galapagos Rift. Science 203, 1073–1083.

Cowan, D.A., 2004. The upper temperature for life—where do we draw the line? Trends Microbiol. 12, 58–60.

Crossey, L.J., Kudo, A.M., McCarville, P., 1994. Post-impact hydrothermal systems: Manson impact structure, Manson, Iowa. In: Lunar and Planet Science Conference XXV, Houston, pp. 299–300.

Grahn, Y., Nõlvak, J., Paris, F., 1996. Precise chitinozoan dating of Ordovician impact events in Baltoscandia. J. Micropaleontol. 15, 21–25.

Horneck, G., Stöffler, D., Eschweiler, U., Hornemann, U., 2001. Bacterial spores survive simulated meteorite impact. Icarus 149, 285–290.

Ivanov, B.A., Deutsch, A., 1999. Sudbury impact event: cratering mechanics and thermal history. In: Dressler, B., Grieve, R.A.F. (Eds.), Large Meteorite Impacts and Planetary Evolution II. GSA Special Paper 339. Geological Society of America, Boulder, CO, pp. 389–397.

Ivanov, B.A., DeNiem, D., Neukum, G., 1997. Implementation of dynamic strength models into 2D hydrocodes: applications for atmospheric breakup and impact cratering. Int. J. Impact Eng. 20, 411–430.

Jõeleht, A., Kirsimäe, K., Plado, J., Versh, E., Ivanov, B., 2005. Cooling of the Kärdla impact crater: II. Impact and geothermal modeling. Meteorit. Planet. Sci. 40, 20–32.

Kashefi, K., Lovley, D., 2003. Extending the upper temperature limit for life. Science 301, 934.

Kirsimäe, K., Suuroja, S., Kirs, J., Kärki, A., Polikarpus, M., Puura, V., Suuroja, K., 2002. Hornblende alteration and fluid inclusions in Kärdla impact crater, Estonia: evidence for impact-induced hydrothermal activity. Meteorit. Planet. Sci. 37, 449–457.

Koeberl, C., Reimold, U.W., 2004. Post-impact hydrothermal activity in meteorite impact craters and potential opportunities for life. In: Norris, R.P., Stootman, F.H. (Eds.), Bioastronomy 2002: Life Among the Stars. IAU Symposium 213, pp. 299–304.

Kring, D.A., 2000. Impact events and their effect on the origin, evolution, and distribution of life. GSA Today 10, 1–7.

Masaitis, V.L., Naumov, M.V., 1993. Puchezh-Katunki astrobleme: preliminary model of hydrothermal circulation system. Meteoritics 28, 390–391.

McCollom, T.M., Schock, E.L., 1997. Geochemical constraints on chemolithoautotrophic metabolism by microorganisms in seafloor hydrothermal system. Geochim. Cosmochim. Acta 61, 4375–4391.

Mojzsis, S.J., Harrison, T.M., 2000. Vestiges of a beginning: clues to the emergent biosphere recorded in the oldest known sedimentary rocks. GSA Today 10, 1–6.

Naumov, M.V., 2002. Impact-generated hydrothermal systems: data from Popigai, Kara, and Puchezh-Katunki impact structures. In: Plado, J., Pesonen, L.J. (Eds.), Impacts in Precambrian Shields. Springer, Berlin, pp. 117–171.

Newsom, H.E., 1980. Hydrothermal alteration of impact melt sheets with implications for Mars. Icarus 44, 207–216.

Newsom, H.E., Brittelle, G.E., Hibbitts, C.A., Crossey, L.J., Kudo, A.M., 1996. Impact crater lakes on Mars. J. Geophys. Res. 101, 14951–14956.

Plado, J., Jõeleht, A., Šogenova, A., 2002. Physical properties. In: Põldvere, A. (Ed.), Soovälja (K-1) Drill Core. Estonian Geological Sections 4, pp. 21–24.

Puura, V., Suuroja, K., 1992. Ordovician impact crater at Kärdla, Hiiumaa Island, Estonia. Tectonophysics 216, 143–156.

Puura, V., Huber, H., Kirs, J., Kärki, A., Suuroja, K., Kirsimäe, K., Kivisilla, J., Kleesment, A., Konsa, M., Preeden, U., Suuroja, S., Koeberl, C., 2004. Geology, petrography, shock petrography, and geochemistry of impactites and target rocks from the Kärdla crater, Estonia. Meteorit. Planet. Sci. 39, 425–451.

Reysenbach, A.-L., Cady, S.L., 2001. Microbiology of ancient and modern hydrothermal systems. Trends Microbiol. 9, 79–86.

Suuroja, K., Suuroja, S., All, T., Floden, T., 2002. Kärdla (Hiiumaa Island, Estonia)—the buried and well-preserved Ordovician marine impact structure. Deep-Sea Res. II 49, 1121–1144.

Thompson, S.L., Lauson, H.S., 1972. Improvements in the Chart D Radiation hydrodynamic Code III: Revised Analytical Equation of State. Sandia National Laboratories, NM, USA.

Van Dover, C.L., 2000. The Ecology of Deep-Sea Hydrothermal Vents. Princeton University Press, Princeton, NY.

Versh, E., Kirsimäe, K., Jõeleht, A., Plado, J., 2005. Cooling of the Kärdla impact crater: I. The mineral parasequence observations. Meteorit. Planet. Sci. 40, 3–19.

CURRICULUM VITAE

EVELIN VERŠ

Date of birth:	February 14th, 1979
Address:	Institute of Geology, University of Tartu Vanemuise 46, 51014 Tartu, Estonia
Phone:	+372 737 5836
E-mail:	evelin.versh@ut.ee

Education

1997	Tallinn Tondiraba High school
2001	University of Tartu, BSc in geology
2002	University of Tartu, MSc in geology and mineralogy

Professional employment

2001–2005	University of Tartu, Museum of Geology; curator of collections (0.5)
2005–2006	MTÜ Loodusajakiri, journal "Eesti Loodus"; editor
2006–...	University of Tartu, Institute of Geology; extr. researcher

Research training

08–12/2003	Humboldt University in Berlin, Museum of Natural History, Institute of Mineralogy
03–06/2004	University of Copenhagen, Geological Institute

Publications

Jõeleht A., Kirsimäe K., Plado J., **Versh E.** and Ivanov B. 2005. Cooling of the Kärdla impact crater: II. Impact and geothermal modeling. *MAPS* 40(1), 20–32.

Jõeleht A., Kirsimäe K., **Versh E.** and Plado J. 2006. Rapid post-impact cooling at Kärdla — Where are the same conditions met? In *First International Conference on Impact Cratering in the Solar System, 08–12 May, 2006.* Abstract Book, ESA, ESTEC, p. 101.

Kirsimäe K., **Versh E.**, Somelar P. and Jõeleht A. 2006. Clays in extraterrestrial environments — The case of impact induced hydrothermal systems. In *Impact craters as indicators for planetary environmental evolution and astrobiology, Östersund (Sweden), June 8–14, 2006.* Abstract Book.

Versh E., Kirsimäe K., Jõeleht A. and Plado J. 2005. Cooling of the Kärdla impact crater: I. The mineral paragenetic sequence observation. *MAPS* 40(1), 3–19.

Versh E., Kirsimäe K., Jõeleht A. in press. Development of potential ecological niches in impact-induced hydrothermal systems: the small-to-medium size impacts. *Planetary and Space Science*. doi:10.1016/j.pss.2005.12.022.

Versh E., Kirsimäe K., Buchardt B., Naumov M.V., Öhman T. and Jõeleht A. 2006. Mineralogical and stable isotope study of impact-induced hydrothermal carbonate minerals. In *First International Conference on Impact Cratering in the Solar System, 08–12 May, 2006.* Abstract Book, ESA, ESTEC, p. 233.

Versh E., Kirsimäe K., Jõeleht J. and Buchardt B. 2006. The stable isotope and mineralogical studies of late-stage IHT carbonate minerals in Kärdla — The fluid source and origin of depleted carbon. In *Impact craters as indicators for planetary environmental evolution and astrobiology, Östersund (Sweden), June 8–14, 2006.* Abstract Book.

CURRICULUM VITAE

EVELIN VERŠ

Sünniaeg:	14. veebruar, 1979
Aadress:	Tartu Ülikooli geoloogia instituut Vanemuise 46, 51014 Tartu
Telefon:	+372 737 5836
E-mail:	evelin.versh@ut.ee

Hariduskäik

1997	Tallinna Tondiraba Keskkool
2001	Tartu Ülikool, BSc geoloogias
2002	Tartu Ülikool, MSc geoloogia ja mineraloogia alal

Teenistuskäik

2001–2005	Tartu Ülikool, geoloogiamuuseum; varahoidja (0,5)
2005–2006	MTÜ Loodusajakiri, "Eesti Loodus"; toimetaja
2006– ...	Tartu Ülikooli geoloogia instituut; erak. teadur

Erialane enesetäiendamine

08–12/2003	Humboldt'i Ülikool Berliinis, Loodusloo muuseum, mineraloogia instituut
03–06/2004	Kopenhaageni Ülikool, Geoloogia Instituut

Publikatsioonid

Jõeleht A., Kirsimäe K., Plado J., **Versh E.** and Ivanov B. 2005. Cooling of the Kärdla impact crater: II. Impact and geothermal modeling. *MAPS* 40(1), 20–32.

Jõeleht A., Kirsimäe K., **Versh E.** and Plado J. 2006. Rapid post-impact cooling at Kärdla — Where are the same conditions met? In *First International Conference on Impact Cratering in the Solar System, 08–12 May, 2006.* Abstract Book, ESA, ESTEC, p. 101.

Kirsimäe K., **Versh E.**, Somelar P. and Jõeleht A. 2006. Clays in extraterrestrial environments — The case of impact induced hydrothermal systems. In

Impact craters as indicators for planetary environmental evolution and astrobiology, Östersund (Sweden), June 8–14, 2006. Abstract Book.

Versh E., Kirsimäe K., Jõeleht A. and Plado J. 2005. Cooling of the Kärdla impact crater: I. The mineral paragenetic sequence observation. *MAPS* 40(1), 3–19.

Versh E., Kirsimäe K., Jõeleht A. in press. Development of potential ecological niches in impact-induced hydrothermal systems: the small-to-medium size impacts. *Planetary and Space Science*. doi:10.1016/j.pss.2005.12.022.

Versh E., Kirsimäe K., Buchardt B., Naumov M.V., Öhman T. and Jõeleht A. 2006. Mineralogical and stable isotope study of impact-induced hydrothermal carbonate minerals. In *First International Conference on Impact Cratering in the Solar System, 08–12 May, 2006.* Abstract Book, ESA, ESTEC, p. 233.

Versh E., Kirsimäe K., Jõeleht J. and Buchardt B. 2006. The stable isotope and mineralogical studies of late-stage IHT carbonate minerals in Kärdla — The fluid source and origin of depleted carbon. In *Impact craters as indicators for planetary environmental evolution and astrobiology, Östersund (Sweden), June 8–14, 2006.* Abstract Book.